Study on convective and non-convective rain of different heavy rainfall events in the pre-monsoon season using WRF-ARW model

M. Sc. Thesis

BY

MD. ADNAN FIHIR

DEPARTMENT OF PHYSICS

KHULNA UNIVERSITY OF ENGINEERING & TECHNOLOGY

KHULNA-9203, BANGLADESH

March-2018

Study on convective and non-convective rain of different heavy rainfall events in the pre-monsoon season using WRF-ARW model

M. Sc. Thesis
BY

MD. ADNAN FIHIR
ROLL NO: 1655555
SESSION: JULY-2016

A thesis submitted in partial fulfillment of the requirements for the degree of Master of Science in the Department of Physics, Khulna University of Engineering & Technology, Khulna-9203.

DEPARTMENT OF PHYSICS
KHULNA UNIVERSITY OF ENGINEERING & TECHNOLOGY
KHULNA-9203, BANGLADESH

MARCH 2016

DECLARATION

This is to certify that the thesis work entitled ***"Study on convective and non-convective rain of different heavy rainfall events in the pre-monsoon season using WRF-ARW model"*** has been carried out by Md. Adnan Fihir in the Department of Physics, Khulna University of Engineering & Technology, Khulna, Bangladesh. The above thesis work or any part of this work has not been submitted anywhere for the award of any degree or diploma.

Signature of Supervisor

(Professor Dr. Md. Mahbub Alam)

Signature of Candidate

Md. Adnan Fihir

DEDICATED TO
MY PARENTS

Acknowledgements

With my great manner it is a pleasure for me to express my deepest sense of gratitude and indebtedness to my reverend supervisor Dr. Md. Mahbub Alam, Professor, Department of Physics, Khulna University of Engineering & Technology, Khulna, for his kind guidance and supervision and for his constant encouragement throughout the research work. His inspiration and friendly cooperation has accelerated my works.

I am indebted to Professor Dr. Shibendra Shekher Sikder, Head, Department of Physics, Khulna University of Engineering & Technology for his strong support in various ways during the entire period of my study in this department. I express my heartfelt gratitude and thanks to Professor Dr. Md. Abdullah Elias Akhter and Professor Dr. Jolly Sultana Department of Physics, Khulna University of Engineering & Technology. Many thanks for their inspiration and advices from the beginning of my study. I gratefully acknowledge Mr. Md. Kamrul Hasan Reza Associate Professor, Mr. Sujit Kumar Shil, Md. Alamgir Hossain, Mr. Sumon Halder, Assistant Professors and Sumon Deb Nath, Lecturer, Department of Physics, KUET for their cooperation regarding writing the thesis.

My personal thankful greetings are to my good friends and well wishers for their help and cooperation. There are numerous people who could not be mentioned individually but their interesting discussions have prompted much thought on various aspects, I would also like to thank them. I would like to express my heart full thanks to my parents, brothers, sisters and nearest relatives for their inspiration, encouragement and multifaceted supports to carry out this thesis work.

Finally, I want to express my gratitude to almighty of god for his mercy.

Md. Adnan Fihir

CONTENTS

List of Figures

List of Table

Nomenclature

AFWA	:	Air Force Weather Agency
ARW	:	Advanced Research WRF
BGD	:	Bangladesh
BMD	:	Bangladesh Meteorological Department
BMJ	:	Betts-Miller-Janjic
BMP	:	Bulk Microphysical Parameterization
BoB	:	Bay of Bengal
BS	:	Bias Score
CAPE	:	Convective Available Potential Energy
CCN	:	Cloud Condensation Nuclei
ECMWF	:	European Centre for Medium-Range Weather Forecasts
ETS	:	Equitable Threat Score
FAA	:	Federal Aviation Administration
FSL	:	Forecast Systems Laboratory
GCM	:	General Circulation model
GMB	:	The Ganges, the Brahmaputra and the Meghna
IPCC	:	Intergovernmental Panel on Climate Change
ISO	:	Intra-seasonal Oscillation
KF	:	Kain-Fritsch
LBC	:	Lateral Boundary Conditions
LCC	:	Lambert Conformal Conic Projection
LES	:	Large Eddy Simulation
MCS	:	Mesoscale Convective System
MIC	:	Many Integrated Core
MM5	:	Mesoscale Model-5
MP	:	Microphysics
MRF	:	Medium Range Forecast
MSKF	:	Multi-Scale Kain-Fritsch
NCAR	:	National Center for Atmospheric Research
NCEP	:	National Centers for Environmental Prediction
NCMRWF	:	National Centre for Medium Range Weather Forecasting
NE	:	Northeastern
NEI	:	North-Eastern India
N-NE	:	North-Northeastern
N-NW	:	North-Northwestern
NW	:	Northwestern

NWP	:	Numerical Weather Prediction
OLR	:	Outgoing Long Wave Radiation
PBL	:	Planetary Boundary Layer
PCR	:	Parameterized-convection Resolution
PR	:	Precipitation Radar
QPFs	:	Quantitative Precipitation Forecasts
RHREs	:	Regional Heavy Rainfall Events
RRTM	:	Rapid Radiative Transfer Model
SD	:	Standard Deviation
SE	:	Southeastern
SPCS	:	State Plane Coordinate System
S-SE	:	South-Southeastern
S-SW	:	South-Southwestern
SW	:	Southwestern
TH	:	Thomson
TOA	:	Top-of-the-Atmosphere
TRMM	:	Tropical Rainfall Measuring Mission
TS	:	Threat Score
UNDP	:	United Nations Development Programme
USL	:	Updraft Source Layer
UTC	:	Universal Time Co-ordinate
VFR	:	Visual Flight Rules
WDM6	:	WRF double-moment 6-class
WMO	:	World Meteorological Organization
WRF	:	Weather Research and Forecasting
WSM5	:	WRF Single-moment 5-class
WSM6	:	WRF Single-moment 6-class
YSU	:	Yonsei University Scheme
ZM	:	Zhang-McFarlane

Abstract

In the present study the Advanced Research WRF (ARW) v3.8.1 model have been used to simulate the heavy rainfall events in the southeastern regions of Bangladesh during 4, 6 and 7 May 2013 and southern region during 15-16 May 2013. The initial and boundary conditions are drawn from the global operational analysis and forecast products of National Center for Environmental Prediction (NCEP-FNL) available at $1^{o} \times 1^{o}$ resolution. The model was configured in single domain, 6 km horizontal grid spacing with 161×183 grids in the east-west and north-south directions and 30 vertical levels. Time step of integration is set to 30 seconds for maintaining computational stability as the model uses third-order Runge-Kutta time integration scheme. In this research, four different microphysics (MP) schemes i.e., Lin *et al*., WSM6, Thompson and WDM6 and four different cumulus parameterization (CP) schemes i.e., Kain-Fritsch (KF), Tiedtke, Zhang-McFarlane (ZM) and Multi-scale Kain-Fritsch (MSKF) are used to simulate the heavy rainfall events. In this research convective rain and non-convective rain have been studied to observe the effect of these rainfalls on total rainfall and area average rainfall, relative humidity, vertical velocity, reflectivity and vorticity have been predicted and analyzed. The different verification methods such as threat score (TS), equitable threat score (ETS), bias score (BS) and standard deviation (SD) have been computed for accuracy of forecast.

Tiedtke scheme has simulated lower rainfall in combination with all chosen MPs in all Bangladesh and also heavy rainfall area on 4, 6 and 7 May. KF scheme coupling with all MPs have simulated similar average rainfall all over Bangladesh on 4 May and WDM6 coupling with KF, ZM and MSKF schemes have simulated almost similar amount of rain in the heavy rainfall region on 7 May. The model simulated heavy rainfall region is shifted from Khepupara to Mongla on 15 May all MPs and CPs and on 16 May, observed maximum rain at Barisal and Patuakhali matched but higher rain area is found at Khepupara. Simulated convective rain position matched with the observed maximum rain on 15 May but the amount is not significant for all MPs and CPs and on 16 May insufficient Convective Rain have simulated. Maximum amount of rain is found mainly non-convective for all MPs and CPs. On 16 May Lin *et al.* scheme coupling with all CPs have simulated almost similar results in the heavy rain area and all over Bangladesh all MPs gives higher results. WSM6 and WDM6 schemes coupling with ZM and MSKF schemes gives the better performance on the basis of Threat Score, Equivalent Threat Score and Bias Score on 4, 6 and 7 May 2013 and during 15-16 May 2013.

Chapter I

Introduction

Convective rain is the rain which happens when the sun heats a water source to the point so that water turns into vapor and rises. By the time it reaches the condensation level, the vapor becomes cooled enough to turn back into water and fall in the form of rain. The rest rainfalls which are not caused by this kind of process are called non–convective rain. This type of precipitation occurs when large air masses rise diagonally as larger–scale atmospheric dynamics force them to move over each other. Non–convective precipitation falls from nimbostratus clouds, while convective precipitation falls from active cumulus and cumulonimbus clouds. These cloud types may occur separately or entangled with each other in the same cloud complex. Tropical rainfall may appear to be essentially convective in nature, but experiments over the eastern tropical Atlantic, northern Australia, and the western equatorial Pacific have shown that almost all convection occurs in association with non–convective rain. The younger parts of the cumulonimbus clouds are 100% convective (Rodrigo, 2002). The clouds become non–convective when convection decays and co–exist with the embedded convective columns of rapid updraft. It is sometimes difficult to distinguish between convective and non–convective rains. Nowadays, the most useful instrument for identifying convective or non–convective rainfall is the meteorological radar, but there is no universal criterion for identifying a pixel as a convective one or non–convective one.

Rainfall is highly variable in space and time and is strongly influenced by orographic forcing. Seasonal prediction of southwest monsoon or summer monsoon rainfall over Bangladesh has considerable application for decision–making in agriculture and water resource sectors. Prediction of heavy rainfall is one of the many challenging problems in meteorology, but very important for issuing timely warnings for the agencies engaged in disaster preparedness and mitigation. Precipitating weather systems in combination with strong wind and flooding have impact and influence on the broad range of activities. The strong moisture–laden winds from the Bay of Bengal (BoB) interact with the topography, causing heavy precipitation over this region. Therefore, heavy precipitation, its timing, location and intensity are certainly key parameters in weather prediction and have significance on operational hydrology.

Cumulus parameterization (CP) schemes must estimate the rate of sub–grid–scale convective precipitation, release of latent heat, and the distribution of heat, moisture, and momentum in the vertical due to convection (Kain and Fritsch, 1993). Cumulus convection modifies the large–scale temperature and moisture fields through detrainment and cumulus–induced subsidence in the environment. The detrainment causes large–scale cooling and moistening, and the cumulus–induced subsidence causes large–scale warming and drying (Arakawa and Schubert, 1974).

Das *et al.* (2012) studied the simulation of seasonal monsoon rainfall over the SAARC region by dynamical downscaling using Weather Research and Forecasting (WRF) Model. Their findings suggest that the large scale seasonal distributions of rainfall observed by different sources are simulated fairly well by the model. Das *et al.* (2008) studied on the skills of different mesoscale models over Indian region during monsoon season. They recommended that the WRF is able to produce best all India rainfall prediction in the day–1 forecast and the mesoscale model (MM5) is able to produce best all India rainfall forecasts in day–3, but eta vertical coordinate (Mesinger *et al.,* 1988) and Reynolds stress equation model (RSM) are able to depict the best distribution of rainfall maxima along the west coast of India.

Bhowmik and Durai (2008) conducted research on multi–model ensemble forecasting of rainfall over Indian monsoon region. They have proposed a method for the ensemble forecasting of rainfall over the Indian monsoon region based on daily outputs of four operational numerical weather prediction (NWP) models in the short–range time scale (up to 48 hours). The method was applied to prepare 24 and 48 hours ensemble forecasting of convective and non–convective rainfall in the test mode daily during the summer monsoon 2006. The inter–comparison revealed that the method was capable to improve the forecast by taking the strength of each constituent model. Clark *et al.* (2007) studied on the comparison of the diurnal precipitation cycle using convection resolving and non–convection resolving mesoscale models which were compared to see if significant improvements could be obtained by using fine enough grid spacing to explicitly resolve convection. They examined the representation of the diurnal cycle by a 5–km grid–spacing configuration of WRF–NMM that did not use a CPS and compared it with a 22–km grid–spacing configuration of WRF–NMM that used a CPS.

Nesbitt and Zipser (2002) conducted research on the diurnal cycle of rainfall and convective intensity according to three years of tropical rainfall measuring mission (TRMM) measurements. They showed that rainfall over the oceans has a significant diurnal cycle that

peaks in the early morning to predawn hours, with a minimum in the late afternoon. Over land, all feature types contribute to an afternoon maximum in precipitation but mesoscale convective system (MCS) rainfall peaks in the early morning. Romatschke and Houze (2001) conducted research on characteristics of precipitating convective and non–convective systems in the pre–monsoon season of south Asia**.** Their TRMM precipitation radar (PR) data showed that the precipitation is more convective in nature and more sensitive to synoptic forcing during the monsoon season.

The effect of diurnal breezes on tropical convection was studied by Houze *et al.* (1981), using radar and other data obtained during the winter monsoon experiment in northwestern Borneo. They observed an extremely regular genesis of nocturnal convection near the coast, propagating offshore and developing through the night and morning hours into a mesoscale convective system that finally dissipates around local noon. In the afternoon, inland convection develops in association with the sea breeze.

A comparison of precipitation forecast skill between small convection allowing and large convection parameterizing ensembles was studied by Clark *et al.* (2009), using convection–allowing resolution (CAR) ensembles with WRF model from a 5–member, 4–km grid–spacing (ENS4) and parameterized–convection resolution (PCR) ensembles with WRF model from a 15–member, 20–km grid–spacing (ENS20). Their computation of various precipitation skill metrics for probabilistic and deterministic forecasts revealed that ENS4 generally provides more accurate precipitation forecasts than ENS20.

Heavy rainfall is often produced by long–lived MCSs or intense mesoscale systems embedded in the mei–yu frontal cloud band (Kuo and Chen 1990; Zhang *et al.*, 2003; Li and Chen, 1998). The presence of a southerly or southwesterly low level jet (Chen and Yu, 1988) to the south side of the mei–yu front significantly helps the development of these heavy rain bearing systems (Chen *et al.,* 2005), by providing warm and moist tropical air and strong uplifting mechanisms (Chen and Li, 1995). Chowdhury (2003) investigated the relationship between the inter–annual variability (IAV) of rainfall over Bangladesh and ENSO for about 40 years (1960s to 1990s). He found that although the summer monsoon rainfall in Bangladesh showed a decreasing (increasing) tendency during strong El Ni˜no (La Ni˜na) years, the quantitative correspondence between the strength of ENSO and the summer rainfall anomaly over Bangladesh was very weak. Schumacher and Johnson (2005) investigated the structure and evolution of extreme rain events using composite radar reflectivity data, and observed two MCS organization patterns occurring frequently in the United States.

The Advanced Research Weather Research and Forecasting (ARW–WRF) model is the new–generation model for both WRF (Skamarock *et al.*, 2008), and is widely used for regional climate research (Leung *et al.,* 2006; Bukovsky and Karoly, 2009; Awan *et al.*, 2011). Alam (2014) studied the effects of microphysics and cumulus parameterization for the prediction of heavy rainfall in post monsoon season. The study showed large variations among the different microphysical schemes. The microphysical schemes have a major impact on time and location of rainfall intensity. Gadgil *et al.,* (2005) expressed concerns about the ability of currently available dynamical systems to produce effective predictions of the monsoon rainfall. Every year in May–June, heavy rainfall events and associated deadly flash floods frequently cause severe property damage in South China and Taiwan. During this season, a quasi–stationary subtropical front, called the mei–yu front, occurs frequently and repeatedly (Ding, 1992).

In Asia, pre–monsoon precipitation systems showed more intense convection in terms of higher echo tops and higher lightning possibility (Kodama *et al.,* 2005). The sensitivity of different types of microphysical schemes and processes on CP were investigated by many Authors (McCumber *et al.,* 1991; Ferrier *et al.,* 1995; Wu *et al.,* 1999; Tao *et al.,* 2003). Tao *et al.* (1990) showed that the dominant microphysical processes were quite different between the convective and stratiform regions and between the mature and decaying stages. Kumar *et al.,* (2010) studied evaluation of physics options of the WRF model to simulate high impact heavy rainfall events over Indian Monsoon region (IMR). Their study shows that WRF model is sensitive to the choice of convective scheme. Betts–Miller–Janjic (BMJ) cumulus scheme is found to produce better results compared to other cumulus schemes for the IMR.

Significant increasing trend in extreme precipitation has been observed in last decades in North America, Europe, Australia, Japan, and other areas (Karl and Knight, 1998; Iwashima *et al.,* 2002; Alexander *et al.* 2006). Kim and Lee (2006) investigated the characteristics of MCSs accompanying heavy rainfall using a single data of Weather Surveillance Radar–1998 Doppler (WSR– 88D). They demonstrated that low–level vertical wind shear plays an important role in the development of quasi–stationary and multi–cell storms, and that convective systems merge and stagnate due to blocking by mountain ranges in Korea. Routray *et al.*, (2010) simulated of heavy rainfall events over Indian monsoon region using WRF–3DVAR data assimilation system. Results from the control experiments also highlight that weather and regional climate model simulations with coarse analysis have high uncertainty in simulating heavy rain events over the IMR and assimilation approaches, such

as the 3DVAR can help reduce this uncertainty. Xukai and Fumin (2015) conducted research on changes in regional heavy rainfall events in China during 1961–2012. Some stations showed significant increasing trends in the southern part of the middle and lower reaches of the Yangtze River and the northern part of South China, while parts of North China, regions between Guangxi and Guangdong, and northern Sichuan showed decreasing trends in the accumulated intensity of regional heavy rainfall events (RHREs).

Khaladkar *et al.*, (2007) studied the performance of NCMRWF models in predicting high rainfall spells during SW monsoon season. They showed that, in general, all the models predicted good rainfall activity along the west coast of India, which is consistent with the observations. Das *et al.*, (2012) simulated the seasonal monsoon rainfall over the SAARC Region by dynamical downscaling using WRF Model. Their findings suggest the large scale seasonal distributions of rainfall observed by different sources are simulated fairly well by the model. Bangladesh is one of the countries of the world most vulnerable to climate change due to its least capacity to address the devastating impacts. According to the IPCC report (IPCC 2007), Bangladesh will experience 5% to 6% increase of rainfall by 2030. Small changes in the mean and standard deviation values can produce relatively large changes in the probability of extreme events (Groisman *et al.*, 1999; Rodrigo, 2002; Chiew, 2006; Su *et al.*, 2006).

Bhanu *et al.* (2012) conducted research on simulation of heavy rainfall events during retreat phase of summer monsoon season over parts of Andhra Pradesh. They noticed that, circulation features and rainfall quantities are validated with observed rainfall of (Indian Meteorological Department) IMD and satellite derived datasets of KALPANA–1. Vitrat and Molteni (2009) studied dynamical extended range prediction of early monsoon rainfall over India. They suggested that the high resolution extended range forecasts could be useful for the prediction a few weeks in advance of sub seasonal events, like the onset of the monsoon. Ranadhur *et al.* (2009) conducted research on impacts of satellite–observed winds and total precipitable water on WRF short–range forecasts over the Indian region during the 2006 summer monsoon. The impacts of assimilating the different satellite dataset were measured in comparison to the control run, which does not assimilate any satellite data. They observed the assimilation of wind speeds resulted in a degradation of the temperature and humidity predictions at lower levels.

Karmakar and Khatun (1995) and Ahmed (1989) studied the probabilistic estimates of rainfall extremes in Bangladesh during the pre–monsoon season. There studies were concentrated only on maximum rainfall events for a limited time period. The skill of the European Centre for Medium–Range Weather Forecasts (ECMWF) seasonal forecasting system (Anderson *et al.*, 2007) has been predicts the monsoon rainfall. They found that this dynamical seasonal forecasting system displays some skill in predicting the monthly–mean precipitation over India after July, but has surprisingly low skill to predict the June precipitation over India. The area around Bangladesh, where a tremendous amount of rainfall occurs in summer, predominantly exhibits sub–monthly–scale intra–seasonal oscillation (ISO), but not 30–60–day ISO (Ohsawa *et al.*, 2000; Murata *et al.*, 2008; Fujinami *et al.*, 2011). The ISO feature allows the sub–monthly–scale ISO to modulate the total seasonal rainfall and the spatial patterns of circulation and convection around Bangladesh.

In the present study the Weather Research and Forecast (WRF–ARW V3.8.1) model has been used to simulate the different heavy rainfall events (4–7 and 15–16 May 2013) in the pre–monsoon (March–May) season over Bangladesh. The objectives of this study are to examine whether the high resolution WRF model is capable of simulating the observed features of heavy rainfall events. In this research four microphysics (MP) schemes and four cumulus parameterization (CP) schemes have been considered to study the rainfall events and try to identify the performance of the MP and CP schemes. The results have been compared with the observed station rainfall of Bangladesh Meteorological Department (BMD). The maximum vertical velocity, reflectivity and relative humidity have also been calculated and analyzed. The model simulated results will be verified by using Threat Score (TS), Equitable Threat Score (ETS), Bias Score (BS) and Standard Deviation (SD).

Chapter II

Review of Literatures

2.1. Rainfall

Rain is a type of precipitation, a product of the condensation of atmospheric water vapour that is deposited on the Earth's surface. It forms when separate drops of water fall to the Earth from clouds. Not all rain reaches the surface; some evaporates while falling through dry air. When none of it reaches the ground, it is called virga, a phenomenon often seen in hot, dry desert regions. Rain plays a role in the hydrologic cycle in which moisture from the oceans evaporates, condenses into drops, precipitates from the sky, and eventually returns to the ocean via rivers and streams to repeat the cycle again. The water vapor from plant respiration also contributes to the moisture in the atmosphere. A major scientific explanation of how rain forms and falls is called the Bergeron process. Rainfall is typically measured using a rain gauge. It is expressed as the depth of water that collects on a flat surface, and is routinely measured with accuracy up to 0.1 mm. Rain gauges are usually placed at a uniform height above the ground, which may vary depending on the country.

Precipitation, especially rain, has a dramatic effect on agriculture. All plants need at least some water to survive; therefore rain is important to agriculture. Plants need varying amounts of rainfall to survive. Agriculture of all nations at least to some extent is dependent on rain. Bangladesh's agriculture, for example, is heavily dependent on the rainfall, especially crops like rice, oilseeds and coarse grains. A delay of a few days in the arrival of the monsoon can, and does, badly affect the economy, as evidenced in the numerous droughts in Bangladesh and India. When classified according to amount of precipitation, rain can be divided into (http://my.athenet.net):

	Types		Rate (mm/hour)
i.	very light rain	when the precipitation rate is	< 0.25
ii.	light rain	when the precipitation rate is between	0.25 – 1
iii.	moderate rain	when the precipitation rate is between	1–4
iv.	heavy rain	when the precipitation rate is between	4–16
v.	very heavy rain	when the precipitation rate is between	16–50
vi.	extreme rain	when the precipitation rate is	> 50

In Bangladesh there are four meteorological seasons, which are a) Pre–monsoon (March to May), b) Southwest Monsoon (June to September), c) Post–monsoon (October to November) and (d) Winter (December to February). These are described below:

2.2 Pre–monsoon Season

Bangladesh has a tropical monsoon climate. During the pre–monsoon season, its climate is characterized by high temperatures and the occurrence of thunderstorms. April is the hottest month. Temperatures of this month range from 27°C along the northeastern foothills to 30°C along the western border. Rainfall from the thunderstorms of this season is copious, varying from 15 cm in the west–central part of the country to more than 80 cm in the northeast. This reflects the effect of orography in the northeastern parts of the country which sets the trigger action for uplift and convectional overturning of the moist air from the Bay of Bengal. The thunderstorm season begins in the northeastern and eastern parts of the country by the first week of March. The thunderstorm activity gradually moves westward, and becomes significant in the western part of the country only before the advent of the summer monsoon in late May or early June. During the early part of the thunderstorm season, a zone of discontinuity crosses the country from southwest to northeast, separating the hot dry air from the dry interior of India, and the warm moist air from the Bay of Bengal. The activity of the thunderstorms during the pre–monsoon season depends upon the supply of moist air from the Bay of Bengal. Since this season is a transitional season between the northerly circulation of winter and southerly circulation of the summer monsoon, the winds from the Bay of Bengal are neither very strong nor continuous.

The hot season from March to May is the traditional period when the winter pattern of pressure and winds gets disturbed prior to the establishment of the summer monsoon and hence, is often referred to as 'pre–monsoon' season. The pre–monsoon hot season is characterized by high temperatures and the occurrence of thunderstorms. April is the hottest month when mean temperatures range from 27°C in the east and south to 31°C in the west–central part of the country. In the western part, summer temperature sometimes reaches up to 40°C. After the month of April, the temperature dampens due to increased cloud cover. The pre–monsoon season is the transition period when the northerly or northwesterly winds of the winter season gradually changes to the southerly or southwesterly winds of the summer monsoon or rainy season (June–September). During the early part of this season, the winds

are neither strong nor persistent. However, with the progression of this season wind speed increases, and the wind direction becomes more persistent.

During the early part of the pre–monsoon season, a narrow zone of air mass discontinuity lies across the country that extends from the southwestern part to the northeastern part. This narrow zone of discontinuity lies between the hot dry airs is coming from the upper Gangetic plain and the warm moist air coming from the Bay of Bengal. As this season progresses, this discontinuity weakens and retreats toward northwest and finally disappears by the end of the season, making room for the onset of the summer monsoon. The rainy season, which coincides with the summer monsoon, is characterized by southerly or southwesterly winds, very high humidity, heavy rainfall, and long consecutive days of rainfall which are separated by short spells of dry days. Rainfall in this season is caused by the tropical depressions that enter the country from the Bay of Bengal. Events and characteristics of pre–monsoon season are discussed in the following sub–sections.

2.2.1 Pre–monsoon Rainfall

The single most dominant element of the climate of Bangladesh is the rainfall. Because of the country's location in the tropical monsoon region, the amount of rainfall is very high. However, there is a distinct seasonal pattern in the annual cycle of rainfall, which is much more pronounced than the annual cycle of temperature. The winter season is very dry, and accounts for only 2–4% of the total annual rainfall. Rainfall during this season varies from less than 2 cm in the west and south to slightly over 4 cm in the northeast. The amount is slightly enhanced in the northeastern part due to the additional uplifting of moist air provided by the Meghalaya Plateau. As the winter season progresses into the pre–monsoon hot season, rainfall increases due to intense surface heat and the influx of moisture from the Bay of Bengal. Rainfall during this season accounts for 10–25% of the total annual rainfall which is caused by the thunderstorms or nor'wester (locally called Kalbaishakhi).

The amount of rainfall in this season varies from about 20 cm in the west central part to slightly over 80 cm in the northeast. The additional uplifting by the Meghalaya Plateau of the moist air causes higher amount of rainfall in the northeast. Rainfall during the rainy season is caused by the tropical depressions that enter the country from the Bay of Bengal. These account for 70% of the annual total in the eastern part, 80% in the southwest, and slightly over 85% in the northwestern part of Bangladesh. The amount of rainfall in this season varies from 100 cm in the west central part to over 200 cm in the south and northeast. Average rainy

days during the season vary from 60 in the west–central part to 95 days in the southeastern and over 100 days in the northeastern part. Geographic distribution of annual rainfall shows a variation from 150 cm in the west–central part of the country to more than 400 cm in the northeastern and southeastern parts. The maximum amount of rainfall has been recorded in the northern part of Sylhet district and in the southeastern part of the country (Cox's Bazar and Bandarban districts).

2.2.2 Pre–monsoon Temperature

January is the coldest month in Bangladesh. However, the cold winter air that moves into the country from the northwestern part of India loses much of its intensity by the time it reaches the northwestern corner of the country. Average temperatures in January vary from about 17°C in the northwestern and northeastern parts to 20–21°C in the coastal areas. In late December and early January, minimum temperature in the extreme northwestern and northeastern parts of the country reaches within 4 to 7 degrees of freezing point. As the winter season progresses into the pre–monsoon hot season, temperature rises, reaching the maximum in April, which is the middle of the pre–monsoon hot season. Average temperatures in April vary from about 27°C in the northeast to 30°C in the extreme west central part of the country. In some places in Rajshahi and Kushtia districts the maximum temperature in summer season rises up to 40°C or more. After April, temperature decreases slightly during the summer months, which coincides with the rainy season. Widespread cloud covers causes dampening of temperature during the later part of the pre–monsoon season. Average temperatures in July vary from about 27°C in the southeast to 29°C in the northwestern part of the country

2.2.3 Pre–monsoon Wind

Western Disturbance is the term used in India, Pakistan, Bangladesh and Nepal to describe an extra tropical storm originating in the Mediterranean that brings sudden winter rain and snow to the northwestern parts of the Indian subcontinent this is a non–monsoonal on pattern driven by the westerlies. The moisture in the Indian subcontinents storms usually originates over the Mediterranean Sea and the Atlantic Ocean. Extra tropical storms are a global, rather than a localized, phenomena with moisture usually carried in the upper atmosphere (unlike tropical storms where it is carried in the lower atmosphere). In the case of the subcontinent, moisture is sometimes shed as rain when the storm system encounters the Himalayas. Western Disturbances are important to the development of the Rabi crop in the northern

subcontinent, which includes the locally important staple wheat. Western Disturbance causes winter and pre monsoon season rainfall across northwest India. Winter months Rainfall has great importance in agriculture, particularly for the Rabi crops. Wheat among them is one of the most important crops, which helps to meet India's food security. During the season, normally 4–5 western disturbances in a month can be seen over northwest India. Some of the western disturbances bring well–distributed and good rainfall, while some pass with negligible rain or sometimes no rain. The Western disturbance affects day–to–day weather of northwest India especially during winter season. It is usually associated with cloudy sky, higher night temperatures, unusual rain etc. Over the Indo–Gangetic plains, it brings cold wave conditions and occasionally dense fog and cold day conditions. These conditions remain stable until it is disturbed by another Western Disturbances.

2.2.4 Thunderstorms/Nor'westers

The regions of high activity for thunderstorms are the northeastern areas of the subcontinent, the Himalayas, east Madhya Pradesh and adjoining areas, south Kerala, northern parts of Pakistan, immediately east of the Aracvalli and the west coast of Sri Lanka. The Andaman Islands and perhaps also the adjoining seas have a high susceptibility to thunderstorms. The smallest frequency is over northern Kashmir, Sind and southeastern Tamil Nadu, the first two being also areas of very low rainfall. The narrow belt of rather few thunderstorms, about 100 km towards the plains from the foot of the Siwaliks, is very interesting. The West Coast between 15^0 and 20^0 N has a relatively smaller number of thunderstorms, in spite of the heavy rainfall. Local orography controls the development of thunderstorms. Northeastern parts of the subcontinent experience severe thunder squalls from March to May called the northeasters or Kalbaishakhi noted for their destructiveness. One or two of them develop into tornadoes every year. The rainfall from March to May is mostly from thundershowers but not so the monsoon rainfall.

Nor'westers are meso–scale severe thunderstorms that occur in Bangladesh during the pre–monsoon season. These are local severe storms. Sometimes tornado cells are embedded in mother thunderstorm cloud. These severe weather events cause fairly widespread destruction of properties and loss of lives throughout Bangladesh. Economic losses are also enormous due to these weather events. Two transition periods between southwest and northeast monsoons over the India–Bangladesh–Pakistan subcontinent are characterized by local severe

storms. In Bangladesh, these transition periods are known as pre–monsoon and post–monsoon seasons. Of these, it is the pre–monsoon season when most of the local severe storms occur over different parts of Bangladesh with frequent intervals. These storms are popularly known as Nor'westers or Kalbaishakhi in Bangladesh, West Bengal and Assam of India and Andhi (dust storms) in North India.

2.2.5 Monsoon Season

Monsoon is traditionally defined as a seasonal reversing wind accompanied by corresponding changes in precipitation but is now used to describe seasonal changes in atmospheric circulation and precipitation associated with the asymmetric heating of land and sea. Usually, the term monsoon is used to refer to the rainy phase of a seasonally changing pattern, although technically there is also a dry phase. Monsoon is a common weather phenomenon in Indian subcontinent. Bangladesh is situated in a very active monsoon region of the world**.** Bangladesh gets much rain during this season. The agro–economic activities of Bangladesh are seriously dependent on monsoon rain. Bangladesh is located over the vast delta of three great rivers, the Ganges, the Brahmaputra and the Meghna (GBM) with total area of about 144,000 sq. kms. The river area is 6.5 % and forest area is 15.6% of the country. The coastal line of the Bay of Bengal is 716 km to the south of the country. It is characterized by very flat plains, which dominate most of the country and never rise more than 10m above sea level. Although there are few mountains higher than 1000 m in the country, the Shillong Plateau of India and Chittagong Hill Tracts of Bangladesh, located near the northeastern and southeastern border with India respectively, have great effects on the amount of rainfall in the adjacent areas. The confluence of many geographical and orographical characteristics makes Bangladesh susceptible to different type of weather hazards.

A monsoon is a seasonal prevailing wind which lasts for several months. The term was first used in English in India, Bangladesh, Pakistan and neighboring countries to refer to the seasonal winds blowing from the Indian Ocean and Arabian Sea in the southwest bringing heavy rainfall to the region. In hydrology, monsoonal rainfall is considered to be that which occurs in any region that receives the majority of its rain during a particular season, and so monsoons are referred to in relation to other regions such as in North America, Sub–Saharan Africa, Brazil and East Asia. The Bay of Bengal (BoB) branch of southwest monsoon flows over the BoB heading towards North–Eastern India (NEI) and Bengal, picking up more moisture from the BoB. Its hits the Eastern Himalaya and provides a huge amount of rain to

the regions of NEI, Bangladesh and West Bengal. Cherrapunji situated on the southern slopes of the astern Himalaya in Shillong, India is one of the wettest places on Earth.

The agriculture of Bangladesh is heavily dependent on the rains, especially crops. A delay of a few days in the arrival of the monsoon can, and does, badly affect the economy, as evidenced in the numerous droughts in Indian subcontinent. The monsoon is widely welcomed and appreciated by city–dwellers as well, for it provides relief from the climax of summer in June. Bangladesh and some regions of Indian like in Assam and places of West Bengal experiences heavy flood, which claims huge number of lives and huge loss of property and causes severe damage to economy. The monsoon area has been defined by Ramage (1971) by the following criteria:

- The prevailing wind direction shifts by at least 120^o between January and July
- The average frequency of prevailing wind directions in January and July exceeds 40 percent.
- The mean resultant wind is at least one of the months exceeding 3 m/sec.
- Less than one cyclone–anticyclone alternation occurs every two years in either month in a 5^o latitude–longitude rectangle.

The monsoon normally reaches the coastal belt of Bangladesh by the last week of May to the first week of June and progressively engulfs the whole country through June. On an average 20–25 rainy days per month during June to August, decreasing to 12–15 days in September. With the advent of the monsoon, the extreme temperatures of summer fall appreciably throughout the country. Although the mean temperature falls hardly by one degree, the maximum temperature falls by 2–5^{o}C over most part of the country except the coastal belts where the fall is by 5–6^{o}C (WMO/UNDP/BGD/79/013, 1986).

2.3 Relative Humidity

Relative humidity is the ratio of the partial pressure of water vapor in the air–water mixture to the saturated vapor pressure of water at those conditions. The relative humidity of air depends not only on temperature but also on pressure of the system of interest. So it is defined as the ratio of the observed vapor pressure to that required for saturation at the same temperature. Designating it as if, we have

$$f = \frac{\omega}{\omega_s} \times 100 = \frac{\rho_w}{\rho_{ws}} \times 100 = \frac{q}{q_s} \times 100 = \frac{e}{e_s} \times 100$$

The multiplication by 100 being for the purpose of expressing it as a percentage

The relative humidity is a measure of the amount of water vapor in the air (at a specific temperature) compared to the maximum amount of water vapor air could hold at that temperature, and is given as a percentage value. Relative humidity depends on the temperature of the air, as warm air can hold more moisture than cold air. A relative humidity of 100 percent indicates that the air is holding all the water it can at the current temperature and any additional moisture at that point will result in condensation. A relative humidity of 50 percent means the air is holding half the amount of moisture that it could. As the temperature decreases, the amount of moisture in the air doesn't change, but the relative humidity goes up (since the maximum amount of moisture that cooler air can hold is smaller). When referring to pet care, the terms humidity and relative humidity are usually used interchangeably. For an example, if we say the appropriate humidity for hermit crabs is 70–80 percent, we are speaking of the relative humidity.

In order for cloud formation and rain to occur, the air where the clouds are forming (or from which the rain originates) must reach 100% relative humidity. Often, rain will fall from air at 100% relative humidity to air where humidity is less than 100% (most people with instruments to measure air humidity are measuring the humidity of this "lower" air, which will likely range from 60–100% humidity during a rainstorm). As the rain falls, this means that some of the rain will evaporate into the water of lesser humidity. The air at lower elevations will not usually reach 100% humidity as a result of this, however. When the air reaches this point, it will feel very wet because the air is completely saturated. It will be foggy and perhaps a bit misty and drizzly, but it takes more than air saturation for rain. For rainfall to begin, the raindrops must be heavier than the surrounding air. Sometimes, there may be 100% humidity, but the raindrops are not large enough to fall...that's why not all clouds create rain. As an interesting side note, most rain actually begins with ice crystals in clouds which draw moisture and then fall when they are sufficiently large.

100% humidity means complete saturation, but rain is usually caused by the air being over saturated by temperature or pressure changes. When it rains, it is common to report the humidity at 100%, but that is just because the rain is the result of the atmosphere shedding the water vapor it can no longer hold so it can remain at 100% humidity. 100% can result in rain, but rain normally results when the atmosphere becomes over saturated with water vapor. 100% humidity is when the atmosphere is holding the maximum amount of water it can. At

this point, fog and dew start to form. If that air were too cool further, then it could not hold that moisture in vapor, and it would precipitate out as rain. The faster the drop in temperature, the harder it will rain. Also think about different layers in the atmosphere. A warm moist air mass can rise, cool, and expand which can raise its humidity past the saturation point. That rain could fall into warmer air and be absorbed back into the air before it hits the ground since that air has not been saturated yet.

2.4 Vorticity

The vorticity is the microscopic measurement of the rotation of a small air parcel. Air parcel has vorticity when the parcel spins as it moves along its path. Although the axis of the rotation can extend in any direction, meteorologists are primarily concerned with the rotational motion about an axis that is perpendicular to the earth's surface. If it does not spin, it is said to have zero vorticity. In the Northern Hemisphere, the vorticity is positive when the parcel has a counterclockwise or cyclonic rotation. It is negative when the parcel has clockwise or anti cyclonic rotation. For turning of the atmosphere, vorticity may be imbedded in the total flow and not readily identified by a flow pattern. The rotation of the Earth imparts vorticity to the atmosphere; absolute vorticity is the combined vorticity due to this rotation and vorticity due to circulation relative to the Earth (relative vorticity). The negative vorticity is caused by anti cyclonic turning; it is associated with downward motion of the air. The positive vorticity is caused by cyclonic turning; it is associated with upward motion of the air. Also the relative vorticity is the air relative to the Earth, disregarding the component of vorticity resulting from Earth's rotation.

The absolute vorticity ω_a is given by the curl of the absolute velocity, while the relative vorticity ω is given by the curl of the relative velocity:

$$\omega_a \equiv \overline{\nabla} \times \overline{V}_a \qquad\qquad \omega \equiv \overline{\nabla} \times \overline{V}$$

In meteorology the general concerned only with the vertical components of absolute and relative vorticity:

$$\eta = \hat{k}.\left(\overline{\nabla} \times \overline{V}_a\right), \quad \zeta = \hat{k}.\left(\overline{\nabla} \times \overline{V}\right)$$

In particular, the vertical component of relative vorticity ζ is highly correlated with synoptic scale weather disturbances. Large positive ζ tends to occur in association with

cyclonic storms in the Northern Hemisphere. Furthermore, η tends to be conserved following the motion in the middle troposphere. Thus, analysis of the η field and its evolution due to advection forms the basis for the simplest dynamical forecast scheme.

2.5 Weather Research & Forecasting Model

The Weather Research and Forecasting (WRF) Model is a next–generation mesoscale numerical weather prediction system designed to serve both atmospheric research and operational forecasting needs. It features two dynamical cores, a data assimilation system, and a software architecture facilitating parallel computation and system extensibility. The model serves a wide range of meteorological applications across scales from tens of meters to thousands of kilometers. The effort to develop WRF began in the latter part of the 1990's and was a collaborative partnership principally among the National Center for Atmospheric Research (NCAR), the National Oceanic and Atmospheric Administration represented by the National Centers for Environmental Prediction (NCEP) and the Forecast Systems Laboratory (FSL) the Air Force Weather Agency (AFWA), the Naval Research Laboratory, the University of Oklahoma, and the Federal Aviation Administration (FAA). WRF offers two dynamical solvers for its computation of the atmospheric governing equations, and the variants of the model are known as WRF–ARW and WRF–NMM. The Advanced Research WRF (ARW) is supported to the community by the NCAR Mesoscale and Micro scale Meteorology Division. The WRF–NMM solver variant was based on the Eta Model, and later Non hydrostatic Mesoscale Model, developed at NCEP. The WRF–NMM is supported to the community by the Developmental Test bed Center.

2.5.1 Microphysics Schemes in WRF–ARW Model

Microphysics includes explicitly resolved water vapor, cloud, and precipitation processes. The model is general enough to accommodate any number of mixing ratio variables, and other quantities such as number concentrations. Four–dimensional arrays with three spatial indices and one species index are used to carry such scalars. Memory, i.e., the size of the fourth dimension in these arrays, is allocated depending on the needs of the scheme chosen, and advection of the species also applies to all these required by the microphysics options. In the current version of the ARW, microphysics is carried out at the end of the time step as an adjustment process, and so does not provide tendencies. The rationale for this is that condensation adjustment should be at the end of the time step to guarantee that the final saturation balance is accurate for the updated temperature and moisture. However, it is also

important to have the latent heating forcing for potential temperature during the dynamical sub–steps, and this is done by saving the microphysical heating as an approximation for the next time step.

Currently, the sedimentation process is accounted for inside the individual microphysics modules, and, to prevent instability in the calculation of the vertical flux of precipitation, a smaller time step is allowed. The saturation adjustment is also included inside microphysics. In the future, however, it might be separated into an individual subroutine to enable the remaining microphysics to be called less frequently than the model's advection step for efficiency.

2.5.1.1 Lin *et al.* Scheme

A sophisticated scheme that has ice, snow and graupel processes, suitable for real–data high–resolution simulations. Lin *et al.* (1983) scheme includes six classes of hydrometeors are included: water vapor, cloud water, rain water, cloud ice, snow, and graupel. All parameterization production terms are based on Lin *et al*. (1983). This is a relatively sophisticated microphysics scheme in WRF, and it is more suitable for use in research studies. The scheme is taken from Purdue cloud model and the details can be found in Chen and Sun (2002) 2–D microphysics scheme. This is one of the first schemes to parameterize snow, graupel, and mixed–phase processes. It has been used extensively in research studies and in mesoscale NWP Model. The scheme includes ice sedimentation and time–split fall terms.

2.5.1.2 WRF Single Moment 6–Class (WSM6) Scheme

The WRF–single–moment–6–class (WSM6) microphysics scheme has been one of the options of microphysical process in the WRF model since August 2004. This scheme predicts the mixing ratios for water vapor, cloud water, cloud ice, snow, rain, and graupel. The characteristics of the cold rain process in the WSM6 scheme follow the revised ice microphysics process (Hong *et al.*, 2004), whereas the warm rain processes are primarily based on the works of Lin *et al.* (1983) and the auto conversion process from Tripoli and Cotton (1980). The daily forecasts at NCAR have shown that the WSM6 scheme works successfully in predicting mesoscale convective systems, but it sometimes overestimates the peak intensity and underestimates the areas of anvil clouds. We attempt to improve such existing deficiencies in the WSM6 scheme by incorporating the prediction of number concentrations for warm rain species. This new method uses a large eddy simulation (LES)–

based approach (Khairoutdinov and Kogan, 2000) to determine the auto conversion rates and allow for a more sophisticated coupling between cloud field and number concentrations of warm species. Double–moment prediction for the warm species in WSM6 scheme will allow more flexibility of the size distribution enabling the mean diameter to evolve in contrast to the one–moment scheme.

WSM6 scheme includes vapor, rain, snow, cloud ice, cloud water and graupel in six different arrays. A new method for representing mixed–phase particle fall speeds for the snow and graupel by assigning a single fall speed to both that is weighted by the mixing ratios, and applying that fall speed to both sedimentation and accumulation processes is introduced. Of the three WSM schemes, the WSM6 scheme is the most suitable for cloud–resolving grids, considering the efficiency and theoretical backgrounds. A new method for representing mixed–phase particle fall speeds for the snow and a scheme with ice, snow and graupel processes suitable for high–resolution simulations. The WSM6 scheme has been developed by adding additional process related to graupel to the WSM5 scheme (Hong and Lim, 2006).

2.5.1.3 Thompson Scheme

The Thompson microphysics scheme is a sophisticated microphysics scheme in the Weather Research and Forecasting (WRF) model. The scheme is very suitable for massively parallel computation as there are no interactions among horizontal grid points. Compared to the earlier microphysics schemes, the Thompson scheme incorporates a large number of improvements. Intel Many Integrated Core (MIC) ushers in a new era of supercomputing speed, performance, and compatibility. It allows the developers to run code at trillions of calculations per second using the familiar programming model. Thus, the development environment is familiar one to a vast number of CPU developers.

A bulk microphysical parameterization (BMP) developed for use with WRF or other mesoscale models. The snow size distribution depends on both ice water content and temperature and is represented as a sum of exponential and gamma distributions. Furthermore, snow assumes a non–spherical shape with a bulk density that varies inversely with diameter as found in observations. A new scheme with ice, snow and graupel processes suitable for high–resolution simulations. This adds rain number concentration and updates the scheme from the one in Version 3.0 New Thompson *et al.* scheme in V3.1. Replacement of Thompson *et al.*, (2007) scheme that was option 8 in V3.0 6–class microphysics with graupel, ice and rain number concentrations also predicted.

2.5.1.4 WRF Double–Moment 6–class (WDM6) Scheme

The WRF double–moment 6–class microphysics scheme (WDM6) implements a double–moment bulk micro physical parameterization of clouds and precipitation and is applicable in mesoscale and general circulation models. The WDM6 scheme enables the investigation of the aerosol effects on cloud properties and precipitation processes with the prognostic variables of cloud condensation nuclei (CCN), cloud water and rain number concentrations. WDM6 extends the WRF single–moment 6–class microphysics scheme (WSM6) by incorporating the number concentrations for cloud and rainwater along with a prognostic variable of CCN number concentration. Moreover, it predicts the mixing ratios of six water species (water vapor, cloud droplets, cloud ice, snow, rain, and graupel), similar to WSM6. Prognostic water substance variables include water vapor, clouds, rain, ice, snow, and graupel for both the WDM6 and WSM6 schemes. Additionally, the prognostic number concentrations of cloud and rain waters, together with the CCN, are considered in the WDM6 scheme. The number concentrations of ice species such as graupel, snow, and ice are diagnosed following the ice–phase microphysics of Hong *et al*. (2004).

2.5.2 Cumulus Parameterization Schemes

These schemes are responsible for the sub–grid–scale effects of convective and/or shallow clouds. The schemes are intended to represent vertical fluxes due to unresolved up drafts and down drafts and compensating motion outside the clouds. They operate only on individual columns where the scheme is triggered and provide vertical heating and moistening profiles. Some schemes provide cloud and precipitation field tendencies in the column, and future schemes may provide momentum tendencies due to convective transport of momentum. The schemes all provide the convective component of surface rainfall. Cumulus parameterizations are theoretically only valid for coarser grid sizes, (e.g., > 10 km), where they necessary to properly release latent heat on a realistic time scale in the convective columns. Where the assumptions about the convective eddies being entirely sub–grid–scale break down for finer grid sizes, sometimes these schemes have been found to be helpful in triggering convection in 5–10 km grid applications. Generally they should not be used when the model can resolve the convective eddies itself.

One of the main options which could potentially affect precipitation severely is the cumulus parameterization. It accounts for unresolved cloud formation. Depending on the grid resolution, convective clouds could be resolved by the explicit scheme, but with the

resolution used here (15 km) it still seems necessary to take into account the unresolved scales. The feedback from these parameterizations to the larger–scale equations of the model is the profile of latent heat release and moistening caused by convection. Two different schemes were used. Even though the efficiency of a given parameterization depends on the concrete event, other cumulus parameterizations have been proved to have less accuracy, e.g. the Anthes–Kuo (Ferretti *et al*., 2000) or Betts–Miller schemes. The KF scheme has demonstrated good performance on several situations and regions (Wang and Seaman, 1997; Kotroni and Lagouvardos, 2001). In the study by Ferretti *et al*. (2000) in the Alpine region, the Grell scheme was better than the KF scheme for some concrete events.

These schemes are responsible for the sub–grid–scale effects of convective and shallow clouds. The schemes are intended to represent vertical fluxes due to unresolved updrafts and downdrafts and compensating motion outside the clouds. The cumulus parameterization are theoretically only valid for coarser grid sizes, (e.g., > 10km), where they are necessary to properly release latent heat on a realistic time scale in the convective columns.

2.5.2.1 K**ain–Fritsch (KF) Scheme**

In the KF scheme the condensates in the updraft are converted into precipitation when their amount exceeds threshold value. In this scheme the convection consumes the convective available potential energy in a certain time scale. The KF scheme also includes the shallow convection other than deep convection. The shallow convection creates non–perceptible condensates and the shallowness of the convection is determined by a vertical extent of the cloud layer that is known by a function of temperature at LCL of rising air parcel. The KF scheme was derived from the Fritsch–Chappell, and its fundamental framework and closure assumptions are described by Fritsch and Chappell (1980). Kain–Fritsch (1990) modified the updraft model in the scheme and later introduced numerous other changes, so that it eventually became distinctly different from the Fritsch–Chappell scheme. It was distinguished from its parent algorithm by referring to the more elaborate code as the KF scheme, beginning in the early 1990s. This is also deep and shallow convection sub–grid scheme using a mass flux approach with downdrafts and convective available potential energy (CAPE) removal time scale. Updraft generates condensate and dump condensate into environment downdraft evaporates condensate at a rate that depends on RH and depth of downdraft leftover condensate accumulates at surface as precipitation.

2.5.2.2 Tiedtke Scheme

The Tiedtke scheme considers a population of clouds where the cloud ensemble is described by a one dimensional bulk model as earlier applied by Yanai *et al.* in a diagnostic study of tropical convection. Cumulus scale downdrafts are included. Various types of convection are represented, i.e., penetrative convection in connection with large–scale convergent flow, shallow convection in suppressed conditions like trade wind cumuli and midlevel convection like extra–tropical organized convection associated with potentially unstable air above the boundary layer and large–scale ascent. The closure assumptions for determining the bulk cloud mass flux are: penetrative convection and midlevel convection are maintained by large–scale moisture convergence and shallow convection by supply of moisture due to surface evaporation. In the Tiedtke scheme, convection is triggered if the parcel's temperature exceeds the environment temperature by a fixed temperature threshold of 0.50 K. This scheme performs well with 0.25 deg. grid resolution. The parameterization produces realistic fields of convective heating and appears to be in fair balance with real data for Numerical Weather Prediction (NWP) as it does not initiate strong adjustment processes (spin–up) in global form.

2.5.2.3 Zhang–McFarlane Scheme

The Zhang–McFarlane scheme is a simplified cumulus parameterization scheme, suitable for use in the general circulation models (GCMs). This parameterization is based on a plume ensemble concept similar to that originally proposed by Arakawa and Schubert (1974). However, it employs three assumptions which significantly simplify the formulation and implementation of the scheme. The first assumption is that an ensemble of convective–scale updrafts with associated saturated downdrafts may exist when the atmosphere is locally conditionally unstable in the lower troposphere. However, the updraft ensemble is comprised only of those plumes which are sufficiently buoyant to penetrate through this unstable layer. The second assumption is that all such plumes have the same upward mass flux at the base of the convective layer. The third assumption is that moist convection, which occurs only when there is CAPE for reversible ascent of an undiluted parcel from the sub–cloud layer, acts to remove CAPE at an exponential rate with a specified adjustment time scale. The performance of the scheme and its sensitivity to choices of disposable parameters is illustrated by presenting results from a series of idealized single–column model tests. These tests demonstrate that the scheme permits establishment of quasi–equilibrium between large–scale

forcing and convective response. However, it is also shown that the strength of convective downdrafts is an important factor in determining the nature of the equilibrium state. Relatively strong down–drafts give rise to an unsteady irregularly fluctuating state characterized by alternate periods of deep and shallow convection. The effect of using the scheme for GCM climate simulations is illustrated by presenting selected results of a multi–year simulation carried out with the Canadian Climate Centre GCM using the new parameterization. Comparison of these results with those for a climate simulation made with the standard model (McFarlane *et al.*, 1992) reveals the importance of other parameterized processes in determining the ultimate effect of introducing the new convective scheme. The radiative response to changes in the cloudiness regime is particularly important in this regard.

2.5.2.4 Multi–Scale Kain–Fritsch (MSKF) Scheme

The MSKF scheme is a mass flux parameterization. It uses the Lagrangian parcel method (e.g., Simpson and Wiggert 1969; Kreitzberg and Perkey 1976), including vertical momentum dynamics (Donner 1993), to estimate whether instability exists, whether any existing instability will become available for cloud growth, and what the properties of any convective clouds might be. Numerous modifications to the Kain–Fritsch convective parameterization have been implemented over the last decade. Most modifications were inspired by feedback from users of the scheme (primarily numerical modelers) and interpreters of the model output (mainly operational forecasters). The specific formulation of the modifications evolved from an effort to produce desired effects in numerical weather prediction while also rendering the scheme more faithful to observations and cloud–resolving modeling studies. The main task of the scheme is to identify potential source layers for convective clouds, that is, updraft source layers (USLs). Beginning at the surface, vertically adjacent layers in the host model are mixed until the depth of the mixture is at least 60 hPa. This combination of adjacent model layers composes the first potential USL. Convective downdrafts are fueled by evaporation of condensate that is generated within the updraft. A fraction of this total condensate is made available for evaporation within the downdraft, based on empirical formulas for precipitation efficiency as a function of vertical wind shear and cloud–base height (Zhang and Fritsch 1986). The method by which the MSKF scheme satisfies its closure assumptions is described in Bechtold *et al.* (2001). In fundamental terms, the MSKF scheme rearranges mass in a column using the updraft, downdraft, and environmental mass fluxes until at least 90% of the CAPE is removed.

2.6 Planetary Boundary Layer (PBL) Parameterizations

The PBL is the layer in the lower part of the troposphere with thickness ranging from a few hundred meters to a few kilometers within which the effects of the Earth's surface are felt by the atmosphere. The PBL processes represent a consequence of interaction between the lowest layer of air and the underlying surface. The interactions can significant impact on the dynamics of the upper air flows. The influences of the small–scale eddy on large scale atmospheric circulations may be included in the model equations. Accurate depiction of meteorological conditions, especially within the PBL, is important for air pollution modeling, and PBL parameterization schemes play a critical role in simulating the boundary layer. It is a very important portion of the atmosphere to correctly model to provide accurate forecasts, e.g., air pollution forecasts (Deardorff 1972; Pleim 2007). As important as the PBL is, it has one basic property whose accurate and realistic prediction is paramount to its correct modeling: its height. After all, the height of the top of the PBL defines its upper boundary. This is critical since PBL parameterizations schemes in WRF–ARW models need to know the extent through which to mix properties such as heavy rainfall, relative humidity, outgoing long wave flux, downward long wave flux. PBL schemes were developed to help resolve the turbulent fluxes of heat, moisture, and momentum in the boundary layer. Another important issue is the interaction between the atmosphere and the surface. The PBL schemes handle the latent and sensible heat fluxes into the atmosphere, the frictional effects with the surface and the strong sub–grid–scale mixing which takes place in the lower levels due to these processes.

2.6.1 Yonsei University (YSU) Scheme

The YSU is the next generation of the Medium Range Forecast (MRF), Non local–K scheme with explicit entrainment layer and parabolic K profile in unstable mixed layer. The YSU scheme is a bulk scheme that expresses non–local mixing by convective large eddies. Non–local mixing is achieved by adding a non–local gradient adjustment term to the local gradient. At the top of the PBL, the YSU scheme uses explicit treatment of the entrainment layer, which is proportional to the surface layer flux (Shin and Hong, 2011; Hong *et al*., 2006).

2.7 Map Projection

Commonly, a map projection is a systematic transformation of the latitudes and longitudes of locations on the surface of a sphere or an ellipsoid into locations on a plane. Map projections are necessary for creating maps. All map projections distort the surface in some fashion.

Depending on the purpose of the map, some distortions are acceptable and others are not; therefore, different map projections exist in order to preserve some properties of the sphere–like body at the expense of other properties. There is no limit to the number of possible map projections. More generally, the surfaces of planetary bodies can be mapped even if they are too irregular to be modeled well with a sphere or ellipsoid. Even more generally, projections are the subject of several pure mathematical fields, including differential geometry and projective geometry. However, map projection refers specifically to a cartographic projection.

2.7.1 Mercator Projection

The Mercator projection is a cylindrical map projection presented by the Flemish geographer and cartographer Gerardus Mercator in 1569. It became the standard map projection for nautical purposes because of its ability to represent lines of constant course, known as rhumb lines loxodromes, as straight segments which conserve the angles with the meridians. While the linear scale is equal in all directions around any point, thus preserving the angles and the shapes of small objects, the Mercator projection distorts the size and shape of large objects, as the scale increases from the Equator to the poles, where it becomes infinite. Although the Mercator projection is still used commonly for navigation, due to its unique properties, cartographers agree that it is not suited to general reference world maps due to its distortion of land area. Mercator himself used the equal–area sinusoidal projection to show relative areas. As a result of these criticisms, modern atlases no longer use the Mercator projection for world maps or for areas distant from the equator, preferring other cylindrical projection or forms of equal–area projection. The Mercator projection is still commonly used for areas near the equator, however, where distortion is minimal.

2.7.2 Lambert Projection

A Lambert conformal conic projection (LCC) is a conic map projection used for aeronautical charts, portions of the State Plane Coordinate System (SPCS), and many national and regional mapping systems. It is one of seven projections introduced by Lambert (1772). This projection is one of the best for middle latitudes. It is similar to the Albers conic equal area projection except that Lambert conformal conic portrays shape more accurately than area. The SPCS uses this projection for all zones that have a greater east–west extent. Conceptually, the projection seats a cone over the sphere of the Earth and projects the surface conformally onto the cone. The cone is unrolled, and the parallel that was touching the sphere is assigned unit scale. That parallel is called the reference parallel or standard parallel.

By scaling the resulting map, two parallels can be assigned unit scale, with scale decreasing between the two parallels and increasing outside them. This gives the map two standard parallels. In this way, deviation from unit scale can be minimized within a region of interest that lies largely between the two standard parallels. Unlike other conic projections, no true secant form of the projection exists because using a secant cone does not yield the same scale along both standard parallels.

Pilots use aeronautical charts based on LCC because a straight line drawn on a Lambert conformal conic projection approximates a great–circle route between endpoints for typical flight distances. The US systems of VFR (visual flight rules) sectional charts and terminal area charts are drafted on the LCC with standard parallels at 33°N and 45°N.

2.8 Arakawa Staggered C–grids

The Arakawa grid system depicts different ways to represent and compute orthogonal physical quantities on rectangular grids used for Earth system models for meteorology and oceanography. For example, the Weather Research and Forecasting Model use the Arakawa Staggered C–Grid in its atmospheric calculations when using the ARW core. The staggered Arakawa C–grid further separates evaluation of vector quantities compared to the Arakawa B–grid e.g., instead of evaluating both east–west (u) and north–south (v) velocity components at the grid center, one might evaluate the u components at the centers of the left and right grid faces, and the v components at the centers of the upper and lower grid faces.

2.9 Atmospheric Radiation

The radiation schemes provide atmospheric heating due to radiative flux divergence and surface downward long–wave and shortwave radiation for the ground heat budget. Long–wave radiation includes infrared or thermal radiation absorbed and emitted by gases and surfaces. Upward long wave radiative flux from the ground is determined by the surface emissivity that in turn depends upon land–use type, as well as the ground (skin) temperature. Shortwave radiation includes visible and surrounding wavelengths that make up the solar spectrum. Hence, the only source is the sun, but processes include absorption, reflection and scattering in the atmosphere and its surfaces. For shortwave radiation, the upward flux is the reflection due to surface albedo. Within the atmosphere the radiation responds to model predicted cloud and water vapor distributions, as well as specified carbon dioxide, and (optionally) tracer gas concentrations. All the radiation schemes in WRF currently are column (one–dimensional) schemes, so each column is treated independently, and the fluxes

correspond to those in infinite horizontally uniform planes, which is a approximation if the vertical thickness of the model layers is much less than the horizontal grid length. This assumption would become less accurate at high horizontal resolution.

2.9.1 Outgoing Long Wave Radiation (OLR)

The Earth Radiation budget is made up of the incoming solar flux and the outgoing Top–of–the–Atmosphere (TOA) radiative fluxes. The outgoing radiative fluxes consist of the reflected part of the incoming solar flux, as well as the thermal flux emitted by the Earth–atmosphere system. The thermal flux is often referred to as OLR. The OLR is a very important parameter for the Earth's radiation budget study as well as for weather/climate model validation purposes. Variations in the OLR reflect the response of the Earth–atmosphere system to solar diurnal forcing. Those variations can be found in particular in surface temperature, cloud cover, cloud top height, and related quantities like precipitation. The OLR is therefore well suited for validation of GCMs simulating the diurnal cycle, as it constitutes the combination of different model aspects. The OLR can be directly estimated from broadband radiance measurements by a satellite instrument such as the GERB. Alternatively, the OLR can be indirectly inferred from narrowband radiance observations. The SEVIRI OLR is obtained from the IR and WV radiance and the satellite viewing angle via a regression scheme. The OLR is currently not operationally derived – the show results are the outcome of a feasibility study. This product is a candidate product for a future reprocessing facility within EUMETSAT to support the derivation of climate–relevant parameters.

2.9.2 Downward Long Wave Radiation

The downward long wave radiation is mostly from the atmosphere. It depends on the temperature and moisture of the atmosphere. The water vapor and other gases, aerosols absorb some solar energy and emit some long wave radiation energy computation of downward long wave radiation from the atmosphere is difficult, even when the distributions of water vapor, carbon dioxide, cloudiness, and temperature are measured. Some satellite measurements like TOVS estimates downward long wave radiation. Little long wave radiation is reflected by the surface: natural surface emission is dominant. It is also difficult to measure and define the surface temperature especially vegetation surface. To combine the above four components makes the calculation of net radiation at the surface. This is not accurate because the errors in each accumulate. So it is developed the research to use some satellite measurements–NOAA, GOES etc.

Chapter III
Model Description and Methodology

3.1 Model Setup

In the present study the Weather Research and Forecast (WRF–ARW Version 3.8.1) model have been used to simulate the pre–monsoon rainfall over Bangladesh. Advance Research WRF (ARW) is a dynamic solver (Skamarock *et al.,* 2005), which is compatible with WRF system to simulate broad spectrum of meteorological phenomena. Weather Research and Forecast model consists of fully compressible non–hydrostatic equations and different prognostic variables. The model vertical coordinate is terrain following hydrostatic pressure and the horizontal grid is Arakawa C–grid staggering. The model has different MP and CP schemes options but in this research we have been used four different microphysics and four cumulus parameterization schemes for the simulation of heavy rainfall events in the pre–monsoon season. The four different MPs are Lin *et al.*, WSM6, Thompson and WDM6 schemes and the four different CPs are KF, Tiedtke, ZM and MSKF schemes. The Lin *et al.* scheme contains prognostic equations for cloud water, rainwater, cloud ice, snow, and graupel mixing ratio, WSM6 for cloud water, rainwater, cloud ice, snow, and graupel mixing ratio, Thompson for cloud water, rainwater, cloud ice, snow, and graupel mixing ratio and WDM6 for cloud water, rainwater, cloud ice, snow, and graupel mixing ratio. The KF scheme includes convective available potential energy and shallow convection, Tiedtke includes cumulus scale downdrafts and various types of convection, i.e., penetrative convection in connection with large–scale convergent flow, shallow convection in suppressed conditions like trade wind cumuli and midlevel convection like extra–tropical organized convection associated with potentially unstable air above the boundary layer and large–scale ascent, ZM includes convective–scale updrafts with associated saturated downdrafts, the same upward mass flux and moist convection and MSKF includes the updraft, downdraft, and environmental mass fluxes until at least 90% of the CAPE is removed. The model has integrated by using initial and lateral boundary conditions (LBCs) from NCEP–FNL analysis at six hourly intervals. Surface layer is treated using Monin–Obukhov and PBL is treated with YSU. Dudhia (1989) scheme has been used for short wave radiation and Rapid Radiative Transfer Model (RRTM) for long wave (Mlawer *et al.* 1997).

Table 3.1: WRF Model and Domain Configurations

Dynamics	Non–hydrostatic
Number of domain	1
Central points of the domain	Central Lat.: 22.80°N, Central Lon.: 90.70°E
Horizontal grid distance	6 km
Integration time step	30 s
Number of grid points	X–direction 161 points, Y–direction 183 points
Map projection	Mercator
Horizontal grid distribution	Arakawa C–grid
Nesting	One way
Vertical co–ordinate	Terrain–following hydrostatic–pressure co–ordinate (30 sigma levels up to 100 hPa)
Time integration	3rd order Runge–Kutta
Spatial differencing scheme	6th order centered differencing
Initial conditions	Three–dimensional real–data (FNL: 1° × 1°)
Lateral boundary condition	Specified options for real–data
Top boundary condition	Gravity wave absorbing (diffusion or Rayleigh damping)
Bottom boundary condition	Physical or free–slip
Diffusion and Damping	Simple Diffusion
Microphysics	(1) Lin *et al*. Scheme (2) WSM6 Scheme (3) Thomson Scheme (4) WDM6 Scheme
Radiation scheme	Dudhia (1989) for short wave radiation/ RRTM long wave Mlawer *et al.* (1997)
Surface layer	Monin–Obukhov similarity theory scheme (Hong and Pan, 1996)
Land surface parameterization	5 Layer Thermal diffusion scheme (Ek *et al*., 2003)
Cumulus parameterization schemes	(1) Kain–Fritsch (KF) Scheme (2) Tiedtke Scheme (3) Zhang–McFarlane (ZM) Scheme (4) Multi–scale Kain–Fritsch (MSKF) scheme
PBL parameterization	Yonsei University Scheme (YSU) (Hong *et al*., 2006)

3.2 Model Domain and Configuration

The model has been configured in single domain, 6 km horizontal grid spacing with 161×183 grids in the east–west and north–south directions and 30 vertical levels. Time step of integration is set to 30 seconds for maintaining computational stability as the model uses third–order Runge–Kutta time integration scheme. The model domain is given in Figure 3.1. The detail of the model and domain configuration is given in Table 3.1:

Figure 3.1: WRF Model Domain for the prediction of heavy rainfall in Bangladesh

3.3 Data and Methodology

Final Reanalysis (FNL) data (1^{o}x1^{o}) collected from National Centre for Environment Prediction (NCEP) is used as initial and lateral boundary Conditions (LBCs) which is updated at six hours interval i.e. the model is initialized with 0000, 0600, 1200 and 1800 UTC initial field of corresponding date. The NCEP FNL data will be interpolated to the model horizontal and vertical grids. There are many MP and CP schemes in WRF–ARW Model.

Table 3.2: Heavy rainfall events and their observed rainfall in the S–SE region of Bangladesh

Events	Heavy Rainfall observed at different stations				
4, 6 & 7 May 2013	Chittagong–209	Hatiya–210	Kutubdia–279	Rangamati–287	Sandwip–217
15–16 May 2013	Barisal–210	Bhola–121	Khepupara–290	Madaripur–129	Patuakhali–246

In this research we have used four different MP schemes and four different cumulus

parameterization schemes. There is limited number of meteorological observation stations in the northeastern and southwestern regions of Bangladesh. For this reason we have added 8 more points in the Bangladesh to see the exact rainfall pattern on Bangladesh Map. There are extracted convective and non–convective rainfall data from WRF Model output at 33 BMD station points with additional 8 points in the northeastern and southwestern regions of Bangladesh. From WRF Model run we made 3 hourly outputs during the study period. This 3 hourly rainfall data converted into daily rainfall data of 4, 6 and 7 May and 15–16 May 2013. For collecting 24, 48 and 72 hour model rainfall data the WRF model has been run with those days with initial condition starting from 0000 UTC of 4 to 0000 UTC of 7 May 2013, 0000 UTC of 15 May to 0000 UTC of 16 May 2013. The model is generated 24 hours as day 1 of model run, 48 hours as day 2 of model run and 72 hours as day 3 of model run. In this research we have calculated total rain on the basis of convective and non-convective rain. The convective and non-convective rains appear directly from the WRF-ARW model output. Txt format data from ctl file of WRF model output has been found using Grid Analysis and Display System (GrADS). These txt data have been converted into Microsoft Excel format and then plotted using SURFER Software. The daily rainfall data of three different rain periods have been plotted of May using 24, 48 and 72–hour lead time prediction for 2013. There is analyzed area average rainfall in the heavy rainfall occurred regions for three events. There is also calculated maximum vertical velocity from the model output, which indicates the maximum convection. Along with maximum vertical velocity, Reflectivity, Relative Humidity and Vorticity have also been calculated. The model simulated results are verified by using four verification methods, i.e., Threat Score (TS), Equitable Threat Score (ETS), Bias Score (BS) and Standard Deviation (SD).

3.4 Verification Methods

The quantitative precipitation forecasts (QPFs) and their improvements on a wide time–scale range, from hours to seasonal, are under heavy and constant demand from the general public and governments around the world (Fritsch and Carbone 2004). The verification of model QPFs is a key factor and the basis for improvement within this process (Olson *et al.* 1995). Thus, it is essential for the verification methods to reflect the model skill on QPFs as accurately as possible, especially for heavy rainfall on short time scales (within a few days) due to its hazardous nature. The most widely used objective verification methods for model QPFs are the threat score (TS), equitable threat score (ETS), and bias score (BS) (Wilks 1995; Ebert *et al.* 2003; Mason 2003).

The schematic of the model QPF verification at any specified threshold for a given accumulation time period in an area is shown in Figure 3.2. The observed rainfall area exceeding the threshold (dotted oval) is labeled O and the model forecast area (gray oval) has labeled F. The intersection of O and F is the hit area H, and the entire verification domain is N. The area of (O–H) is misses (occurred but not predicted), (F–H) is false alarms (predicted but did not happen) and [N–(F+O–H)] is correct negatives (correctly predicted to not occur). The dashed box (denoted by N_s) marks the conditions for a small verification area. The areas used here are calculated by their latitude–longitude. The area of a latitude–longitude rectangle is proportional to the difference in the longitudes. The area enclosed by latitude–longitude is given by the following formula,

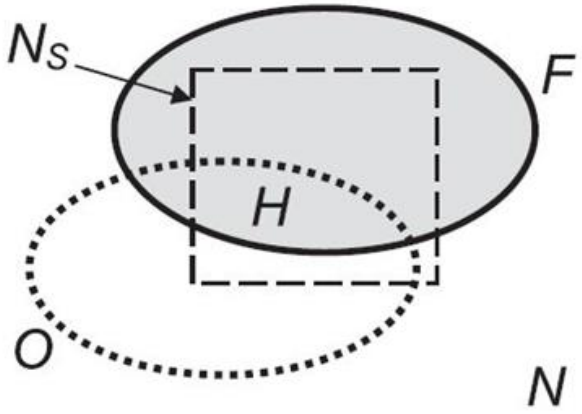

Figure 3.2: Schematic of the model QPF verification

$$A = \frac{2 \times \pi \times \mathrm{R}^2 |\sin(\mathrm{lat1}) - \sin(\mathrm{lat2})||\mathrm{lon1} - \mathrm{lon2}|}{360}$$

$$= \left(\frac{\pi \times \mathrm{R}^2}{180}\right) |\sin(\mathrm{lat1}) - \sin(\mathrm{lat2})||\mathrm{lon1} - \mathrm{lon2}| \qquad (1)$$

Where, R is defined as the radius of the earth having value of 6400 km.

We can define from Figure 3.2 at any given rainfall threshold over an accumulation period, the observed rain area exceeding the criterion is O and the model–predicted area is F. Their intersection (i.e., the hit area) is denoted by H, while the entire verification domain is N.

3.4.1 Threat Score (TS)

The TS measures the fraction of observed and/or forecast events that were correctly predicted. It can be thought of as the accuracy when correct negatives have been removed from consideration, that is, TS is only concerned with forecasts that count. It is sensitive to hits and penalizes both misses and false alarms. It does not distinguish source of forecast

error. Depends on Climatological frequency of events (poorer scores for rarer events) since some hits can occur purely due to random chance. The TS has a value between 0 and 1 (as the hit area cannot be greater than the union of O and F), and a higher one represents better performance. The TS is defined as

$$TS = H / (O + F - H) \quad (2)$$

Where O = Observed heavy rain area; F = Model predicted heavy rain area; H = Intersected area between observed (O) and model predicted (F) heavy rain area. The TS is also called the critical success index.

3.4.2 Equitable Threat Score (ETS)

The ETS measures the fraction of observed and/or forecast events that were correctly predicted, adjusted for hits associated with random chance (for example, it is easier to correctly forecast rain occurrence in a wet climate than in a dry climate). The ETS is often used in the verification of rainfall in NWP models because its "equitability" allows scores to be compared more fairly across different regimes. It is sensitive to hits because it penalizes both misses and false alarms in the same way. It does not distinguish the source of forecast error. The ETS differs from the TS only in that a value of R is subtracted from both the denominator and numerator, as seen in Eq. (3), and thus can become negative but still capped by unity [–1/3≤ ETS≤ 1; Schaefer (1990); Baldwin and Kain (2006)]. Given in Eq. (4), R is the expected area for a random distribution of F to fall inside O just by chance (i.e., the random hit area). Due to this assumption of R being random and thus reflecting no model skill, it is excluded from the calculation of ETS and is therefore subtracted. Considered a fairer measure than the TS, the ETS is perhaps more widely used (Cartwright and Krishnamurti 2007). The ETS is denoted as

$$ETS = (H - R) / (O + F - H - R) \quad (3)$$

Where, $$R = (O/N) * (F/N) * N = F * (O/N) = O * (F/N) \quad (4)$$

Where N = Entire verification domain. The ETS is also called the Gilbert skill score.

3.4.3 Bias Score (BS)

The BS is the ratio of the relative sizes of the rain areas in the forecast to the observations and, thus, can vary from 0 to infinity but ideal value is 1 (Wilks 1995; Ebert *et al*. 2003). It measures the ratio of the frequency of forecast events to the frequency of observed events. It indicates whether the forecast system has a tendency to under forecast (BS<1) or over

forecast (BS>1) events. It does not measure how well the forecast corresponds to the observations, only measures relative frequencies. In Figure 3.2, it is clear that the same TS or ETS can result from either an over forecast or an under forecast of rain by the model, and thus the BS often needs to be provided alongside to interpret the verification results more properly (Pasaric and Juras 2011). The Bias Score is defined as

$$BS = F/O \tag{5}$$

3.4.4 Standard Deviation (SD)

The SD is a measure that is used to quantify the amount of variation or dispersion of a set of data values. A low standard deviation indicates that the data points tend to be close to the mean (also called the expected value) of the set, while a high standard deviation indicates that the data points are spread out over a wider range of values. The SD of a random variable, statistical population, data set, or probability distribution is the square root of its variance. It is algebraically simpler, though in practice less robust, than the average absolute deviation. A useful property of the SD is that, unlike the variance, it is expressed in the same units as the data. There are also other measures of deviation from the norm, including average absolute deviation, which provide different mathematical properties from SD.

In addition to expressing the variability of a population, the SD is commonly used to measure confidence in statistical conclusions. For example, the margin of error in polling data is determined by calculating the expected SD in the results if the same poll were to be conducted multiple times. This derivation of a SD is often called the "standard error" of the estimate or "standard error of the mean" when referring to a mean. It is computed as the SD of all the means that would be computed from that population if an infinite number of samples were drawn and a mean for each sample were computed. It is very important to note that the SD of a population and the standard error of a statistic derived from that population are quite different but related. The reported margin of error of a poll is computed from the standard error of the mean and is typically about twice the SD – the half–width of a 95 percent confidence interval. The formula for the SD deviation is

$$\sigma = \sqrt{\frac{\sum(x - \mu)2}{N}}$$

Where x is the observed value of the sample item μ is the mean value of these observations and *N* is the number of observations in the sample.

Chapter IV
Results and Discussion

In this research we have analyzed 24, 48 and 72 hour predicted rainfall for 33 meteorological stations of Bangladesh but presented only 24 hour predicted rainfall. We have also presented and compared time variation of station rainfall in the heavy rainfall area in the following subsection. We have also analyzed the convective rain, non–convective rain, area average rain, relative humidity, vertical velocity, reflectivity and vorticity and the model simulated results are verified by four verification methods (e. g., Threat Score, Equitable Threat Score, Bias Score and Standard Deviation). All of the above is discussed in the following sub–sections. For this purpose, GrADS, Microsoft Excel and SURFER Software have been used.

4.1 Heavy rainfall event at 4, 6 and 7 May 2013

The four different microphysics schemes (e.g. Lin *et al*., WSM6, Thompson and WDM6) and four different cumulus parameterization schemes (e.g., Kain–Fritsch, Tiedtke, Zhang–McFarlane and Multi–scale Kain–Fritsch) in WRF Model have been used to simulate the different parameters of heavy rainfall events of 4, 6 and 7 May 2013.

4.1.1 Observed and Model Simulated Rainfall on 4 May 2013

The observed rainfall over Bangladesh on 4, 6 and 7 May 2013 is presented in Figures 2(a–c). The heavy rainfall is observed in the southern and southeastern (SE) regions and light rainfall is found in the other regions of Bangladesh on 4 May (Figure 2a). The heavy rainfall is found at Chittagong, Comilla, Cox's Bazar, Hatiya, Kutubdia, M.Court, Rangamati, Sandwip, Sitakunda and Srimangal regions are 70, 54, 72, 81, 93, 126, 135, 147, 130 and 50 mm respectively.

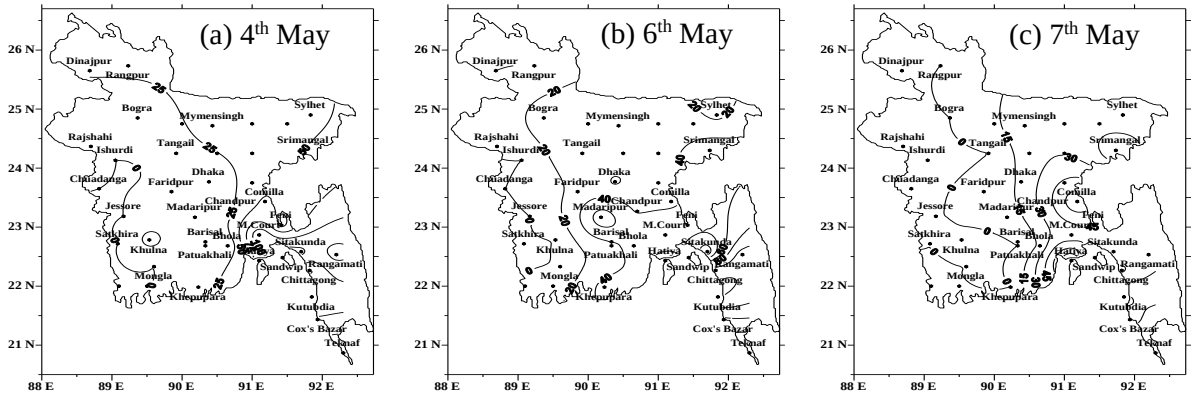

Figure 2: Distribution of (a–c) observed rainfall for 4, 6 and 7 May 2013 all over Bangladesh.

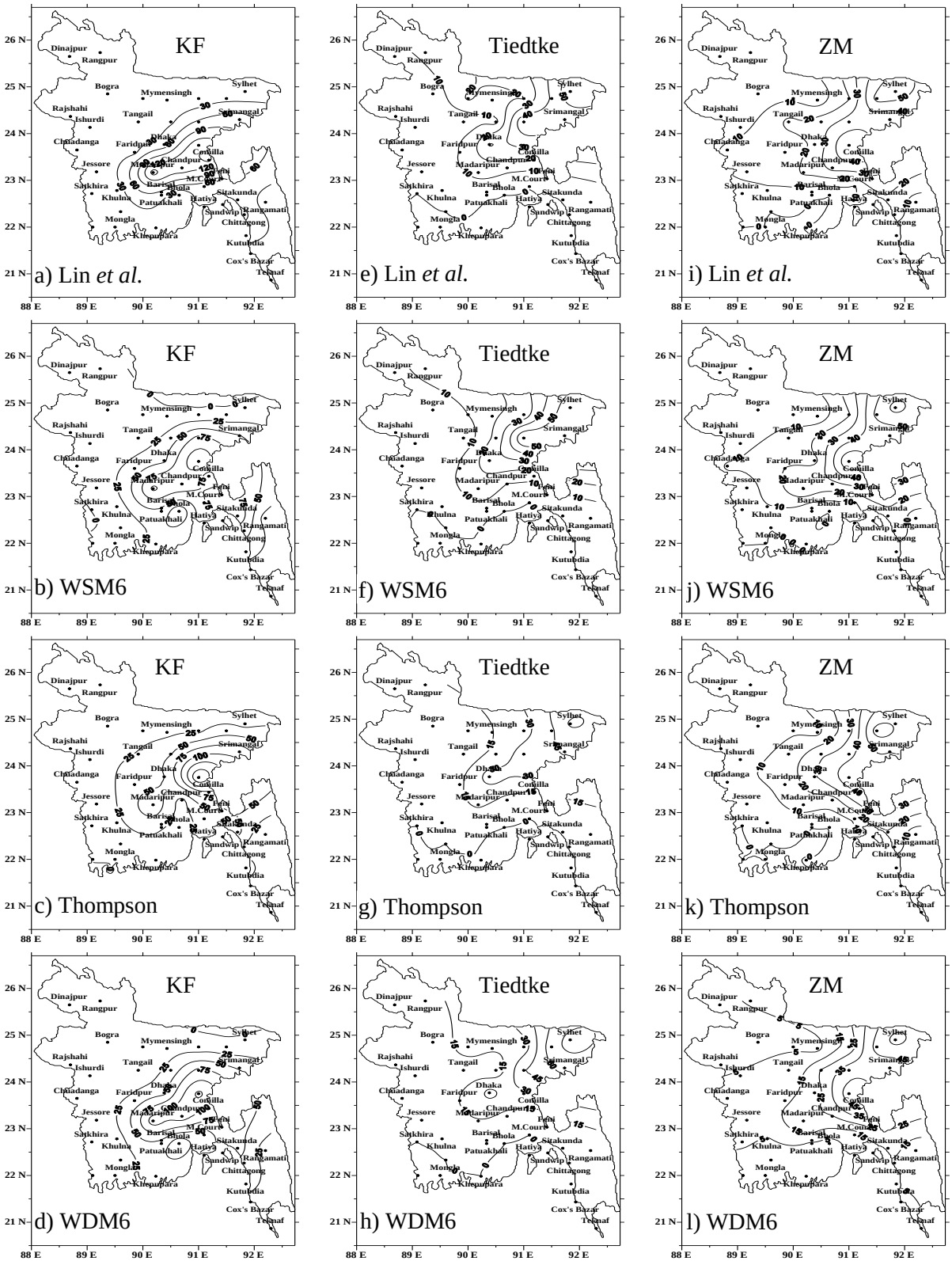

Figure 3: Distribution of model simulated (a–l) rainfall using Lin *et al.*, WSM6, Thompson and WDM6 schemes in combination with KF, Tiedtke and ZM schemes on 4 May with the initial condition at 0000 UTC of 4 May 2013.

The model simulated rainfall using four different MP schemes coupling with four different CP schemes on 4 May 2013 is presented in Figure 3(a–l) and Figure 6(a–d). The Lin–KF and

WSM6–KF combinations have simulated heavy rainfall (Figure 3(a–b)) in the central, SE and eastern regions and light rainfall in other regions of Bangladesh. Maximum rainfalls found at Barisal, Chandpur, Chittagong, Comilla, Feni, Hatiya, Madaripur, Sandwip, Sitakunda and Srimangal regions are 56, 139, 68, 156, 59, 52, 163, 69, 54 and 77 mm for Lin–KF (Figure 3a) and 50, 100, 63, 60, 89, 68, 106, 72, 96 and 51 mm for WSM6–KF (Figure 3b) combinations respectively. The Thompson–KF combination has simulated heavy rainfall (Figure 3c) in the central, northeastern (NE) and eastern regions and light rainfall in other regions of Bangladesh. Model simulated maximum rainfalls found at Comilla, Madaripur, Sandwip, Sitakunda and Srimangal regions are 97, 71, 55, 58 and 92 mm respectively.

The WDM6–KF combination has simulated heavy rainfall (Figure 3d) in the central to eastern and SE regions and light rainfall in other regions of Bangladesh. Maximum rainfalls found at Chandpur, Comilla, Feni, Hatiya, Madaripur, Sandwip and Sitakunda regions are 115, 96, 65, 62, 114, 51 and 62 mm respectively. The Lin–Tiedtke, WSM6–Tiedtke, Thompson–Tiedtke and WDM6–Tiedtke combinations have simulated heavy rainfall (Figures 3(e–h)) in the NE regions and light rainfall in other regions of Bangladesh. The Lin–Tiedtke, WSM6–Tiedtke, Thompson–Tiedtke and WDM6–Tiedtke combinations have not simulated so much rainfall but at Srimangal and Sylhet regions the rainfalls are 44 and 58 mm for Lin–Tiedtke (Figure 3e), 58 and 57 mm for WSM6–Tiedtke (Figure 3f), 47 and 62 mm for Thompson–Tiedtke (Figure 3g) and 66 and 80 mm for WDM6–Tiedtke (Figure 3h) combinations respectively.

The Lin–ZM and WSM6–ZM combinations have simulated heavy rainfall (Figures 3(i–j)) in the eastern and NE regions and light rainfall in other regions of Bangladesh. Maximum rainfalls found at Comilla and Sylhet regions are 42 and 56 mm for Lin–ZM (Figure 3i) and 42 and 63 mm WSM6–ZM (Figure 3j) combinations respectively. The Thompson–ZM and WDM6–ZM combinations have simulated heavy rainfall (Figures 3(k–l)) in the eastern to NE regions and light rainfall in other regions of Bangladesh. Maximum rainfalls found at Comilla, Srimangal and Sylhet regions are 41, 50 and 51 mm (Figure 3k) for Thompson–ZM and 46, 36 and 58 mm for WDM6–ZM (Figure 3l) combinations respectively.

The Lin–MSKF and WSM6–MSKF combinations have simulated heavy rainfall (Figures 6(a–b)) in the central to SE and NE regions and light rainfall in other regions of the country. Maximum rainfalls observed at Chittagong, Comilla, Dhaka, Sandwip and Srimangal regions are 43, 107, 45, 65 and 50 mm for Lin–MSKF (Figure 6a) and 58, 77, 40, 55 and 75 mm for WSM6–MSKF (Figure 6b) combinations respectively. The Thompson–MSKF and WDM6–

MSKF combinations have simulated heavy rainfall (Figures 6(c–d) in the SE and NE regions and light rainfall in other regions of Bangladesh. Maximum rainfall has been simulated at Comilla, Feni, Sitakunda and Srimangal regions and are 41, 47, 76 and 98 mm for Thompson–MSKF (Figure 6c) and 50, 36, 28 and 44 mm for WDM6–MSKF (Figure 6d) combinations respectively.

The model simulated maximum rainfall is almost matched with the observed rainfall for KF and MSKF schemes in combination with WSM6 and WDM6 schemes.

4.1.2 Observed and Model Simulated Rainfall on 6 May 2013

The heavy rainfall is observed in the southern to SE and NE regions and light rainfall is found in the other regions of Bangladesh on 6 May 2013 (Figure 2b). The maximum amount of rainfall is observed at Bhola, Chittagong, Cox's Bazar, Feni, Kutubdia, Madaripur, Rangamati and Srimangal regions and the amounts are 58, 112, 76, 55, 122, 74, 112 and 53 mm respectively.

The model has simulated very heavy rainfall using four different MP schemes coupling with four different CP schemes on 6 May 2013 and the results are presented in Figures 4(a–l) and Figures 6(e–h). The Lin–KF, WSM6–KF, Thompson–KF and WDM6–KF combinations have simulated heavy rainfall (Figures 4(a–d)) in the central to southern and SE regions and light rainfall in other regions of Bangladesh.

Maximum rainfalls simulated at Barisal, Chandpur, Chittagong, Comilla, Dhaka, Feni, Hatiya, Khepupara, Khulna, Madaripur, M.Court, Patuakhali and Sandwip regions and the rainfall amounts are 28, 85, 86, 95, 84, 73, 141,82, 95, 116, 163, 146 and 130 mm for Lin–KF (Figure 4a), 79, 72, 76, 82,65, 93, 127, 77, 101, 62, 94, 101 and 103 mm for WSM6–KF (Figure 4b), 120, 80, 52, 93, 99, 86, 72, 61, 86, 94, 128, 112 and 45 mm for Thompson–KF (Figure 4c) and 75, 59, 78, 93, 91, 89, 86, 74, 55, 53, 107, 93 and 81 mm for WDM6–KF (Figure 4d) combinations respectively.

The Lin–Tiedtke has simulated heavy rainfall (Figure 4e) at Comilla and Srimangal regions and the rainfall amounts are 73 and 85 mm respectively and the light rainfall is simulated in other regions of Bangladesh. The WSM6–Tiedtke has simulated heavy rainfall (Figure 4f) at Chandpur, Comilla, Dhaka, M.Court, Srimangal and Sylhet regions and the rainfall amounts are 88, 49, 57, 72, 107 and 50 mm respectively and the light rainfall is simulated in other regions of Bangladesh. The Thompson–Tiedtke combination has not simulated (Figure 4g) so much rainfall all over the country.

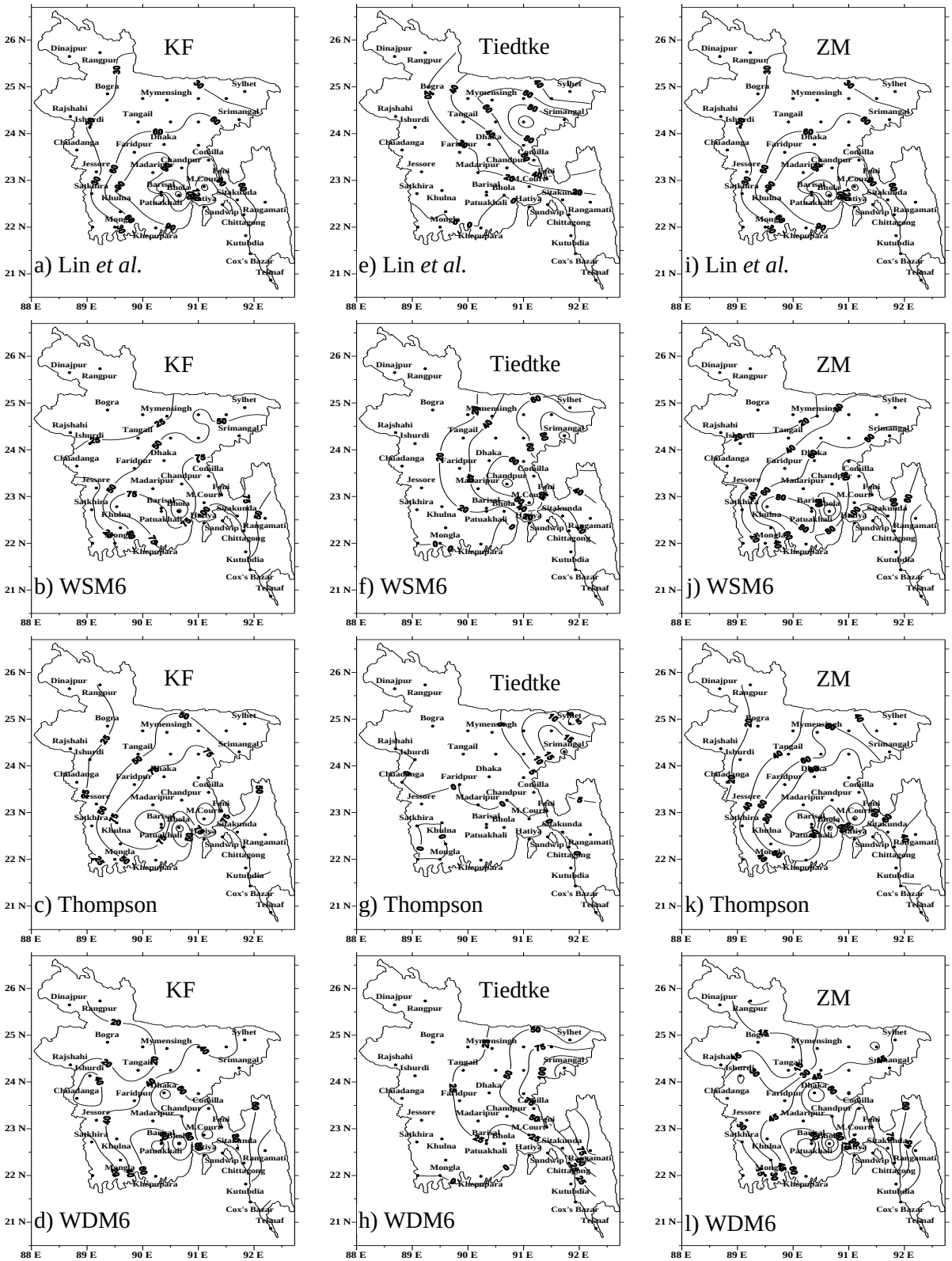

Figure 4: Distribution of model simulated rainfall (a–l) using Lin *et al.*, WSM6, Thompson and WDM6 schemes in combination with KF, Tiedtke and ZM schemes on 6 May with the initial condition at 0000 UTC of 6 May 2013.

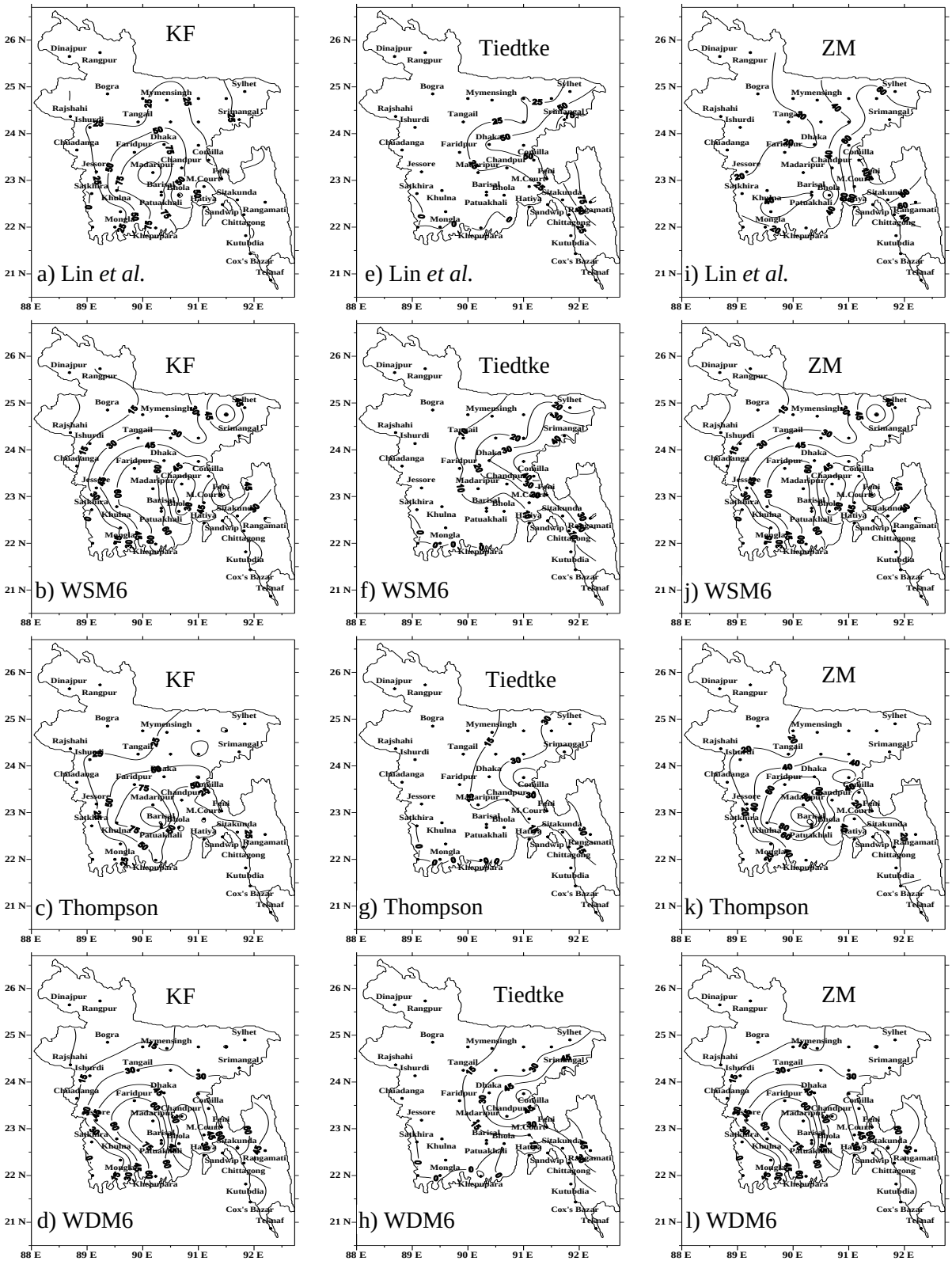

Figure 5: Distribution of model simulated rainfall using (a–l) Lin *et al.*, WSM6, Thompson and WDM6 schemes in combination with KF, Tiedtke and ZM schemes on 7 May with the initial condition at 0000 UTC of 7 May 2013.

The WDM6–Tiedtke has simulated very heavy rainfall (Figure 4h) in the eastern to SE and NE regions and light rainfall in other regions of Bangladesh. Maximum rainfalls are

simulated at Comilla, Rangamati and Srimangal regions are 67, 111 and 143 mm respectively.

The Lin–ZM, WSM6–ZM, Thompson–ZM and WDM6–ZM combinations have simulated heavy rainfall (Figures 4(i–l)) on 6 May with the initial condition at 0000 UTC of 6 May in the central to SE regions and light rainfall in other regions of Bangladesh. Maximum rainfalls are simulated at Chittagong, Comilla, Dhaka, Feni, Hatiya, Khulna, M.Court, Patuakhali and Sandwip regions and the rainfall amounts are 86, 95, 84, 73, 141, 95, 163, 146 and 130 mm for Lin–ZM (Figure 4i), 76, 82, 64, 93, 127, 101, 94, 101 and 103 mm for WSM6–ZM (Figure 4j), 80, 93, 99, 86, 72, 86, 128, 112 and 45 mm for Thompson–ZM (Figure 4k) and 78, 93, 91, 89, 86, 55, 107,93 and 81 mm for WDM6–ZM (Figure 4l) combinations respectively.

The Lin–MSKF has simulated heavy rainfall (Figure 6e) on 6 May at Chandpur, Chittagong, Comilla, Dhaka, Faridpur, Hatiya, Khepupara, Khulna, Madaripur, M.Court, Patuakhali and Sandwip regions and the rainfall amounts are 85, 86, 95, 84, 76, 141, 82, 95, 116, 163, 146 and 130 mm respectively light rainfall in other regions of Bangladesh.

The WSM6–MSKF combination has simulated heavy rainfall (Figure 6f) in the southern to SE regions and light rainfall in other regions of Bangladesh. Maximum rainfalls simulated at Barisal, Chittagong, Comilla, Feni, Hatiya, Khulna, M.Court, Patuakhali, Sandwip and Sitakunda regions are 79, 76, 82, 93, 127, 101, 94, 101, 103 and 100 mm respectively. The Thompson–MSKF and WDM6–MSKF combinations have simulated heavy rainfall (Figures 6(g–h)) in the central to SE regions and light rainfall in other regions of Bangladesh. Maximum rainfall are simulated at Barisal, Chittagong, Comilla, Dhaka, Feni, Hatiya, Khulna, Madaripur, M.Court, Patuakhali, Sandwip and Sitakunda regions and the rainfall amounts are 120, 80, 93, 99, 86, 72, 86, 94, 128, 112, 45 and 43 mm for Thompson–MSKF (Figure 6g) and 75, 78, 93, 91, 89, 86, 55, 53, 107, 93, 81 and 82 mm for WDM6–MKSF (Figure 6h) combinations respectively. The model simulated maximum rainfall is almost matched with the observed rainfall in the SE region for all MPs coupling with KF, ZM and MSKF schemes and in NE region for Tiedtke scheme on 6 May.

4.1.3 Observed and Model Simulated Rainfall on 7 May 2013

The heavy rainfall is observed in the southern to SE regions and light rainfall is found in other regions of Bangladesh on 7 May (Figure 2c). The heavy rainfall is found at Comilla,

Hatiya, Kutubdia, Cox's Bazar and Teknaf regions and the rainfall amounts are 75, 100, 64, 54 and 87 mm respectively.

The model has simulated rainfall using four different MP schemes coupling with four different CP schemes on 7 May and the results are presented in Figures 5(a–l) and Figures 6(i–l) with the initial conditions at 0000 UTC of 7 May 2013.The Lin–KF, WSM6–KF and Thompson–KF combinations have simulated heavy rainfall (Figures 5(a–c)) in the central to southern regions and light rainfall in other regions of Bangladesh. Maximum rainfalls simulated at Barisal, Dhaka, Faridpur, Hatiya, Khepupara, Khulna and Patuakhali regions are 80, 83, 69, 57, 92, 75 and 89 mm for Lin–KF, 65, 59, 66, 53, 68, 58and 70 mm for WSM6–KF and 134, 60, 72, 51, 52, 80 and 75 mm for Thompson–KF combinations respectively. The WDM6–KF combination has simulated heavy rainfall (Figure 5d) in the SW to SE regions and light rainfall in other regions of Bangladesh.

Maximum rainfalls simulated at Barisal, Cox's Bazar, Faridpur, Feni, Khepupara, Khulna, Kutubdia, Madaripur, Patuakhali and Sitakunda regions are 85, 64, 64, 70, 70, 56, 79, 91, 86 and 78 mm respectively. The Lin–Tiedtke has simulated heavy rainfall (Figure 5e) on 7 May at Dhaka, Rangamati and Srimangal regions and the rainfall amounts are 56, 102 and 86 mm respectively. The WSM6–Tiedtke and Thompson–Tiedtke (Figure 5(f–g)) combinations has simulated slight rainfall all over the country on 7 May. The WDM6–Tiedtke has simulated heavy rainfall (Figure 5h) on 7 May at Rangamati and Srimangal regions and the rainfall amounts are 55 and 63 mm respectively and light rainfall in other regions of Bangladesh.

The Lin–ZM combination has simulated heavy rainfall (Figure 5i) on 7 May at Comilla, Feni, M.Court, Mongla, Rangamati, Sandwip, Sitakunda and Srimangal regions and the rainfall amounts are 100, 104, 82, 53, 62, 63, 92 and 70 mm respectively. The WSM6–ZM and Thompson–ZM combinations have simulated heavy rainfall (Figures 5(j–k)) on 7 May in the central to southern regions and light rainfall in other regions of Bangladesh. Maximum rainfalls are simulated at Barisal, Dhaka, Faridpur, Feni, Hatiya, Khepupara, Madaripur and Patuakhali regions and the rainfall amounts are 65, 59, 66, 80, 53, 68, 70 and 70 mm for WSM6–ZM (Figure 5j) and 134, 60, 72, 51, 52, 80, 97 and 75 mm for Thompson–ZM (Figure 5j) combinations respectively. Heavy rainfall has been simulated using WDM6–ZM schemes combination (Figure 5l) on 7 May at Barisal, Comilla, Cox's Bazar, Faridpur, Feni, Jessore, Khepupara, Khulna, Kutubdia, Madaripur, Patuakhali and Sitakunda regions and the rainfall amounts are 85, 52, 64, 64, 70, 50, 70, 54, 79, 91, 86 and 78 mm respectively.

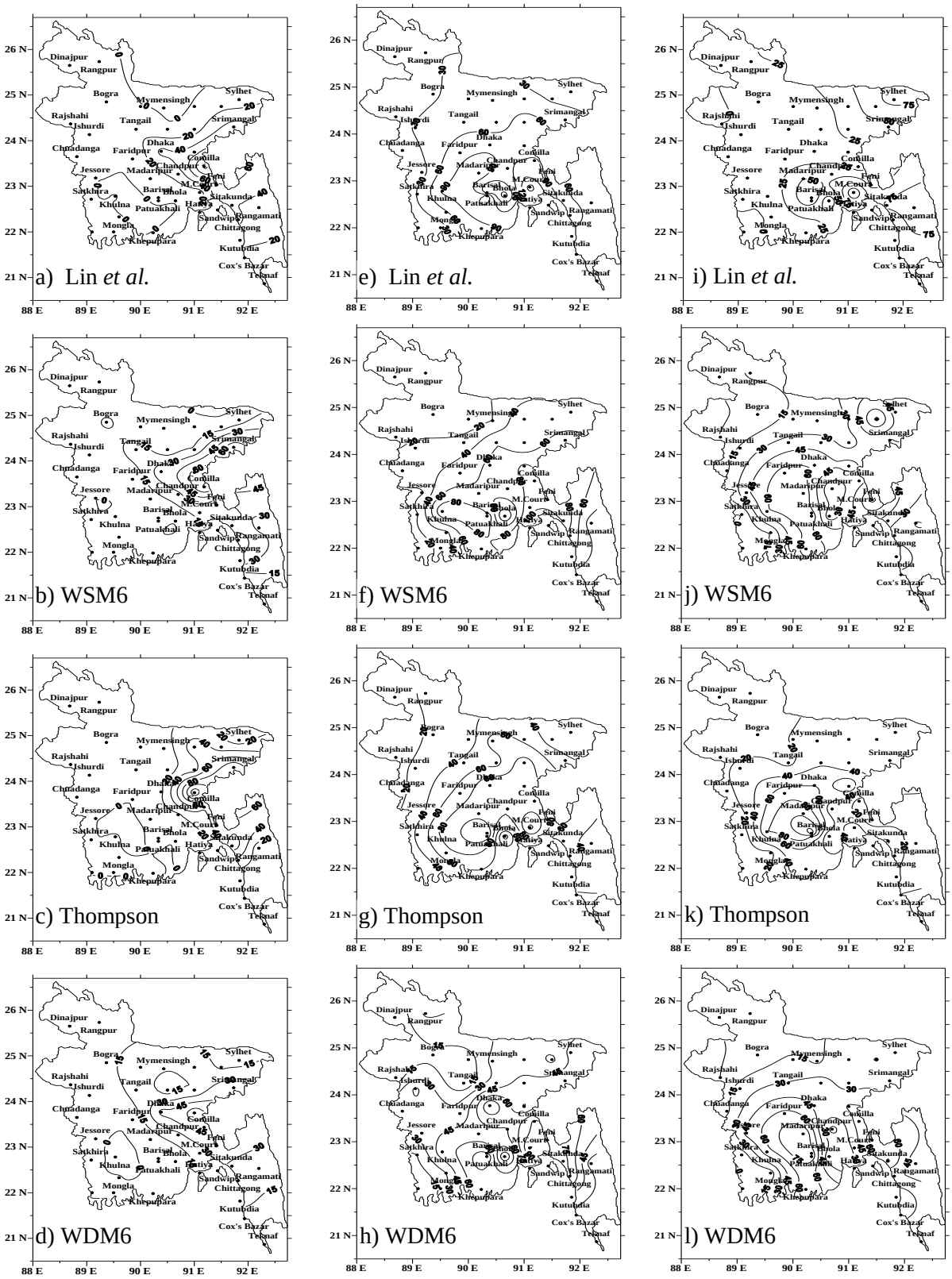

Figure 6: Distribution of model simulated rainfall on (a–d) 4 May, (e–h) 6 May and (i–l) 7 May using Lin *et al*., WSM6, Thompson and WDM6 schemes coupling with MSKF with the initial condition at 0000 UTC of 4, 6 and 7 May respectively.

The Lin–MSKF has simulated heavy rainfall (Figure 6i) on 7 May at Barisal, Chittagong, Cox's Bazar, Hatiya, Kutubdia, Madaripur, M.Court, Patuakhali, Rangamati, Sitakunda and

Sylhet regions and the rainfall amounts are 78, 60, 72, 76, 67, 50, 126, 63, 95, 81 and 81 mm respectively. The WSM6–MSKF and Thompson–MSKF combinations have simulated heavy rainfall (Figures 6(j–k)) in the central to southern regions and light rainfall in other regions of Bangladesh. Maximum rainfall has been simulated at Barisal, Dhaka, Faridpur, Feni, Khepupara, Madaripur and Patuakhali regions and the rainfall amounts are 65, 59, 66, 80, 68, 70 and 70 mm for WSM6–MSKF (Figure 6j)and 134, 60, 72, 51, 80, 97 and 75 mm for Thompson–MSKF (Figure 6k) combinations respectively. The WDM6–MSKF has simulated heavy rainfall (Figure 6l) on 7 May at Barisal, Cox's Bazar, Faridpur, Feni, Khepupara, Kutubdia, Madaripur, Patuakhali and Sitakunda regions and the rainfall amounts are 85, 64, 64, 70, 70, 79, 91, 86 and 78 mm respectively. The model simulated maximum rainfall is almost matched with the observed rainfall on 7 May 2013 in the SE region. Therefore, KF, ZM and MSKF coupling with all MPs are better for simulating heavy rainfall in the study area.

4.1.4 Model Simulated Convective Rainfall on 4 May 2013

The model simulated convective rains using four different MP schemes coupling with four different CP schemes on 4 May 2013 are presented in Figures 7(a–l) and Figures 10(a–d) respectively for the initial conditions at 0000 UTC of 4 May. The Lin–KF, WSM6–KF and Thompson–KF combinations have simulated significant amount of convective rain (Figures 7(a–c)) in the central to eastern and NE regions and light convective rain in other regions of Bangladesh. Model simulated maximum convective rains at Barisal, Chandpur, Comilla, Dhaka, Feni, Hatiya, Madaripur, M.Court, Sandwip, Sitakunda and Srimangal regions are 45, 56, 50, 43, 42, 52, 45, 43, 62, 53 and 53 mm for Lin–KF (Figure 7a), 47, 43, 32, 45, 82, 67, 55, 64, 69, 77 and 51 mm for WSM6–KF (Figure 7b) and 69, 67, 66, 84, 39, 58, 24, 62, 30, 18 and 31 mm for Thompson–KF (Figure 7c) combinations respectively. The WDM6–KF combination has simulated maximum convective rainfalls of 45, 45, 44, 50, 43, 54, 60, 43, 51, 61 and 47 mm (Figure 7d) at Barisal, Chandpur, Chittagong, Comilla, Dhaka, Feni, Hatiya, Khepupara, Madaripur, Patuakhali, Sandwip, Sitakunda and Srimangal regions respectively.

The significant amount of convective rains simulated at Srimangal and Sylhet regions are 41 and 40 mm for Lin *et al.* (Figure 7e), 55 and 43 mm for WSM6 (Figure 7f), 47 and 34 mm for Thompson (Figure 7g) and 66 and 36 mm for WDM6 (Figure 7h) coupling with Tiedtke cumulus parameterization scheme.

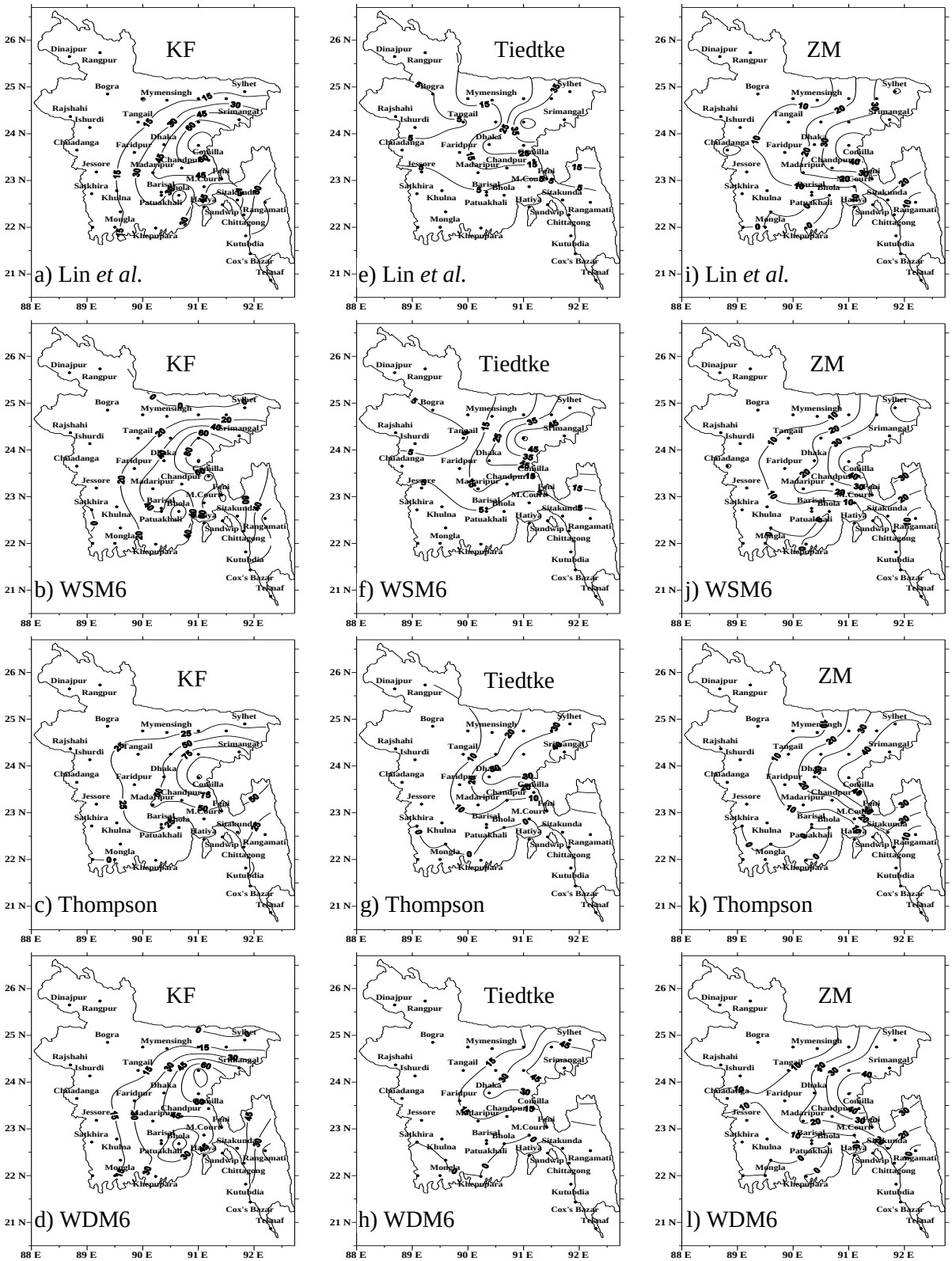

Figure 7: Distribution of model simulated convective rain on 4 May using (a–d) KF, (e–h) Tiedtke and (i–l) ZM schemes in combination with Lin *et al.*, WSM6, Thompson and WDM6 schemes with the initial condition at 0000 UTC of 4 May 2013.

The significant amount of convective rainfalls simulated at Srimangal and Sylhet regions are 41 and 40 mm for Lin *et al.* (Figure 7i), 55 and 43 mm for WSM6 (Figure 7j), 47 and 34 mm

for Thompson (Figure 7k) and 66 and 36 mm for WDM6 (Figure 7l) coupling with ZM cumulus parameterization scheme. Little amount of convective rain has simulated in the eastern side of Bangladesh using MSKF scheme in combination with Lin *et al.*, WSM6, Thompson and WDM6 (Figures 10(a–d)) schemes and almost no convective rain in other regions of the country on 4 May 2013. The significant amount of convective rain is simulated in the central to eastern and NE regions by KF and ZM schemes and central to NE region by Tiedtke scheme coupling with all MPs. Little amount of convective rain has simulated in the eastern side of Bangladesh using MSKF scheme.

4.1.5 Model Simulated Convective Rainfall on 6 May 2013

The model simulated convective rain using four different MP schemes coupling with four different CP schemes on 6 May 2013 are presented in Figures 8(a–l) and Figures 10(e–h) respectively for the initial conditions at 0000 UTC of 6 May. The KF scheme has simulated significant amount of convective rain in combination with four different MPs (Figures 8(a–d)) in the central to western region and light convective rain in other regions of Bangladesh. Model simulated maximum convective rainfalls at Barisal, Chandpur, Comilla, Dhaka, Faridpur, Hatiya, Khulna, Madaripur, M.Court and Patuakhali regions are 77, 62, 51, 74, 74, 78, 50, 80, 63 and 78 mm for Lin–KF (Figure 8a), 69, 67, 66, 84, 67, 58, 54, 75, 62 and 66 mm Thompson–KF (Figure 8c) combinations respectively. KF scheme has also simulated maximum convective rain at Chandpur, Comilla, Dhaka and Hatiya regions and the amounts are 55, 49, 81 and 58 mm (Figure 8b) and 52, 46, 77 and 62 mm (Figure 8d) coupling with WSM6 and WDM6 schemes respectively.

The Lin–Tiedtke has simulated convective rains (Figure 8e) at Comilla and Srimangal regions and the amounts are 44 and 30 mm respectively. The Thompson–Tiedtke has simulated little amount of convective rain (Figure 8g) in the NE region of Bangladesh and almost no convective rain in other regions of Bangladesh. The WSM6 and WDM6 coupling with Tiedtke has simulated significant amounts of convective rain at Chandpur, Comilla and Srimangal regions are 34, 35 and 32 mm (Figure 8f) and 32, 45 and 36 mm (Figure 8h) respectively. The ZM scheme coupling with Lin *et al.* and Thompson schemes have simulated significant amounts of convective rain at Barisal, Chandpur, Comilla, Dhaka, Faridpur, Hatiya, Khulna, Madaripur, M.Court, Mymensingh, Patuakhali and Tangail regions and the amounts are 77, 62, 51, 74, 74, 78, 50, 80, 63, 44, 78 and 50 mm (Figure 8i) and 69, 67, 66, 84, 67, 58, 54, 75, 62, 51, 66 and 44 mm (Figure 8k) respectively.

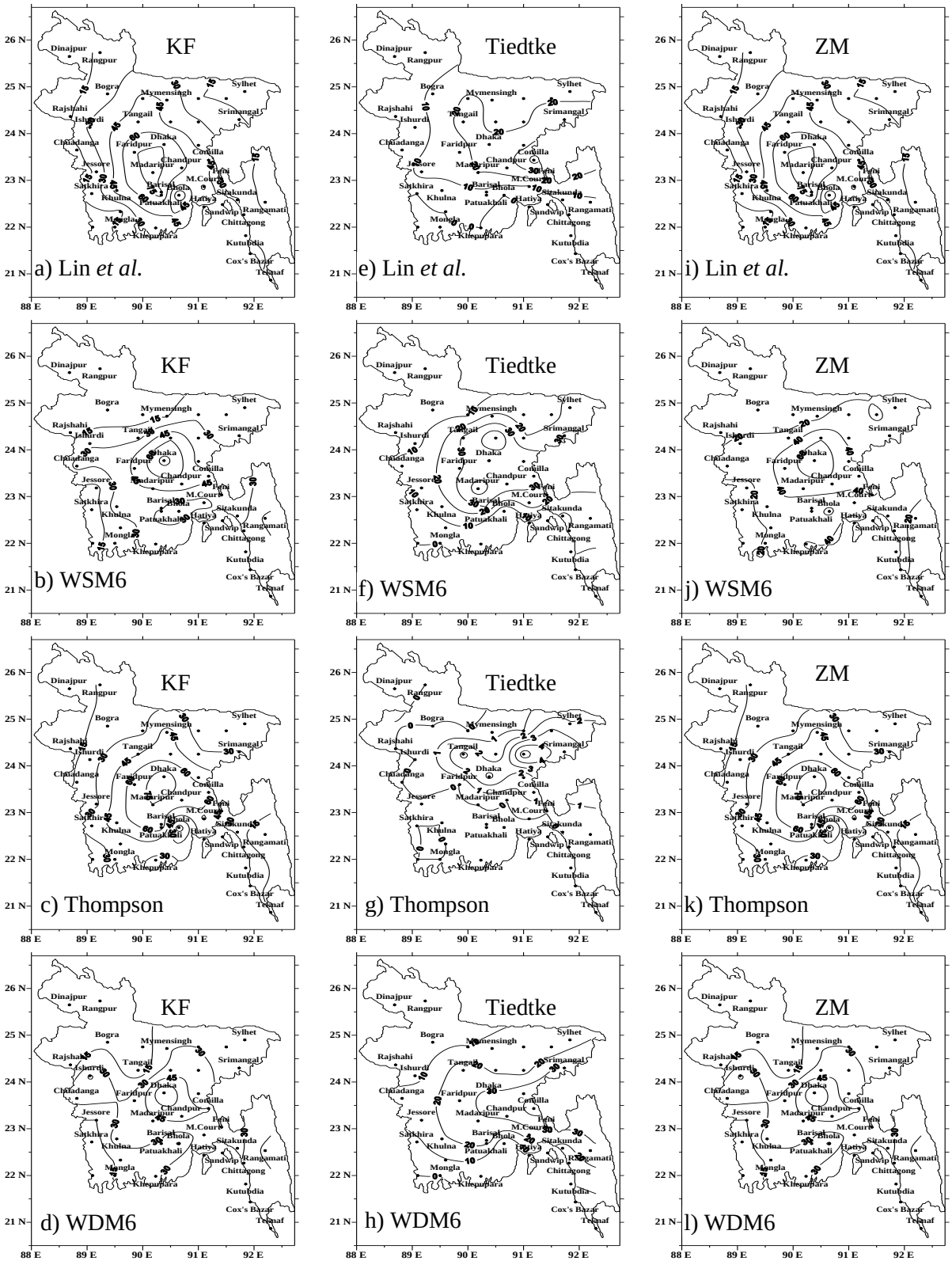

Figure 8: Distribution of model simulated convective rain on 6 May using (a–d) KF, (e–h) Tiedtke and (i–l) ZM schemes in combination with Lin *et al.*, WSM6, Thompson and WDM6 schemes with the initial condition at 0000 UTC of 6 May 2013.

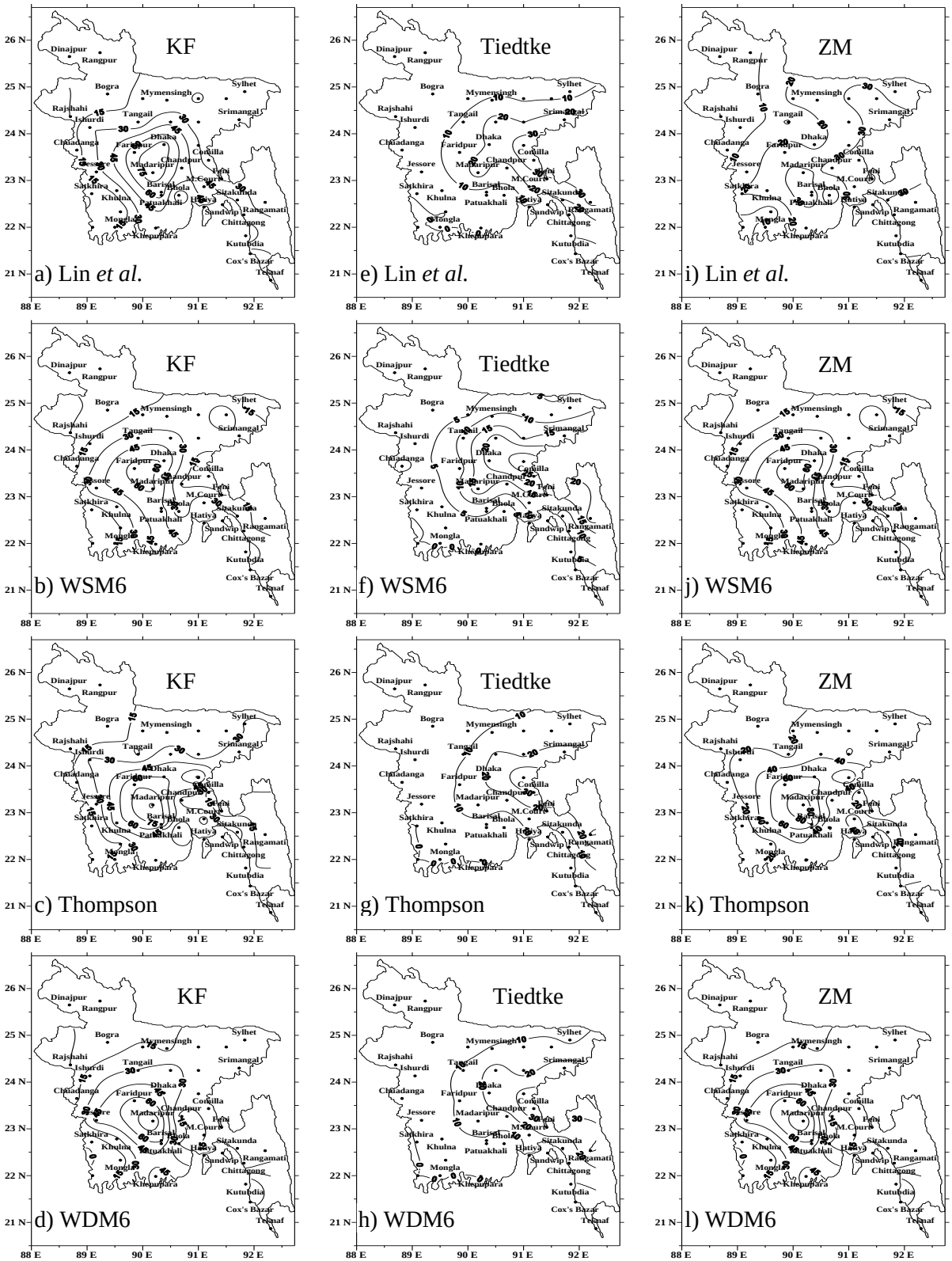

Figure 9: Distribution of model simulated convective rain on 7 May using (a–d) KF, (e–h) Tiedtke and (i–l) ZM schemes in combination with Lin *et al.*, WSM6, Thompson and WDM6 schemes with the initial condition at 0000 UTC of 7 May 2013.

The ZM scheme coupling with WSM6 and WDM6 schemes have simulated significant amount of convective rain at Chandpur, Comilla, Dhaka, Feni, Hatiya and Madaripur regions

and the amounts are 55, 49, 81, 41, 58 and 44 mm (Figure 8j) and 52, 46, 77, 41, 62 and 41 mm (Figure 8l) respectively.

The MSKF scheme coupling with Lin *et al.* and Thompson schemes have simulated significant amounts of convective rain at Barisal, Chandpur, Comilla, Dhaka, Faridpur, Hatiya, Khulna, Madaripur, M.Court and Patuakhali regions and the amounts are 77, 62, 51, 74, 74, 78, 50, 80, 63 and 78 mm for Lin–MSKF (Figure 10e) and 69, 67, 66, 84, 67, 58, 54, 75, 62 and 66 mm for Thompson–MSKF (Figure 10g) combinations respectively. The MSKF coupling with WSM6 and WDM6 schemes have simulated significant amount of convective rain in the central to eastern and NE regions and light convective rain in other regions of Bangladesh.

Model simulated maximum convective rain is found at Chandpur, Comilla, Dhaka, Feni, Hatiya, Khulna and Madaripur regions and the amounts are 55, 49, 81, 41, 58, 40 and 44 mm for WSM6–MSKF (Figure 10f) and 52, 46, 77, 41, 62, 39 and 41 mm for WDM6–MSKF (Figure 10h) combinations respectively. The significant amount of convective rain is simulated in the central to western region by KF scheme and central to eastern and NE regions by Tiedtke, ZM and MSKF schemes coupling with all MPs with little exceptions.

4.1.6 Model Simulated Convective Rainfall on 7 May 2013

The model simulated convective rain on 7 May 2013 using four different MP schemes coupling with four different CPs have presented in Figures 9(a–l) and Figures 10(i–l) for the initial condition at 0000 UTC of 7 May. The KF scheme has simulated significant amount of convective rain in combination with four different MPs (Figures 9(a–d)) in the central to western and southern regions and light convective rain in other regions of Bangladesh. The maximum convective rain is simulated at Barisal, Dhaka, Faridpur, Khepupara, Kutubdia, Madaripur, M.Court, Patuakhali and Sandwip regions and the amounts are 66, 82, 69, 45, 61, 88, 56, 64 and 50 mm for Lin–KF (Figure 9a), 48, 59, 66, 50, 45, 62, 45, 56 and 42 mm for WSM6–KF (Figure 9b), 85, 60, 72, 41, 16, 92, 51, 49 and 43 mm for Thompson–KF (Figure 9c) and 64, 42, 64, 52, 78, 90, 14, 52, and 48 mm for WDM6–KF (Figure 9d) combinations respectively.

The moderate convective rain has simulated at Comilla and Rangamati regions and the amounts are 38 and 33 mm for Lin *et al.* (Figure 9e), 33 and 31 mm for Thompson (Figure 9g) and 40 and 31 mm for WDM6 (Figure 9h) coupling with Tiedtke scheme.

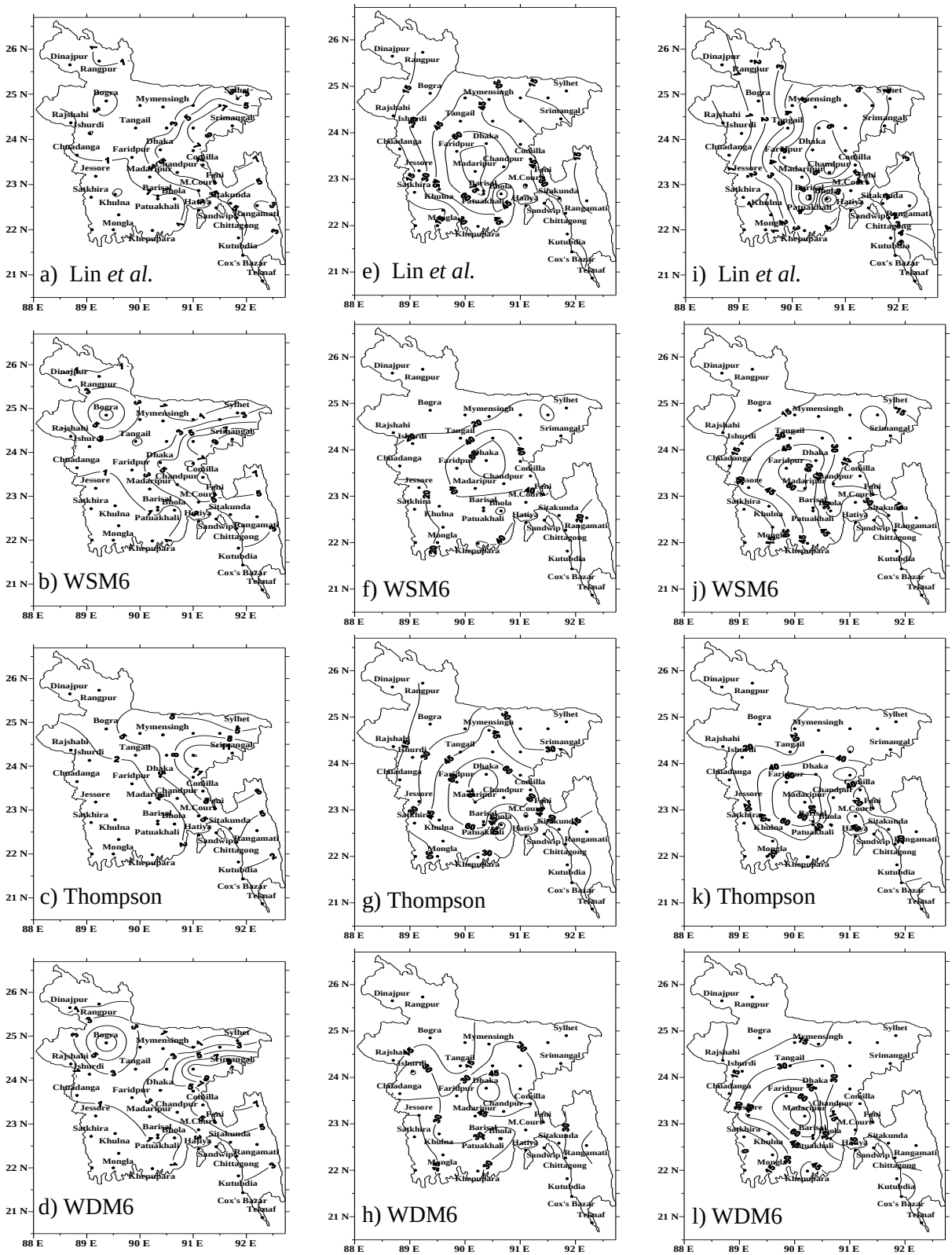

Figure 10: Distribution of model simulated convective rain using Lin *et al.*, WSM6, Thompson and WDM6 schemes in combination with MSKF scheme on (a–d) 4 May, (e–h) 6 May and (i–l) 7 May with the initial condition at 0000 UTC of 4, 6 and 7 May respectively.

Little amount of convective rain has simulated in the eastern side of Bangladesh for WSM6–Tiedtke combination (Figure 9f) and almost no convective rain is simulated for this combination in other regions of the country on 7 May 2013.

The Lin–ZM combination has simulated convective rain at Feni, Patuakhali and Sandwip regions and the amounts are 41, 41 and 42 mm respectively (Figure 9i). The significant amount of convective rain has simulated at Barisal, Dhaka, Faridpur, Jessore, Khepupara, Kutubdia, Madaripur, M.Court, Patuakhali and Sandwip regions and the amounts are 48, 59, 66, 42, 50, 45, 62, 45, 56 and 42 mm for WSM6–ZM (Figure 9j), 84, 60, 72, 22, 40, 16, 92, 51, 49 and 43 mm for Thompson–ZM (Figure 9k) and 66, 47, 68, 46, 56, 77, 90, 18, 50 and 41 mm for WDM6–ZM (Figure 9l) combinations respectively.

The Lin–MSKF has simulated little amount of convective rain (Figure 10i) in the eastern side and almost no convective rain in other regions of the country on 7 May 2013. The significant amount of convective rain has simulated at Barisal, Dhaka, Faridpur, Jessore, Khepupara, Madaripur and Patuakhali regions and the amounts are 48, 59, 66, 42, 50, 62 and 56 mm for WSM6–MSKF (Figure 10j), 84, 60, 72, 22, 40, 92 and 49 mm for Thompson–MSKF (Figure 10k) and 64, 42, 64, 50, 52, 90 and 52 mm for WDM6–MSKF (Figure 10l) combinations respectively on 7 May 2013.

The significant amount of convective rain is simulated in the central to western region by KF, ZM and MSKF schemes and central to eastern regions by Tiedtke scheme in combination with all MPs with little exception.

4.1.7 Model Simulated Non–Convective (NC) Rainfall on 4 May 2013

The model simulated NC rain using four different MP schemes coupling with four different CPs on 4 May 2013 have presented in Figure 11(a–l) and Figure 14(a–d) respectively for the initial condition at 0000 UTC of 4 May. The Lin–KF combination has simulated maximum amount of NC rain (Figure 11a) at Chandpur, Comilla, Dhaka and Madaripur regions and the amounts are 83, 105, 52 and 118 mm respectively. The KF scheme coupling with WSM6 and WDM6 schemes have simulated significant amount of NC rain at Chandpur, Comilla and Madaripur regions and the amounts are 49, 28 and 51 mm (Figure 11b) and 70, 46 and 71 mm (Figure 11d) respectively and light NC rain in other regions of Bangladesh. The Thompson–KF combination has simulated little amount of NC rain (Figure 11c) in the eastern side of Bangladesh and almost no NC rain in other regions of the country.

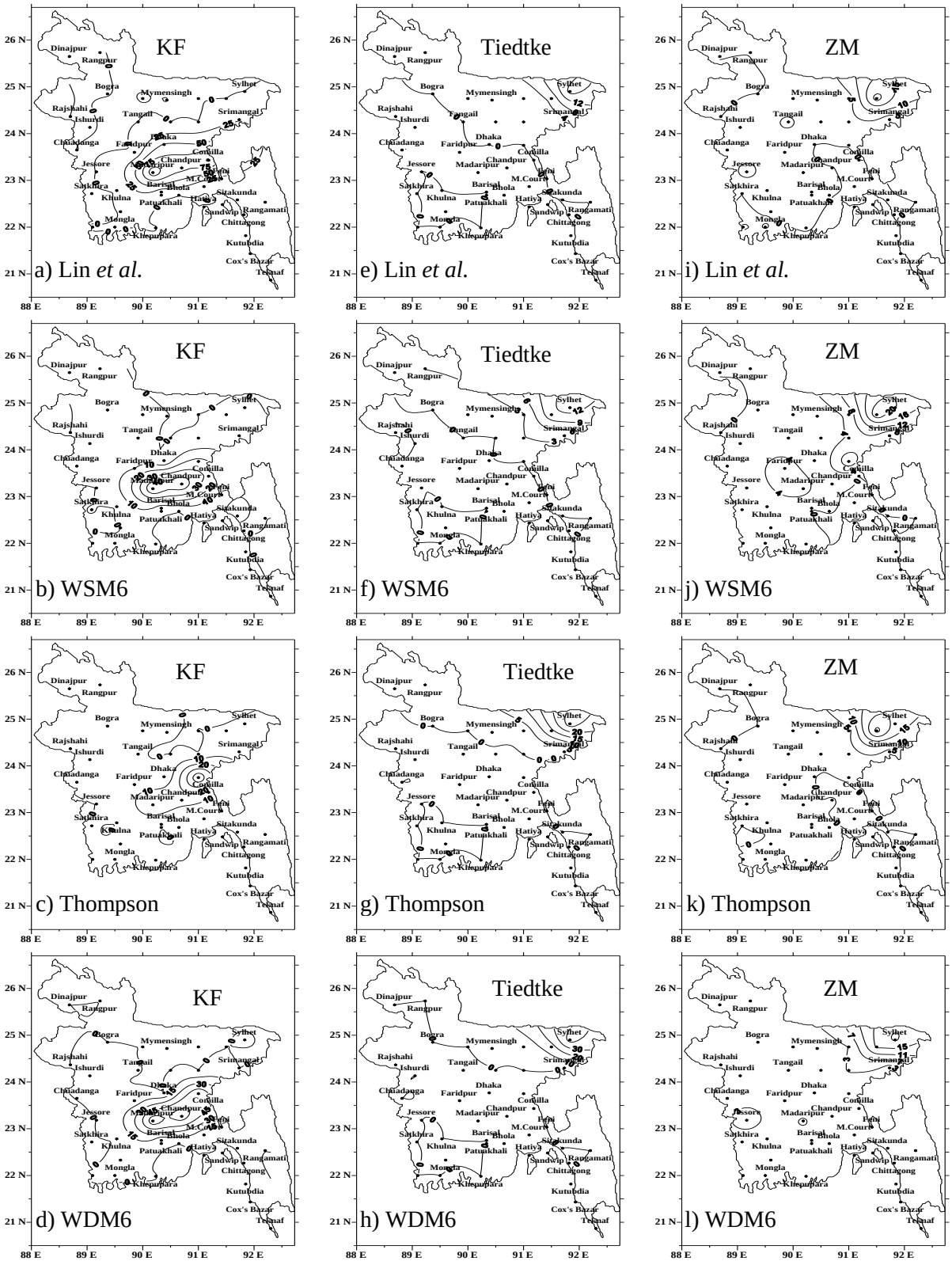

Figure 11: Distribution of model simulated NC rain on 4 May using (a–d) KF, (e–h) Tiedtke and (i–l) ZM schemes in combination with Lin *et al*., WSM6, Thompson and WDM6 schemes with the initial condition at 0000 UTC of 4 May 2013.

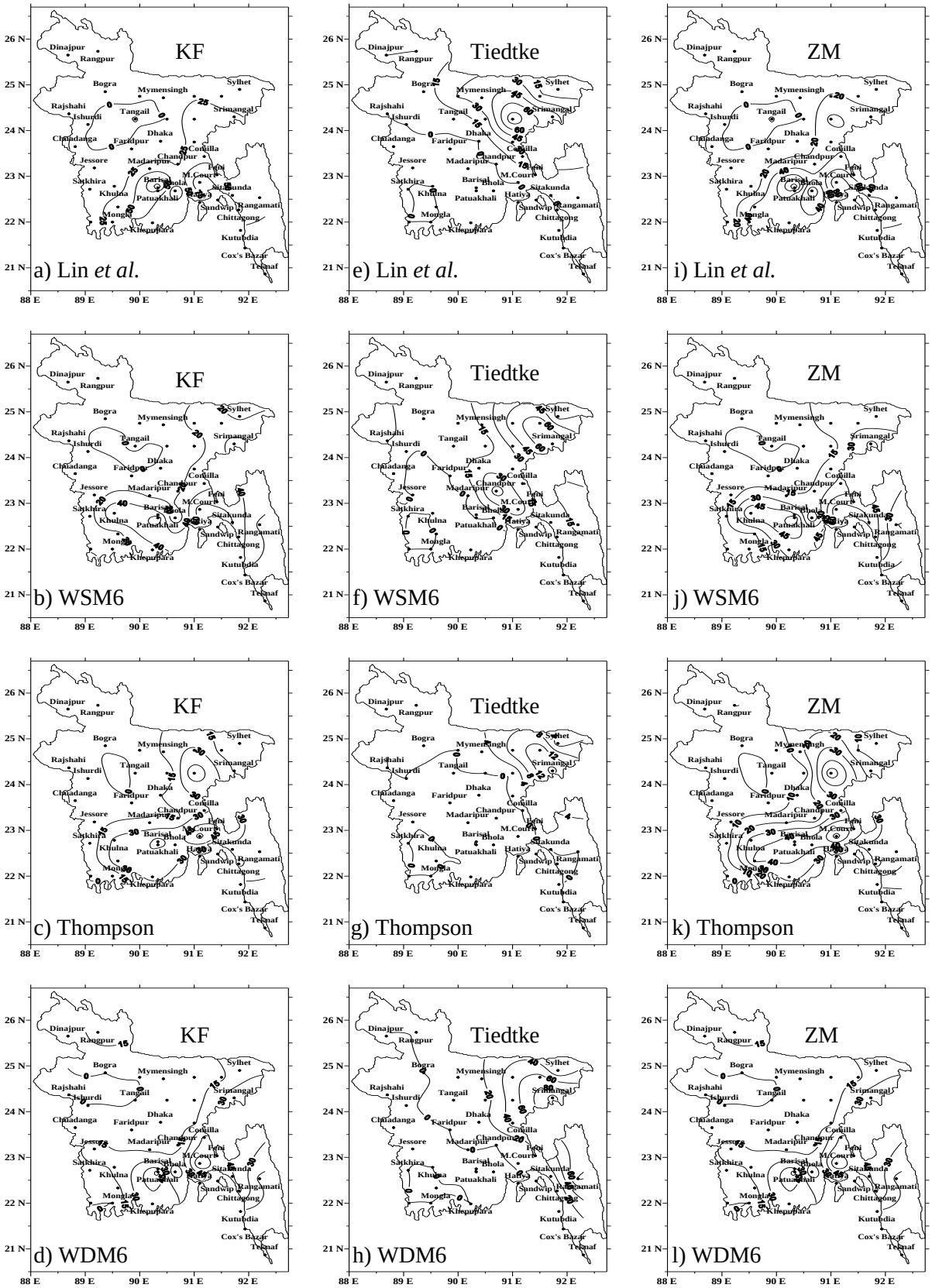

Figure 12: Distribution of model simulated NC rain on 6 May using (a–d) KF, (e–h) Tiedtke and (i–l) ZM schemes in combination with Lin *et al*., WSM6, Thompson and WDM6 schemes with the initial condition at 0000 UTC of 6 May 2013.

The Tiedtke scheme coupling with Lin *et al.*, WSM6 and Thompson schemes have simulated little amount of NC rain (Figures 11(e–g)) in the NE region of Bangladesh and almost no NC rain in other regions of the country. The WDM6–Tiedtke combination has simulated significant amount of NC rain at Sylhet region and the amount is (Figure 11h) is 44 mm and light NC rain in other regions. Little amount of NC rain has simulated in the NE region of Bangladesh using ZM scheme in combination with Lin *et al.*, WSM6, Thompson and WDM6 (Figures 11(i–l)) schemes and almost no NC rain in other regions of the country on 4 May 2013.

The Lin–MSKF, WSM6–MSKFand Thompson–MSKF combinations have simulated significant amount of NC rain (Figure 14(a–c)) in the central to eastern and NE regions and light NC rain in other regions of Bangladesh. Model simulated maximum NC rain is found at Chittagong, Comilla, Feni, Sandwip, Sitakunda and Srimangal regions and the amounts are 37, 100, 60, 35 and 40 mm for Lin–MSKF (Figure 14a), 52, 69, 50, 29 and 63 mm for WSM6–MSKF (Figure 14b) and 30, 31, 17, 69 and 85 mm for Thompson–MSKF (Figure 14c) combinations respectively. The WDM6–MSKF combination has simulated moderate NC rain (Figure 14d) at Comilla and Dhaka regions and the amount is 44 mm respectively and light NC rain in other regions of Bangladesh.

The significant amount of NC rain is simulated in the central to eastern and NE regions by KF and MSKF schemes coupling with all MPs. Little amount of NC rain has simulated in the NE region of Bangladesh using Tiedtke and ZM schemes.

4.1.8 Model Simulated NC Rain on 6 May 2013

The model simulated Non–convective (NC) rain using four different MP schemes coupling with four different CP schemes on 6 May 2013 has been presented in Figures 12(a–l) and Figures 14(e–h) respectively for the initial conditions at 0000 UTC of 6 May. The KF scheme coupling with Lin *et al.* and WSM6 schemes have simulated significant amount of NC rain in the central to eastern regions and light convective rain in other regions of Bangladesh. Maximum NC rain is found at Barisal, Chittagong, Comilla, Feni, Hatiya, Khepupara, M.Court, Patuakhali and Sandwip regions and the amounts are 120, 56, 44, 52, 64, 47, 100, 68 and 100 mm for Lin–KF (Figure 12a) and 47, 49, 33, 52, 69, 36, 70, 75 and 86 mm for WSM6–KF (Figure 12b) combinations respectively. The significant amount of NC rain has been simulated at Barisal, Chittagong, Comilla, Feni, Khepupara, M.Court, Patuakhali and Sitakunda regions and the amounts are 50, 33, 27, 48, 34, 66, 46 and 25 mm for Thompson–

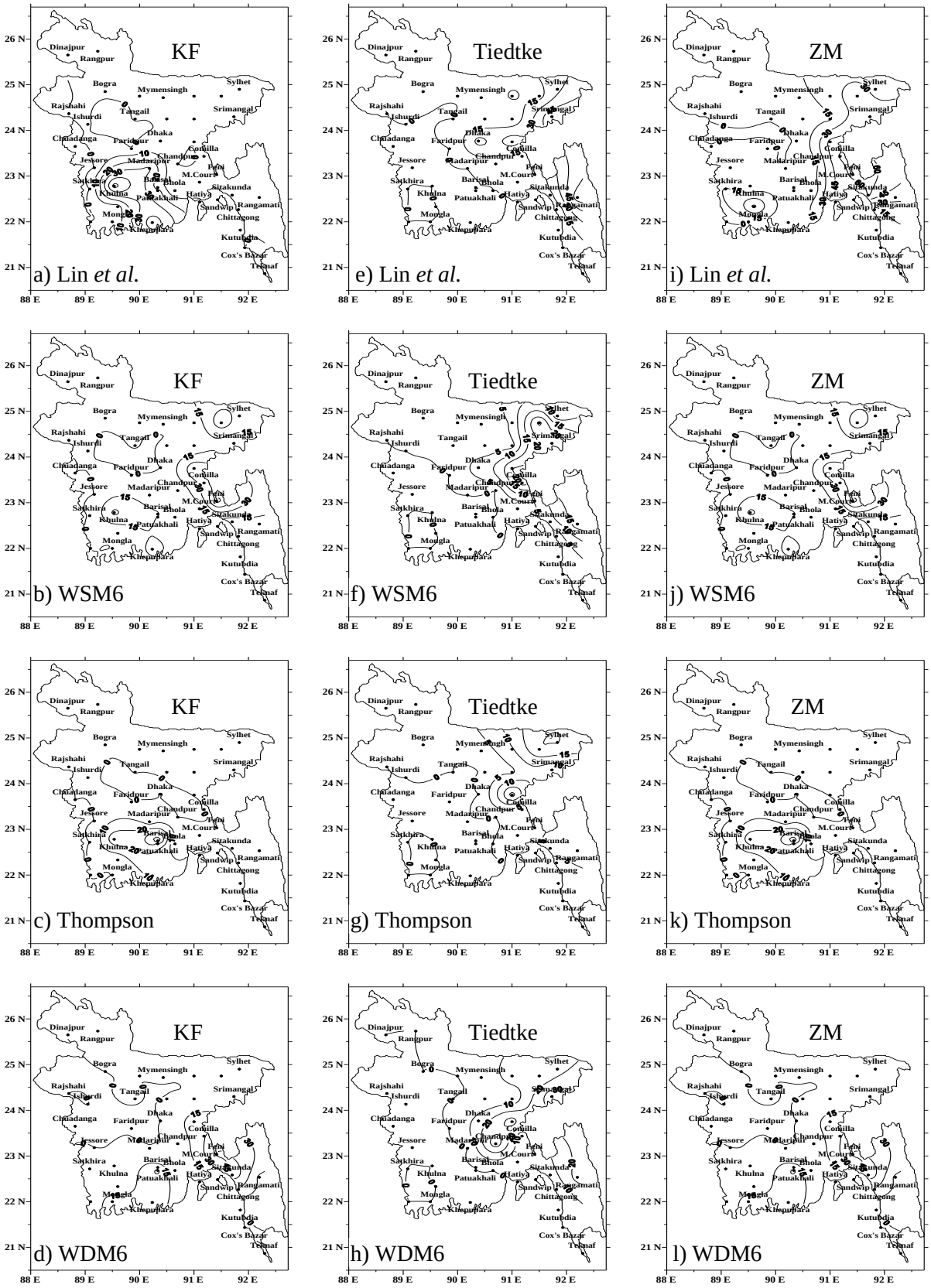

Figure 13: Distribution of model simulated NC rain on 7 May using (a–d) KF, (e–h) Tiedtke and (i–l) ZM schemes in combination with Lin *et al*., WSM6, Thompson and WDM6 schemes with the initial condition at 0000 UTC of 7 May 2013.

KF (Figure 12c) and 45, 49, 48, 49, 45, 76, 67 and 46 mm for WDM6–KF (Figure 12d) combinations respectively. The model has simulated significant amount of 54 mm NC rain at Srimangal region for Lin–Tiedtke (Figure 12e); the simulated NC rainfall amounts at Chandpur, M.Court and Srimangal regions are 53, 46 and 75 mm for WSM6–Tiedtke (Figure 12f), At Rangamati and Srimangal regions are 82 and 107 mm for WDM6–Tiedtke (Figure 12h) combinations respectively and the model has simulated light rain in other regions of Bangladesh. The Thompson–Tiedtke has simulated little amount of NC rain (Figure 12g) in the NE region of Bangladesh and almost no NC rain in other regions of the country.

The ZM scheme in combination with Lin *et al.*, WSM6, Thompson and WDM6 ((Figures 12(i–l)) schemes has simulated significant amount of NC rain in the eastern to southern region and light NC rain in other regions of Bangladesh. Maximum NC rain is found at Barisal, Feni, Khepupara, M.Court, Patuakhali and Sandwip regions and the amounts 120, 52, 47, 100, 68 and 102 mm for Lin–ZM (Figure12i), 47, 52, 36, 70, 75 and 86 mm for WSM6–ZM (Figure 12j), 50, 48, 34, 66, 46 and 15 mm for Thompson–ZM (Figure 12k) and 45, 48, 45, 76, 67 and 44 mm for WDM6–ZM (Figure 12l) combinations respectively.

The Lin–MSKF, WSM6–MSKF, Thompson–MSKF and WDM6–MSKF combinations have simulated significant amount of NC rain (Figures 14(e–h)) in the southern region and light NC rain in some other regions of Bangladesh. Maximum NC rainfalls simulated at Barisal, Chittagong, Feni, M.Court, Patuakhali and Sandwip regions are 120, 56, 52, 100, 68 and 102 mm for Lin–ZM (Figure 14e), 47, 48, 52, 70, 75 and 86 mm for WSM6–ZM (Figure 14f), 50, 33, 48, 66, 46 and 15 mm for Thompson–ZM (Figure 14g) and 45, 49, 48, 76, 67 and 44 mm for WDM6–ZM (Figure 14h) combinations respectively.

The significant amount of NC rain is simulated in the south–southeastern region by KF, ZM and MSKF schemes and eastern to NE by Tiedtke scheme coupling with Lin *et al.* and WSM6 schemes.

4.1.9 Model Simulated NC Rainfall on 7 May 2013

The model simulated NC rain using four different MPs coupling with four different CPs on 7 May 2013 has been presented in Figure 13(a–l) and Figure 14(i–l) for the initial conditions at 0000 UTC of 7 May respectively. The Lin–KF has simulated significant amount of NC rain (Figure 13a) at Khepupara and Khulna regions where the rainfall amounts are 47 and 55 mm respectively and light NC rain in other regions of Bangladesh. The WSM6–KF and

Thompson–KF combinations have simulated significant amount of NC rain at Feni is 65 mm (Figure 13b) and at Barisal is 49 mm (Figure 13c) respectively and light NC rain in other regions of Bangladesh. The WDM6–KF combination has simulated significant amount of NC rain (Figure 13d) at Feni and Sitakunda regions where the rainfall amounts are 47 and 56 mm respectively.

The Lin–Tiedtke has simulated significant amount of NC rain (Figure 13e) at Rangamati and Srimangal regions where the rainfall amounts are 69 and 60 mm respectively and light NC rain in other regions of Bangladesh. The Tiedtke scheme in combination with WSM6 and Thompson schemes have simulated little amount of NC rain (Figure 13(f–g)) in the eastern to NE region of Bangladesh and almost no NC rain in other regions of the country. The WDM6–Tiedtke combination has simulated moderate NC rain (Figure 13h) at Chandpur and Srimangal regions where the rainfall amounts are 36 and 38 mm respectively and light NC rain in other regions of Bangladesh.

The Lin–ZM has simulated significant amount of NC rain (Figure 13i) at Comilla, Feni, Hatiya, M.Court, Mongla and Sitakunda regions where the rainfall amounts are 62, 63, 58, 46, 50 and 62 mm respectively. The WSM6–ZM combination has simulated significant amount of NC rain (Figure 13j) at Feni and Khulna regions where the rainfall amounts are 65 and 40 mm respectively and light NC rain in other regions of Bangladesh. The Thompson–ZM has simulated significant amount of NC rain (Figure 13k) at Barisal region is 45 mm. The WDM6–ZM combination has simulated significant amount of NC rain (Figure 13l) at Feni, Patuakhali and Sitakunda regions where the rainfall amounts are 47, 34 and 56 mm respectively and light NC rain in other regions of Bangladesh.

The Lin–MSKF combination has simulated significant amount of NC rain (Figure 14i) at Barisal, Chittagong, Cox's Bazar, Kutubdia, Madaripur, M.Court, Patuakhali, Rangamati, Sitakunda and Sylhet regions and the amounts of rainfalls are 72, 58, 66, 62, 46, 122, 57, 93, 79 and 78 mm respectively. TheWSM6–MSKF, Thompson–MSKF and WDM6–MSKF combinations have simulated significant amount of NC rain at Feni and Khulna regions where the rainfall amounts are 65 and 40 mm (Figure 14j) and at Barisal region is 51 mm (Figure 14k) and at Feni and Sitakunda regions are 49 and 52 mm (Figure 14l) respectively and light NC rain in other regions of Bangladesh.

NC rain has simulated in the south–southeastern region of Bangladesh by all CP and MP schemes and maximum amount of NC is simulated by the MSKF scheme on 7 May 2013.

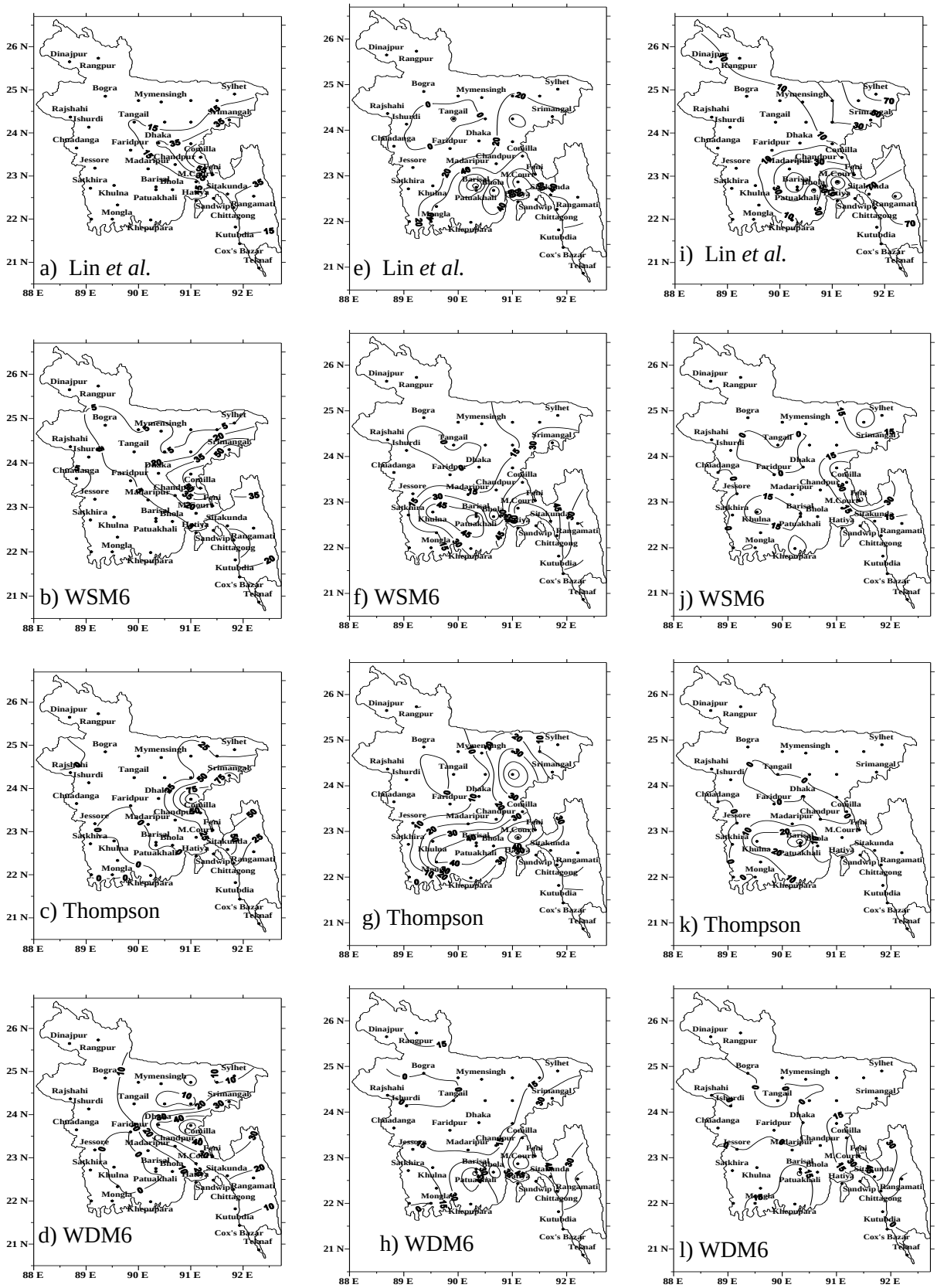

Figure 14: Distribution of model simulated NC rain using Lin *et al.*, WSM6, Thompson and WDM6 schemes in combination with MSKF scheme on (a–d) 4 May, (e–h) 6 May and (i–l) 7 May with the initial condition at 0000 UTC of 4, 6 and 7 May respectively.

4.1.9 Area average rainfall at 4, 6 and 7 May 2013

All Bangladesh observed and model simulated station average rainfall and station average observed and model simulated heavy rainfall in the S–SE region of the country using different MPs in combination with different CPs at 4, 6 and 7 May 2013 are presented in Figures 15(a–c) and Figures 15(d–f) respectively. The KF scheme coupling with Lin *et al.*, WSM6, Thompson and WDM6 schemes have simulated (Figure 15a) almost similar all Bangladesh station average rainfall as observed from 35 meteorological stations of all over Bangladesh on 4 May 2013 and other CP schemes in combination with four MP schemes have simulated much less average all Bangladesh rainfall than the observed. The Tiedtke scheme coupling with all MP schemes have simulated lowest average rainfall than that of observed all over Bangladesh.

The KF, ZM and MSKF schemes coupling with all MPs have simulated (Figures 15(b–c)) higher station average rainfall and Tiedtke scheme has simulated lower rainfall than that of observed from 35 meteorological stations of all over Bangladesh on 6 and 7 May 2013. The KF, ZM and MSKF schemes coupling with Lin *et al.* scheme have simulated maximum rainfall and Thompson–Tiedtke has simulated lowest station average rainfall on 6 and 7 May.

Lin *et al*, WSM6, Thompson and WDM6 schemes coupling with Tiedtke scheme has simulated minimum amount of rain in the heavy rainfall area on 4, 6 and 7 May where the observed rainfall is significantly higher (Figures 15(d–f)). On 4 May, all MPs coupling with Tiedtke and ZM schemes have simulated almost no rain and KF and MSKF schemes have simulated little amount of rain in the heavy rainfall region (Figure 15d). On 6 May, all MPs coupling with Tiedtke scheme has simulated almost no rain and KF, ZM and MSKF schemes have simulated heavy rain in the heavy rainfall region (Figure 15e), but the amount is also lower than that of observed. On 7 May, WDM6 coupling with KF, ZM and MSKF schemes have simulated almost similar amount of rain in the heavy rainfall region and all other combinations have simulated lower rain (Figure 15f), except Lin–ZM and Lin–MSKF combinations.

Tiedtke scheme has simulated lower rainfall in combination with all chosen MPs in all Bangladesh and also heavy rainfall area on 4, 6 and 7 May. KF scheme coupling with all MPs have simulated similar average rainfall all over Bangladesh on 4 May and WDM6 coupling with KF, ZM and MSKF schemes have simulated almost similar amount of rain in the heavy rainfall region on 7 May.

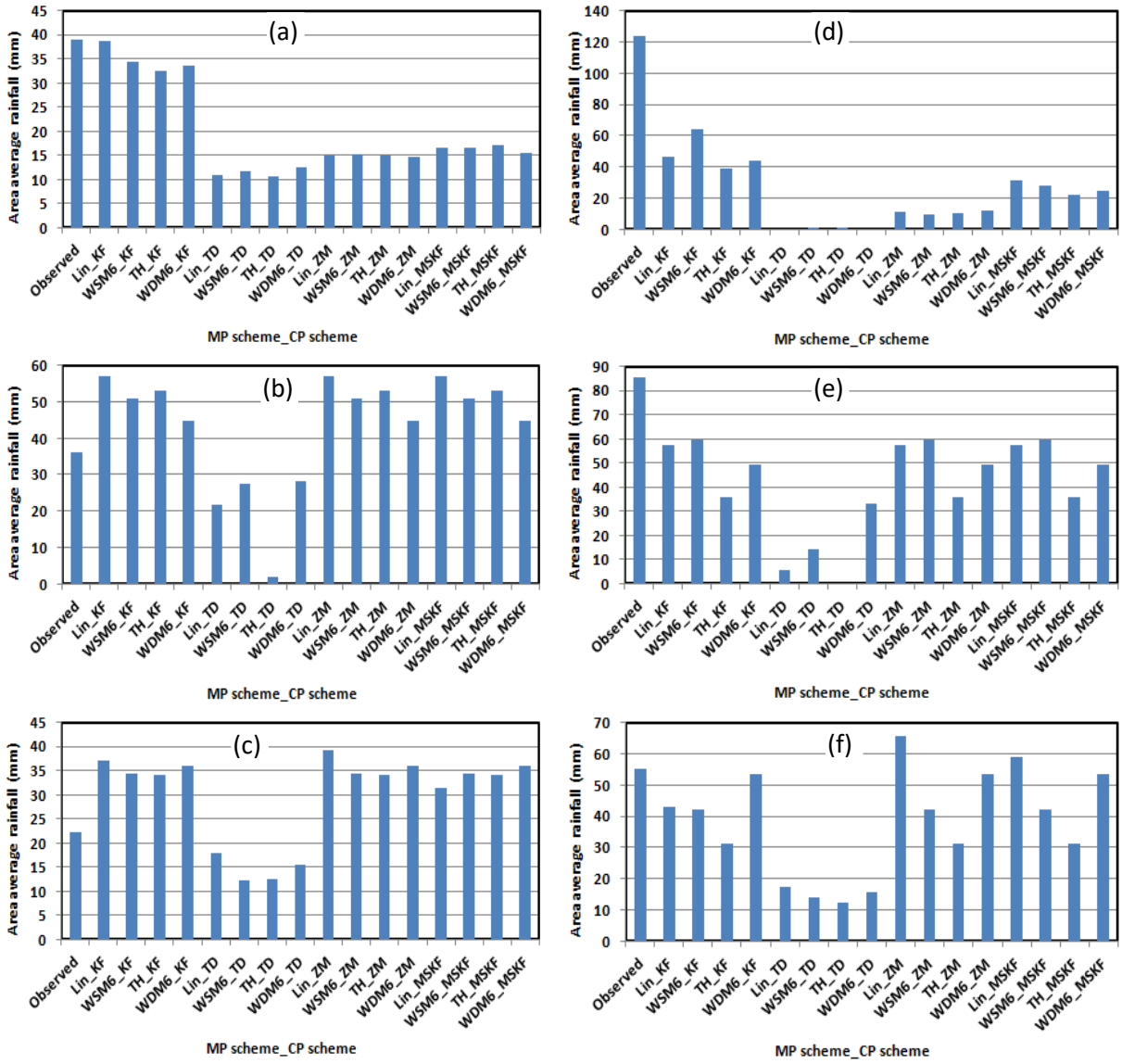

Figure 15: Station average (a–c) all Bangladesh observed and model simulated rainfall and (d–f) heavy rainfall in the S–SE region of the country using different MPs in combination with different CPs at 4, 6 and 7 May 2013 respectively.

4.1.11 Relative Humidity on heavy rainfall days of 4, 6 and 7 May 2013

The model simulated RH at 850 hPa level has been analyzed for the heavy rainfall days at 4, 6 and 7 May 2013 at 0900, 1200 and 0600 UTC using four different MP schemes coupling with four different CP schemes. The distribution pattern of RH is presented for all MPs and CPs with the initial condition at 0000 UTC of 6 May as shown in Figures 16(a–p). The KF and Tiedtke schemes coupling with all MPs have simulated high RH (90–95%) in the central to NE regions and low RH (50–70%) in the western to NW regions of Bangladesh and the ZM and MSKF schemes coupling with all MPs have simulated high RH (95–100%) in the central to eastern and NE regions and comparatively low RH in the western to NW regions of

the country on 4 May (Figure not shown). The distribution patterns of RH on 4 and 6 May are similar for all MPs in combination with all CPs all over Bangladesh but on 6 May the higher RH system shifted towards west from east. The model simulated higher RH almost covered all over the country on 7 May (Figure not shown) with the initial condition of 0000 UTC of 7 May.

All CPs coupling with all MPs have simulated higher RH in the eastern and NE regions of the country on 4 May and almost all over Bangladesh on 6 and 7 May 2013. The maximum amount of rainfall is simulated in a region where RH is significantly high. This suggests that the amount of rainfalls in an area is directly proportional to the RH of that area.

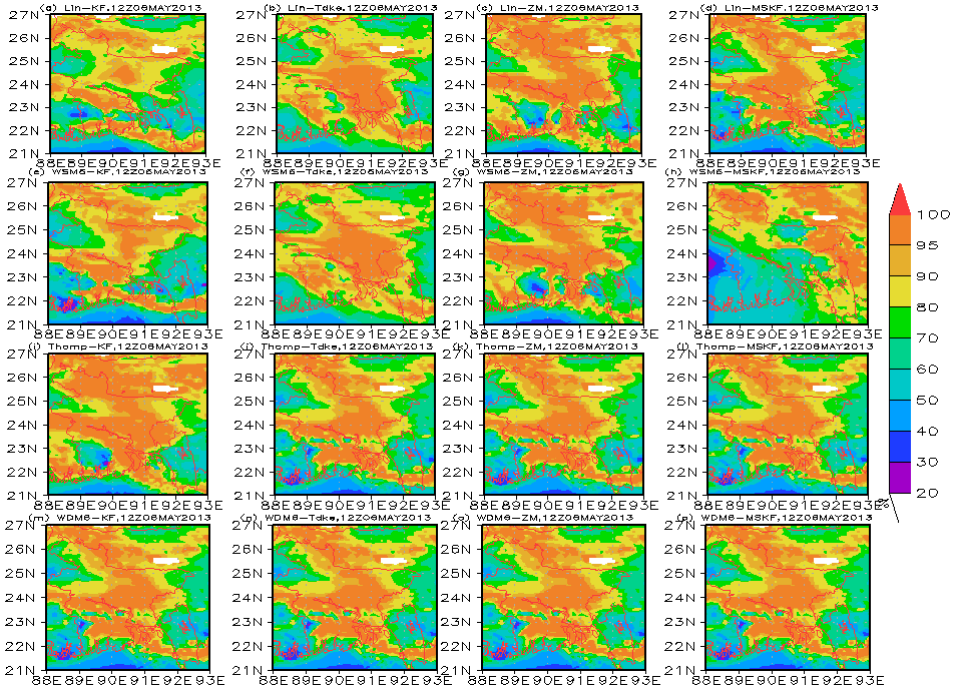

Figure 16: Model simulated RH at 850 hPa level using (a–d) Lin *et al*., (e–h) WSM6, (i–l) Thompson and (m–p) WDM6 schemes in combination with KF, Tiedtke, ZM and MSKF schemes respectively at 1200 UTC of 6 May with the initial condition at 0000 UTC of 6 May 2013.

4.1.12 Vertical Velocity at 4, 6 and 7 May 2013

The model simulated vertical velocity at 300 hPa level has been analyzed and plotted at 1200 UTC, 0900 UTC and 1200 UTC of 4, 6 and 7 May 2013 using four different MPs coupling with four different CPs and are shown in Figures 17(a–p) respectively. KF scheme in combination with four different MP schemes has simulated maximum vertical velocity of 5 ms^{-1} in the central region but it is directed from west towards southern region of the country.

ZM scheme in combination with four different MP schemes has simulated maximum vertical velocity of 5 ms^{-1} in the western to central region of the country. MSKF scheme in combination with different MPs have simulated maximum vertical velocity 5 ms^{-1} in the central region but it is directed from west towards eastern region of the country at 1200 UTC of 4 May with the initial conditions at 0000 UTC of 4 May. Tiedtke scheme in combination with four different MP schemes has simulated maximum vertical velocity equals to 2–2.5 ms^{-1} (Figure not shown) in the western region of the country at 1200 UTC of 4 May with the initial condition at 0000 UTC of 4 May.

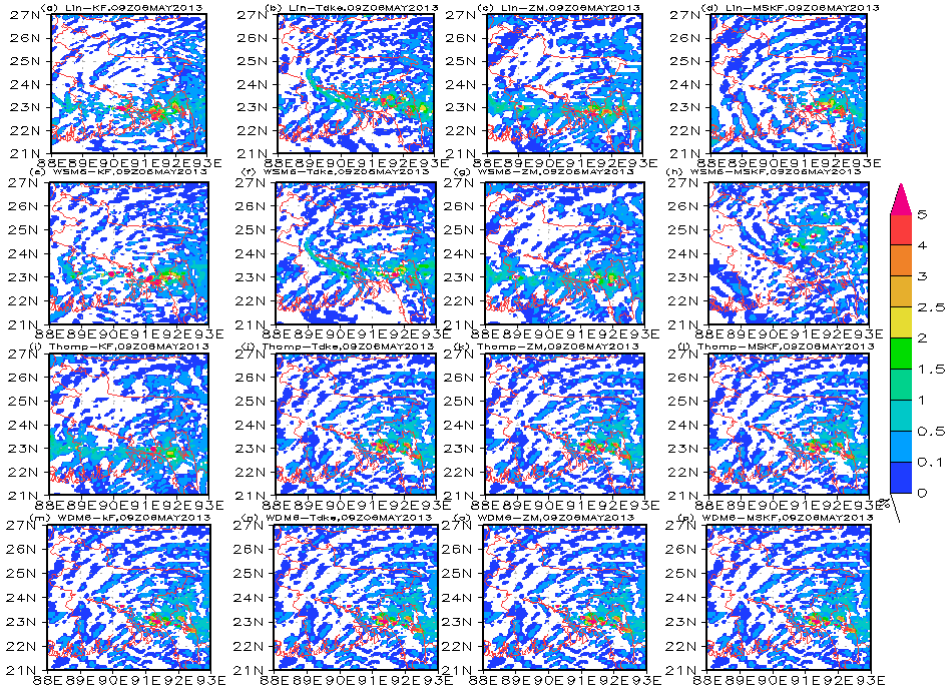

Figure 17: Model simulated vertical velocity at 300 hPa level using (a–d) Lin *et al.*, (e–h) WSM6, (i–l) Thompson and (m–p) WDM6 schemes in combination with KF, Tiedtke, ZM and MSKF schemes respectively at 0900 UTC of 6 May with the initial condition at 0000 UTC of 6 May 2013.

KF, Tiedtke, ZM and MSKF schemes in combination with different MPs have simulated maximum vertical velocity of 5 ms^{-1} in the central to eastern region of the country (Figures 17(a–p)) at 0900 UTC of 6 May with the initial conditions at 0000 UTC of 6 May. KF and MSKF schemes in combination with four different MP schemes have simulated maximum vertical velocity of 5 ms^{-1} in the southwestern and in the southern to eastern regions (Figure not shown) of the country respectively at 1200 UTC of 7 May with the initial condition at 0000 UTC of 7 May 2013. Tiedtke and ZM schemes in combination with four different MP

schemes have simulated maximum vertical velocity of 1–2 ms^{-1} in the south–southeastern region of the country at 1200 UTC of 7 May with the initial condition at 0000 UTC of 7 May.

KF and MSKF schemes in combination with Lin *et al.* and WDM6 schemes have simulated maximum vertical velocity of 5 m s^{-1} in the central to S-SE region with the initial conditions at 0000 UTC 4, 6 and 7 May 2013. Tiedtke and ZM schemes in combination with all MPs have simulated less vertical velocity during the simulation period. The vertical velocity is higher means more convection and more rainfall to occur.

4.1.13 Reflectivity at 4, 6 and 7 May 2013

The model simulated reflectivity at 850 hPa level has been analyzed at 1200 UTC, 0900 UTC and 1200 UTC of 4, 6 and 7 May 2013 using four different MPs coupling with four different CPs and plotted for 0900 UTC of 6 May in Figures 18(a–p) respectively. KF and MSKF schemes in combination with four different MP schemes have simulated maximum reflectivity of 54 dBZ in the west to east through central region of the country at 1200 UTC of 4 May with the initial conditions at 0000 UTC of 4 May. ZM scheme in combination with four different MP schemes have simulated maximum reflectivity of 54 dBZ in the western to central region of the country and Tiedtke scheme in combination with four different MP schemes have simulated less reflectivity of 20–30 dBZ (Figure not shown) in the western to eastern through the central region of the country at 1200 UTC of 4 May with the initial condition at 0000 UTC of 4 May. KF, Tiedtke, ZM and MSKF schemes in combination with different MPs have simulated maximum reflectivity of 54 dBZ in the western to eastern through southern region of the country as shown in Figures 18(a–p) at 0900 UTC of 6 May except little anomalies with the initial condition at 0000 UTC of 6 May. Lin–Tiedtke and WSM6–Tiedtke have simulated reflectivity of 20–30 dBZ and Lin–MSKF has simulated maximum in the northeastern region of the country.

KF and MSKF schemes in combination with four different MP schemes have simulated maximum reflectivity of 54 dBZ in the southwestern and in the southern to eastern regions (Figure not shown) of the country respectively at 1200 UTC of 7 May with the initial conditions at 0000 UTC of 7 May 2013. Tiedtke and ZM schemes in combination with four different MP schemes have not simulated sufficient reflectivity (Figure not shown) all over the country at 1200 UTC of 7 May with the initial conditions at 0000 UTC of 7 May. KF and MSKF schemes in combination with four different MP schemes have simulated maximum reflectivity of 54 dBZ in different regions at 4, 6 and 7 May 2013.

The probability of heavy rain is higher in those regions where the reflectivity is higher. It has seen that where the reflectivity is higher, the amount of convective and non–convective rain is also higher in that region during 4, 6 and 7 May 2013. Higher reflectivity is directly proportional to the higher amounts of rainfall.

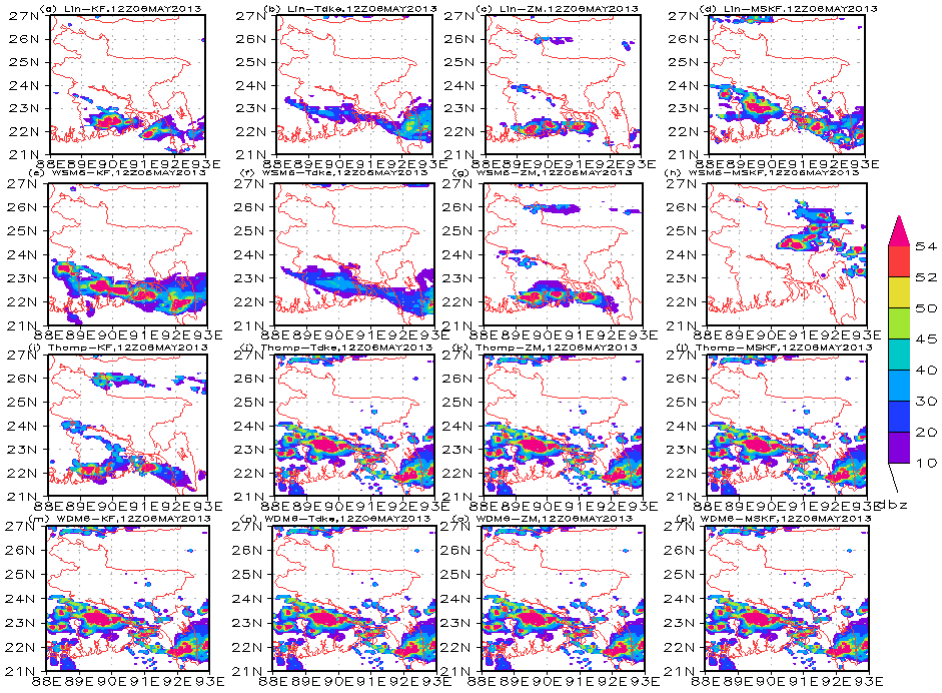

Figure 18: Model simulated reflectivity at 850 hPa level using (a–d) Lin *et al*., (e–h) WSM6, (i–l) Thompson and (m–p) WDM6 schemes in combination with KF, Tiedtke, ZM and MSKF schemes respectively at 1200 UTC of 6 May with the initial condition at 0000 UTC of 6 May 2013.

4.1.14 Vorticity at 4, 6 and 7 May 2013

The model simulated vorticity at 850 hPa level has been analyzed at 1200 UTC of 4, 6 and 7 May 2013 using four different MPs coupling with four different CPs and plotted for 1200 UTC of 6 May in Figures 19(a–p) respectively. KF and MSKF schemes in combination with four different MP schemes have simulated maximum vorticity of 60×10^{-5}/s in the west to east through central region of the country at 1200 UTC of 4 May with the initial conditions at 0000 UTC of 4 May. ZM scheme in combination with WSM6, Thompson and WDM6 schemes has simulated maximum vorticity of 60×10^{-5}/s in the western to central region and Lin *et al.* scheme has simulated in the western to eastern through central region of the country. Tiedtke scheme in combination with four different MP schemes have simulated maximum Vorticity band (Figure not shown) in the southwestern region of the country at 1200 UTC of 4 May with the initial conditions at 0000 UTC of 4 May. KF, Tiedtke, ZM and

MSKF schemes in combination with different MPs have simulated maximum vorticity of 60×10^{-5}/s in the western to eastern through southern region of the country can be seen from Figures 18(a–p) at 1200 UTC of 6 May except Lin–Tiedtke and WSM6–Tidetke with the initial conditions at 0000 UTC of 6 May. Lin–Tiedtke and WSM6–Tiedtke have simulated vorticity of (30–40) $\times10^{-5}$/s in the southwestern region of the country.

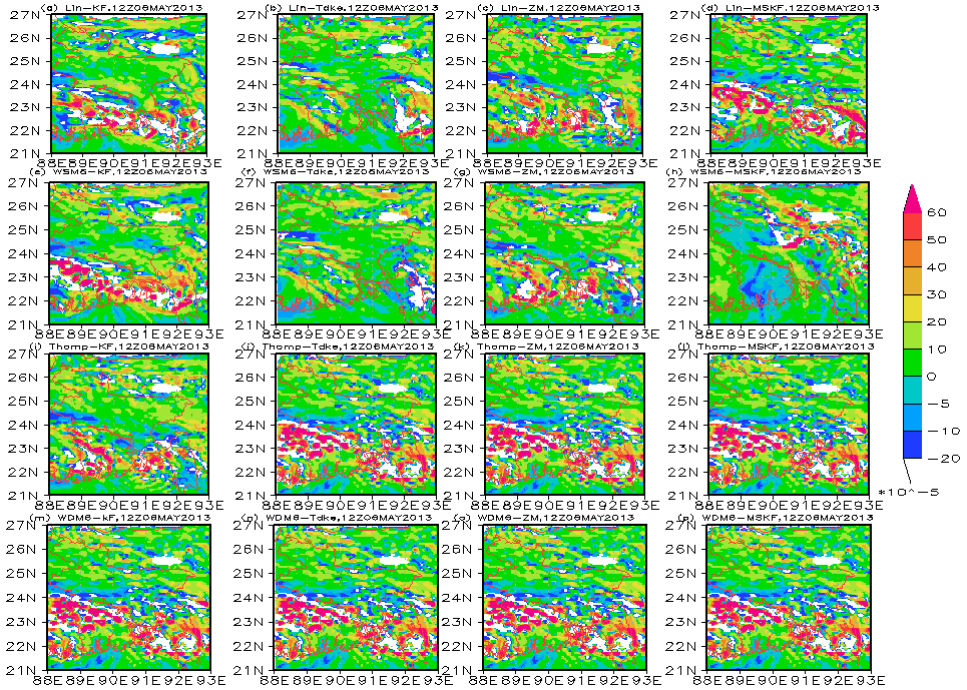

Figure 19: Model simulated vorticity at 850 hPa level using (a–d) Lin *et al*., (e–h) WSM6, (i–l) Thompson and (m–p) WDM6 schemes in combination with KF, Tiedtke, ZM and MSKF schemes respectively at 1200 UTC of 6 May with the initial condition at 0000 UTC of 6 May 2013.

KF, ZM and MSKF schemes in combination with four different MP schemes have simulated maximum vorticity of 60×10^{-5}/s in the western to eastern regions through southern regions (Figure not shown) of the country respectively at 1200 UTC of 7 May with the initial conditions at 0000 UTC of 7 May 2013. Tiedtke scheme in combination with four different MP schemes have not simulated sufficient vorticity (Figure not shown) all over the country at 1200 UTC of 7 May with the initial conditions at 0000 UTC of 7 May.

KF, ZM and MSKF schemes in combination with Thompson and WDM6 schemes have simulated maximum vorticity of 60×10^{-5}/s in the western to eastern region through central and southern region with the initial condition at 0000 UTC 4, 6 and 7 May 2013 respectively. It is observed that where the vorticity is higher the amounts of rainfall are also higher.

Tiedtke and ZM schemes in combination with all MPs have simulated less vertical vorticity during the simulation period.

4.1.15 Different verification methods of rainfall at 4, 6 and 7 May 2013

For the prediction of correct forecast threat score (TS), equitable threat score (ETS), bias score (BS) and Standard Deviation (SD) have been estimated for different heavy rainfall events. The model simulated heavy rain predicted region, predicted area (km^2), observed heavy rainfall region and intersected regions and intersected area (km^2) have been identified for different combination of MPs and CPs on 4, 6 and 7 May 2013 and are presented in Table 1–Table 3 for the initial conditions at 0000 UTC of 4, 6 and 7 May respectively. The observed heavy rain region lies between 90.7–92.3^{o}E and 22.5–25.1^{o}N and the area is 47486.78 km^2.

Table 1: Threat score, equitable threat score, bias score and standard deviation for the heavy rainfall region on 4 May for different combination of MPs and CPs with the initial condition at 0000 UTC of 4 May 2013

CPs	MPs	Threat Score TS = H/(O+F–H)	Equitable Threat Score ETS = (H–R)/(O+F–H–R)	Bias Score BS = F/O	Standard Deviation
KF	Lin	0.471	0.397	1.14	42.46
	WSM6	0.434	0.349	1.39	34.68
	Thompson	0.502	0.424	1.38	34.42
	WDM6	0.453	0.377	1.16	33.46
Tiedtke	Lin	0.416	0.371	0.47	15.10
	WSM6	0.286	0.241	0.42	16.80
	Thompson	0.185	0.141	0.38	15.11
	WDM6	0.274	0.239	0.30	19.49
ZM	Lin	0.580	0.529	0.78	15.18
	WSM6	0.189	0.121	0.72	16.76
	Thompson	0.488	0.431	0.76	17.17
	WDM6	0.662	0.615	0.90	15.43
MSKF	Lin	0.488	0.437	0.65	23.33
	WSM6	0.473	0.418	0.68	21.44
	Thompson	0.459	0.398	0.82	28.88
	WDM6	0.469	0.408	0.81	16.75

The highest and lowest values of TS are found 0.662 and 0.185 for WDM6–ZM and Thompson–Tiedtke combinations respectively. The highest and lowest values of ETS are found from WDM6–ZM and WSM6–ZM combinations and are 0.615 and 0.121 respectively. The highest and lowest values of BS are found from WSM6–KF and Thompson–Tiedtke combinations and are 1.39 and 0.38 respectively. The highest and lowest values of SD are

found from Lin–KF and Lin–Tiedtke combinations are 42.46 and 15.10 respectively. The lower values of SD indicate the similarity of the model simulated and observed rainfall.

TS and ETS are applicable to validate the accuracy of forecasts without the contribution from the correct rejections events. The accuracy of forecasts is higher as TS and ETS approaches to the maximum value of unity. The obtained TS and ETS scores suggest that the WDM6–ZM combination give the better forecast among all studied combinations. The bias score is greater than 1 for all MPs in combination with KF scheme and suggests that the KF scheme over–predicts the rain occurrence and other CPs under predicts rain occurrence. The bias score is 0.90 for WDM6–ZM combination indicates the better performance.

The maximum values of TS, ETS and BS are found 0.662, 0.615 and 0.90 respectively and the minimum value of SD is found 15.43 for WDM6–ZM combination, which suggest that the WDM6–ZM combination gives the better performance than those of other combinations on 4 May 2013.

Table 2: TS, ETS, BS and SD for the heavy rainfall region on 6 May for different combination of MPs and CPs with the initial condition at 0000 UTC of 6 May 2013

CPs	MPs	Threat Score TS = H/(O+F–H)	Equitable Threat Score ETS = (H–R)/(O+F–H–R)	Bias Score BS = F/O	Standard Deviation
KF	Lin	0.711	0.633	1.12	40.10
	WSM6	0.718	0.631	1.39	33.19
	Thompson	0.608	0.491	1.53	32.44
	WDM6	0.626	0.519	1.38	29.62
Tiedtke	Lin	0.386	0.300	0.61	27.32
	WSM6	0.463	0.372	0.73	27.58
	Thompson	0.079	0.034	0.22	4.57
	WDM6	0.641	0.559	0.92	31.39
ZM	Lin	0.711	0.633	1.12	40.10
	WSM6	0.801	0.742	1.16	33.19
	Thompson	0.550	0.443	1.11	32.44
	WDM6	0.565	0.450	1.33	29.62
MSKF	Lin	0.711	0.633	1.12	40.10
	WSM6	0.775	0.709	1.20	33.19
	Thompson	0.416	0.273	1.45	32.44
	WDM6	0.581	0.496	0.83	29.62

The heavy rain observed region lies between 89.9–92.3^{o}E and 21.9–24.5^{o}N and the area is 71555 km^2 on 6 May 2013. The model simulated heavy rain predicted region, predicted area (km^2), intersected regions and intersected area (km^2) have been identified for different combination of MPs and CPs on 6 May 2013 for the initial condition at 0000 UTC of 6 May

and are presented in Table 2. The KF scheme coupling with Lin *et al.*, WSM6, Thompson and WDM6 schemes have simulated heavy rain predicted region and intersected region of observed and model simulated heavy rain predicted region lies between 89.2–92.3°E & 21.9–25.1°N and 89.9–92.3°E & 21.9–24.5°N respectively. The Tiedtke scheme coupling with different MPs have simulated heavy rain predicted region and intersected region of observed and model simulated heavy rain predicted region lies between 90.1–92.3°E & 21.9–25.1°N and 90.1–92.3°E & 21.9–24.5°N respectively.

The ZM scheme coupling with different MPs have simulated heavy rain predicted region and intersected region of observed and model simulated heavy rain predicted region lies between 89.3–91.7°E & 21.9–25.2°N and 89.9–92.3°E & 21.9–25.5°N respectively. The MSKF scheme coupling with MPs have simulated heavy rain predicted region and intersected region of observed and model simulated heavy rain predicted region lies between 89.3–92.3°E & 21.9–25.8°N and 89.9–92.3°E & 21.9–24.5°N respectively.

The obtained TS scores 0.801 and 0.718 for WSM6–ZM and WSM6–KF combinations and 0.711 for Lin *et al.* scheme coupling with KF, ZM and MSKF gives the better forecast. Thompson–Tiedtke combination gives the worse forecast among all the combinations. The obtained ETS score 0.742 and 0.034 also suggests that the WSM6–ZM and Thompson–Tiedtke combinations give the better and worse forecast among all studied combinations. The bias score (Table 2) for all MPs in combination with KF, ZM and MSKF schemes suggest the over prediction of rain–occurrence and Tiedtke scheme under predicts the rain occurrence all over the country. The highest value of SD 40.10 is found for Lin–KF, Lin–ZM and Lin–MSKF combinations and lowest value 4.57 is found for Thompson–Tiedtke combination. The maximum values of TS and ETS are found 0.801 and 0.742 respectively and BS and SD are found 1.16 and 33.19 for WSM6–ZM combination, which suggest that the WSM6–ZM combination gives the better performance than those of other combinations on 6 May 2013.

The observed heavy rain region lies between 90.6–91.5°E and 21.9–24.2°N and the area is 23764 km^2 on 7 May 2013. The KF scheme coupling with Lin *et al.*, WSM6, Thompson and WDM6 schemes have simulated heavy rain predicted region and intersected region are 89.3–92.0°E & 22.0–24.1°N and 90.6–91.5°E & 22.0–24.1°N respectively with the initial conditions at 0000 UTC of 7 May 2013. The Tiedtke scheme coupling with MPs has simulated heavy rain predicted region and intersected regions are 90.2–92.3°E & 22.0–25.1°N and 90.6–91.5°E & 22.0–24.2°N respectively. The ZM scheme coupling with MPs has simulated heavy rain predicted region and intersected regions are 89.2–92.3°E & 22.0–25.0°N

and 90.6–91.5°E & 22.0–24.2°N respectively. The MSKF scheme coupling with MPs has simulated heavy rain predicted region and intersected regions are 89.2–92.0°E & 21.9–24.2°N and 90.6–91.9°E & 21.9–24.2°N respectively. The value of obtained TS is 0.522 and 0.147 for WDM6–MSKF and WSM6–MSKF combinations and gives the better forecast and worse forecast. The values of ETS are 0.478 and 0.087, which also suggest that the WDM6–MSKFand WSM6–MSKF combinations give the better and worse forecast among all studied combinations. The bias score (Table 3) suggests the over prediction of rain–occurrence all over the country for all MPs in combination with KF, ZM, Tiedtke and MSKF schemes. The highest and lowest values of BS are found from WDM6–Tiedtke and WDM6–KF combinations and are 3.03 and 1.39 respectively. The highest and lowest values of SD are found 32.99 and 13.48 for Lin–MSKF and WSM6–Tiedtke & Thompson–Tiedtke combinations.

Table 3: TS, ETS, BS and SD for the heavy rainfall region on 7 May for different combination of MPs and CPs with the initial condition at 0000 UTC of 7 May 2013

CPs	MPs	Threat Score TS = H/(O+F–H)	Equitable Threat Score ETS = (H–R)/(O+F–H–R)	Bias Score BS = F/O	Standard Deviation
KF	Lin	0.306	0.255	2.03	28.01
	WSM6	0.323	0.268	2.74	22.66
	Thompson	0.313	0.264	1.84	28.35
	WDM6	0.312	0.268	1.39	26.13
Tiedtke	Lin	0.343	0.288	2.74	23.52
	WSM6	0.302	0.245	2.93	13.48
	Thompson	0.318	0.264	2.42	13.48
	WDM6	0.293	0.234	3.03	18.00
ZM	Lin	0.362	0.309	2.60	28.63
	WSM6	0.328	0.272	2.87	22.66
	Thompson	0.358	0.310	1.93	28.35
	WDM6	0.295	0.241	2.44	26.13
MSKF	Lin	0.335	0.287	1.78	32.99
	WSM6	0.147	0.087	2.74	22.66
	Thompson	0.312	0.261	2.12	28.35
	WDM6	0.522	0.478	2.48	26.13

The maximum values of TS and ETS are found 0.522 and 0.478 respectively and BS and SD are found 2.48 and 26.13 for WDM6–MSKF combination, which suggest that the WDM6–MSKF combination gives the better performance than those of other combinations on 7 May 2013.

4.2 Heavy rainfall event during 15–16 May 2013

The four different microphysics schemes (e.g. Lin *et al*., WSM6, Thompson and WDM6) and four different cumulus parameterization schemes (e.g., KF, Tiedtke, ZM and MSKF) in WRF Model have been used to simulate the different parameters of heavy rainfall event during 15–16 May 2013.

4.2.1 Observed and Model Simulated Rainfall on 15 May 2013

The observed rainfall over Bangladesh at 15 and 16 May 2013 is presented in Figures 20(a–b). The heavy rainfall is observed at Barisal, Bhola, Feni, Hatiya, Khepupara, Madaripur and Patuakhali regions are 95, 78, 67, 54, 232, 50 and 123 mm respectively on 15 May (Figure 20a) and light rainfall is found in other regions of Bangladesh.

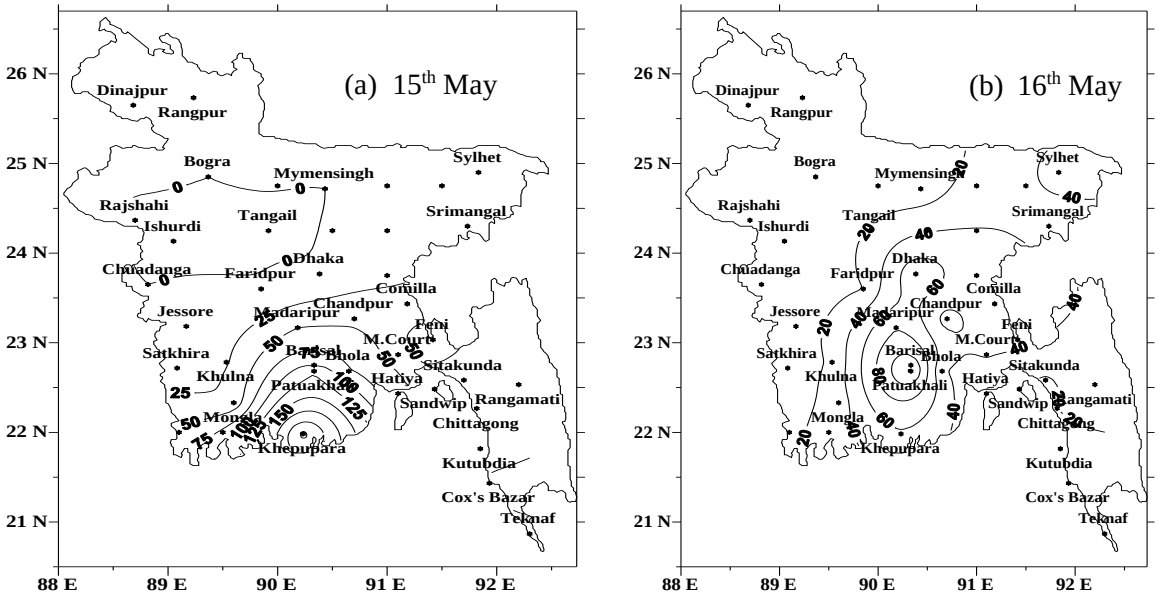

Figure 20: Distribution of observed rainfall at (a) 15 and (b) 16 May 2013 respectively.

The model simulated rainfall using four different MP schemes coupled with four different CPs on 15 May 2013 is presented in Figures 21(a–l) and Figures 23(a–d). The Lin–KF combination is simulated heavy rainfall at Mongla, Patuakhali and Satkhira regions are 265, 51 and 76 mm (Figure 21a) respectively and light rainfall in other regions of the country.

The WSM6–KF, Thompson–KF and WDM6–KF combinations have simulated heavy rainfall at Bhola, Khulna and Mongla regions and the rainfall amounts are 77, 60 and 78 mm (Figure 21b) and 71, 151 and 90 mm (Figure 21c) and 59, 79 and 70 mm (Figure 21d) respectively and the model has simulated light rainfall in other regions of the country on 15 May. The Lin–Tiedtke regions where the rainfall amounts combination has simulated heavy rainfall

(Figure 21e) at Mongla, Patuakhali and Satkhira regions are 265, 51 and 76 mm respectively and the other combination has simulated light rainfall in other regions of the country.

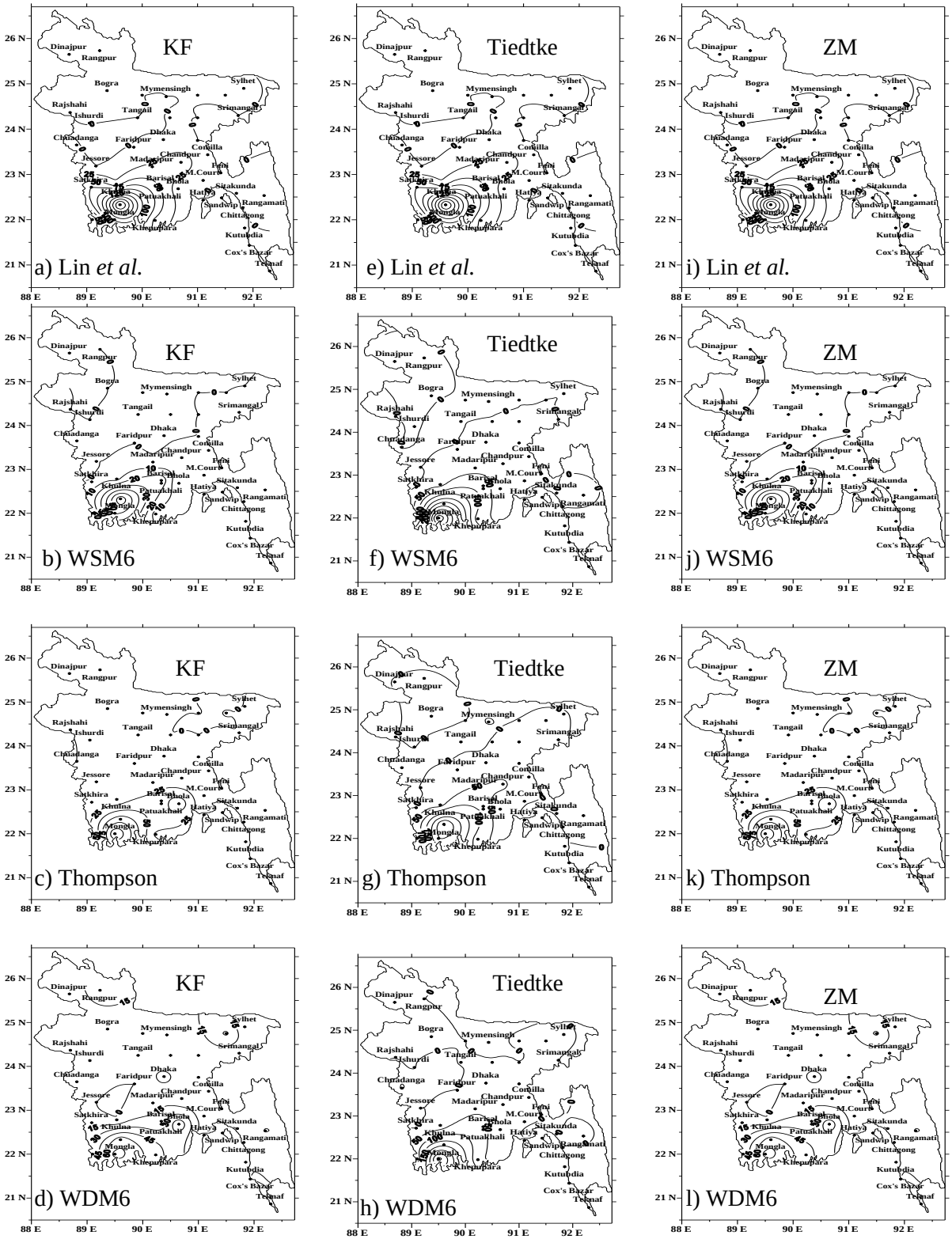

Figure 21: Distribution of model simulated (a–l) rainfall using Lin *et al*., WSM6, Thompson and WDM6 schemes in combination with KF, Tiedtke and ZM schemes on 15 May with the initial condition at 0000 UTC of 15 May 2013.

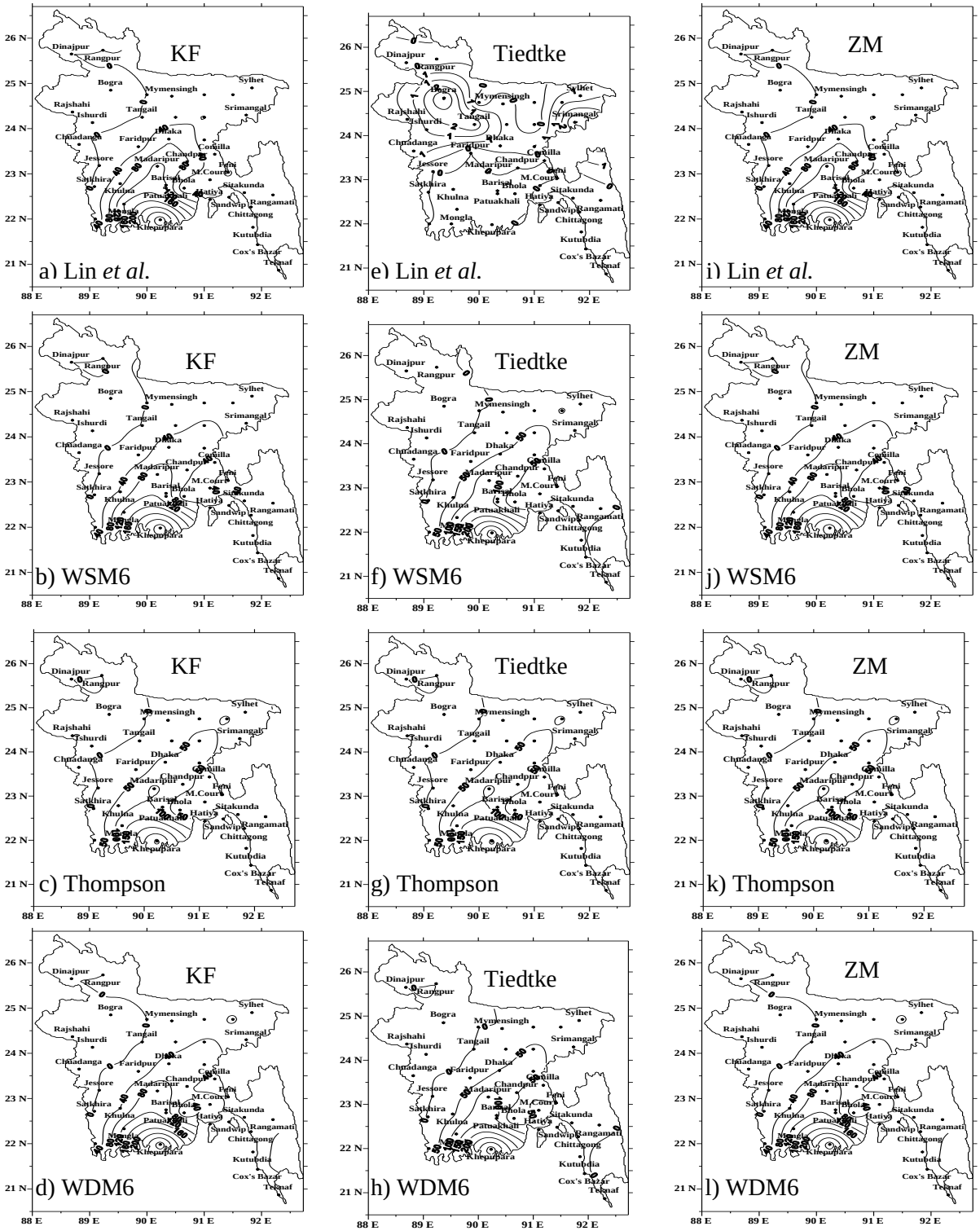

Figure 22: Distribution of model simulated (a–l) rainfall using Lin *et al*., WSM6, Thompson and WDM6 schemes in combination with KF, Tiedtke and ZM schemes on 16 May with the initial condition at 0000 UTC of 16 May 2013.

The WSM6–Tiedtke has simulated heavy rainfall (Figure 21f) at Barisal, Khepupara, Mongla and Patuakhali regions where the rainfall amounts are 80, 71, 276 and 86 mm respectively and light rainfall in other regions of Bangladesh. The Thompson–Tiedtke and WDM6–

Tiedtke combinations have simulated heavy rainfall at Barisal, Chandpur, Khepupara, Madaripur, Mongla and Patuakhali regions where the rainfall amounts are 79, 63, 69, 55, 311 and 91 mm (Figure 21g) and 73, 28, 61, 42, 187 and 67 mm (Figure 21h) respectively.

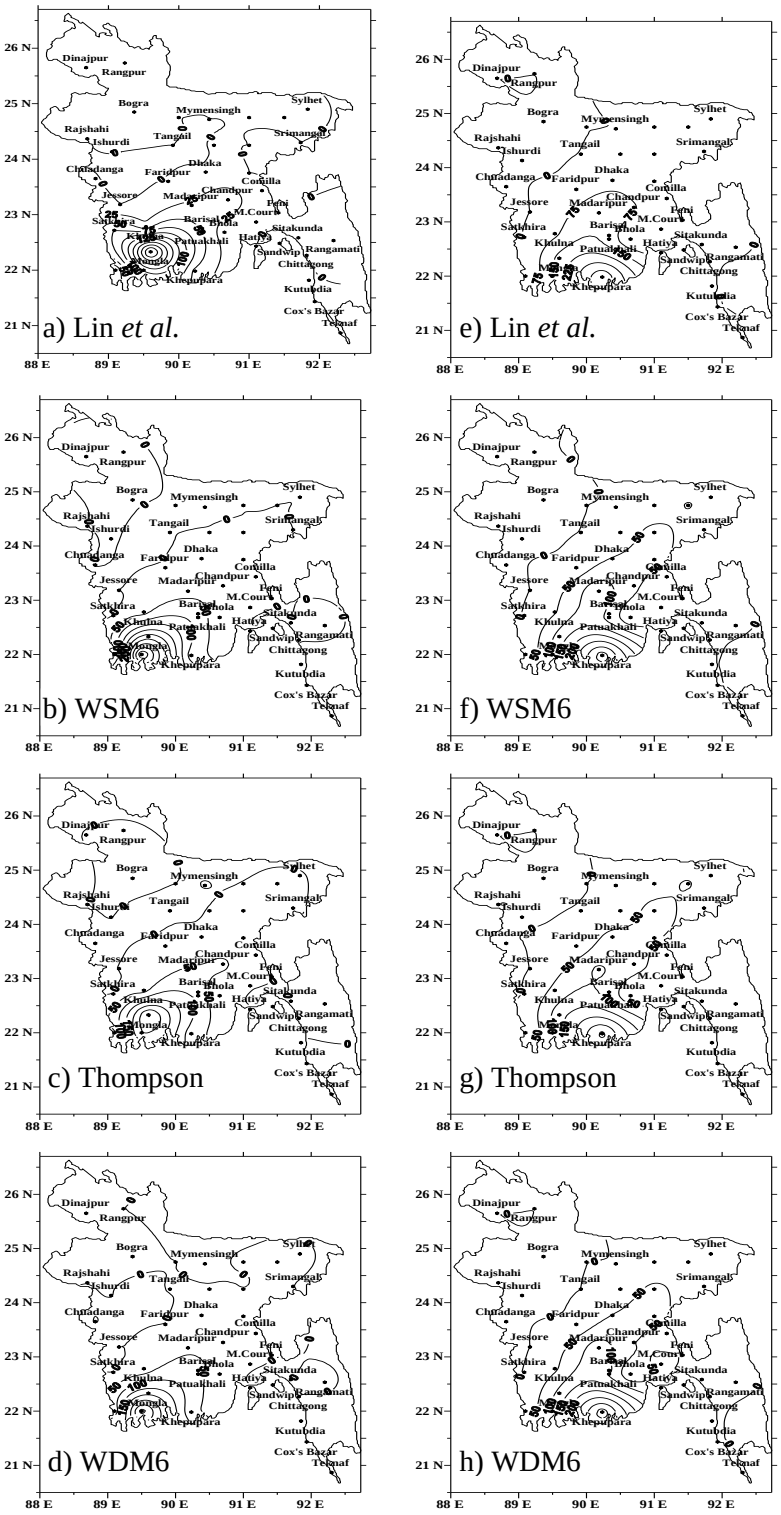

Figure 23: Distribution of model simulated rainfall using Lin *et al.*, WSM6, Thompson and WDM6 schemes in combination with MSKF scheme on (a–d) 15 May and (e–h)16 May with the initial conditions at 0000 UTC of 15 and 16 May respectively.

The Lin–ZM has simulated heavy rainfall (Figure 21i) at Mongla, Patuakhali and Satkhira regions where the rainfall amounts are 265, 51 and 76 mm respectively and light rainfall in other regions of Bangladesh. The WSM6–ZM, Thompson–ZM and WDM6–ZM combinations have simulated heavy rainfall at Bhola, Khulna and Mongla regions where the rainfall amounts are 77, 60 and 78 mm (Figure 21j), 71, 151 and 90 mm (Figure 21k) and 59, 79 and 70 mm (Figure 21l) respectively and light rainfall in other regions of Bangladesh. The Lin–MSKF combination has simulated heavy rainfall of 265, 51 and 76 mm (Figure 23a) at Mongla, Patuakhali and Satkhira regions respectively. The WSM6–MSKF has simulated heavy rainfall (Figure 23b) at Barisal, Khepupara, Mongla and Patuakhali regions where the rainfall amounts are 80, 71, 276 and 86 mm respectively. Thompson and WDM6 schemes in combination with MSKF scheme has simulated heavy rainfall at Barisal, Chandpur, Khepupara, Madaripur, Mongla and Patuakhali regions where the rainfall amounts are 79, 63, 69, 55, 311 and 91 mm (Figure 23c) and 73, 28, 61, 42, 187 and 67 mm (Figure 23d) respectively.

The model simulated significantly heavy rainfall region is almost matched with the observed rainfall on 15 May 2013 for KF and ZM schemes in combination with all MPs but the position of maximum rainfall has shifted from Khepupara to Mongla.

4.2.2 Observed and Model Simulated Rainfall on 16 May 2013

The heavy rainfall is observed at Barisal, Comilla, Dhaka, Khepupara, Madaripur and Patuakhali regions where the rainfall amounts are 115, 61, 75, 58, 79 and 123 mm (Figure 20b) respectively on 16 May. The model simulated very heavy rainfall using four different MP schemes coupling with four different CPs on 16 May 2013 are presented in Figures 22(a–l) and Figures 23(e–h). The KF scheme coupling with Lin *et al.*, WSM6, Thompson and WDM6 schemes have simulated heavy rainfall at Barisal, Chandpur, Dhaka, Feni, Hatiya, Khepupara, Khulna, Madaripur, Mongla and Patuakhali regions where the rainfall amounts are 124, 84, 77, 45, 50, 350, 67, 133, 161 and 106 mm for Lin–KF (Figure 22a), 104, 46, 68, 55, 35, 309, 44, 115, 127 and 96 mm for WSM6–KF (Figure 22b), 81, 64, 67, 51, 43, 316, 62, 112, 134 and 75 mm for Thompson–KF (Figure 22c) and 98, 42, 59, 34, 46, 344, 39, 121, 127 and 90 mm for WDM6–KF (Figure 22d) combinations respectively.

The Lin–Tiedtke has not simulated (Figure 22e) so much rainfall all over the country. The Tiedtke scheme coupling with WSM6, Thompson and WDM6 schemes have simulated heavy rainfall (Figures 22(f–h)) in the central to southern and SW regions of Bangladesh and light

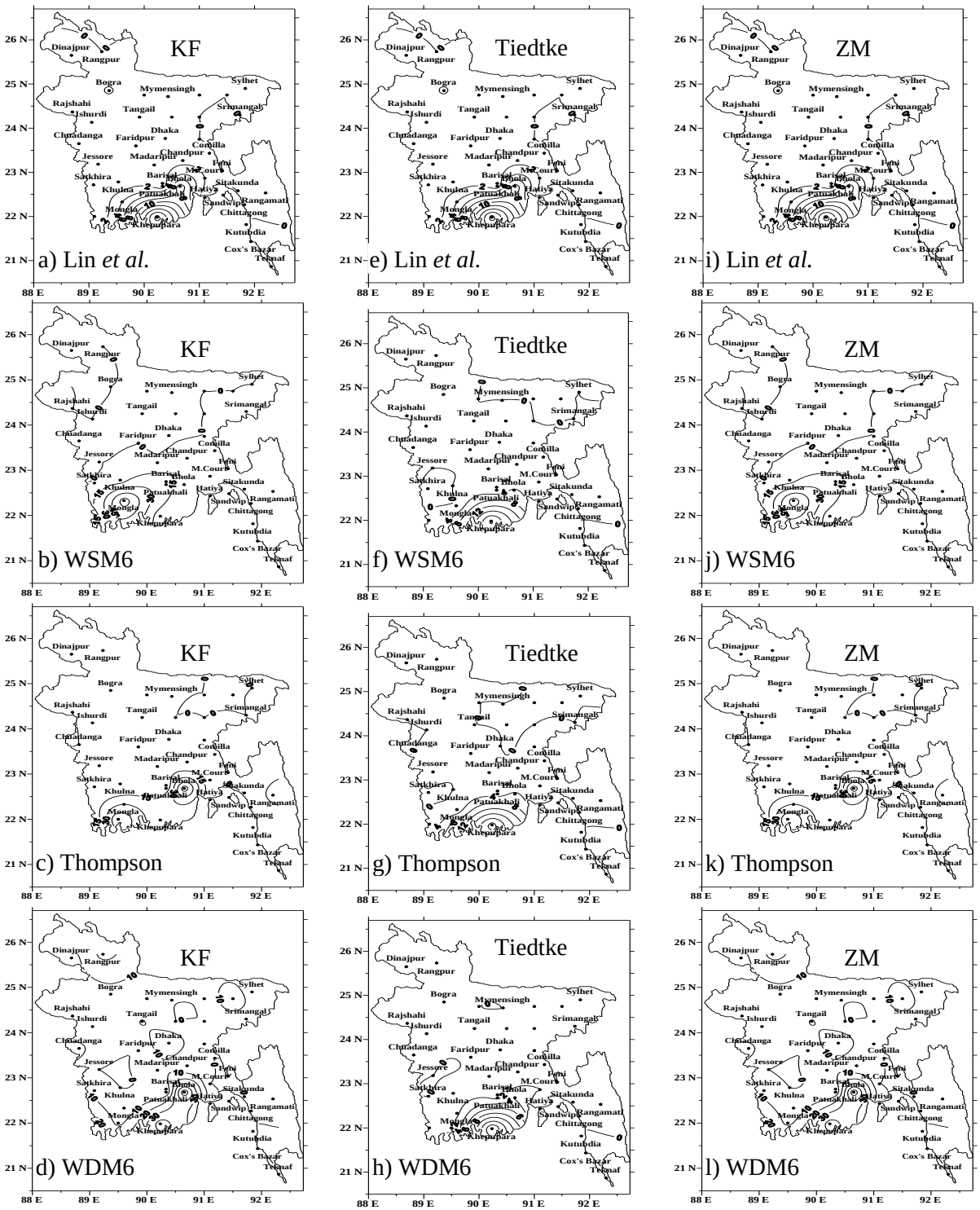

Figure 24: Distribution of model simulated (a–l) convective rain using Lin *et al.*, WSM6, Thompson and WDM6 schemes in combination with KF, Tiedtke and ZM schemes on 15 May with the initial condition at 0000 UTC of 15 May 2013.

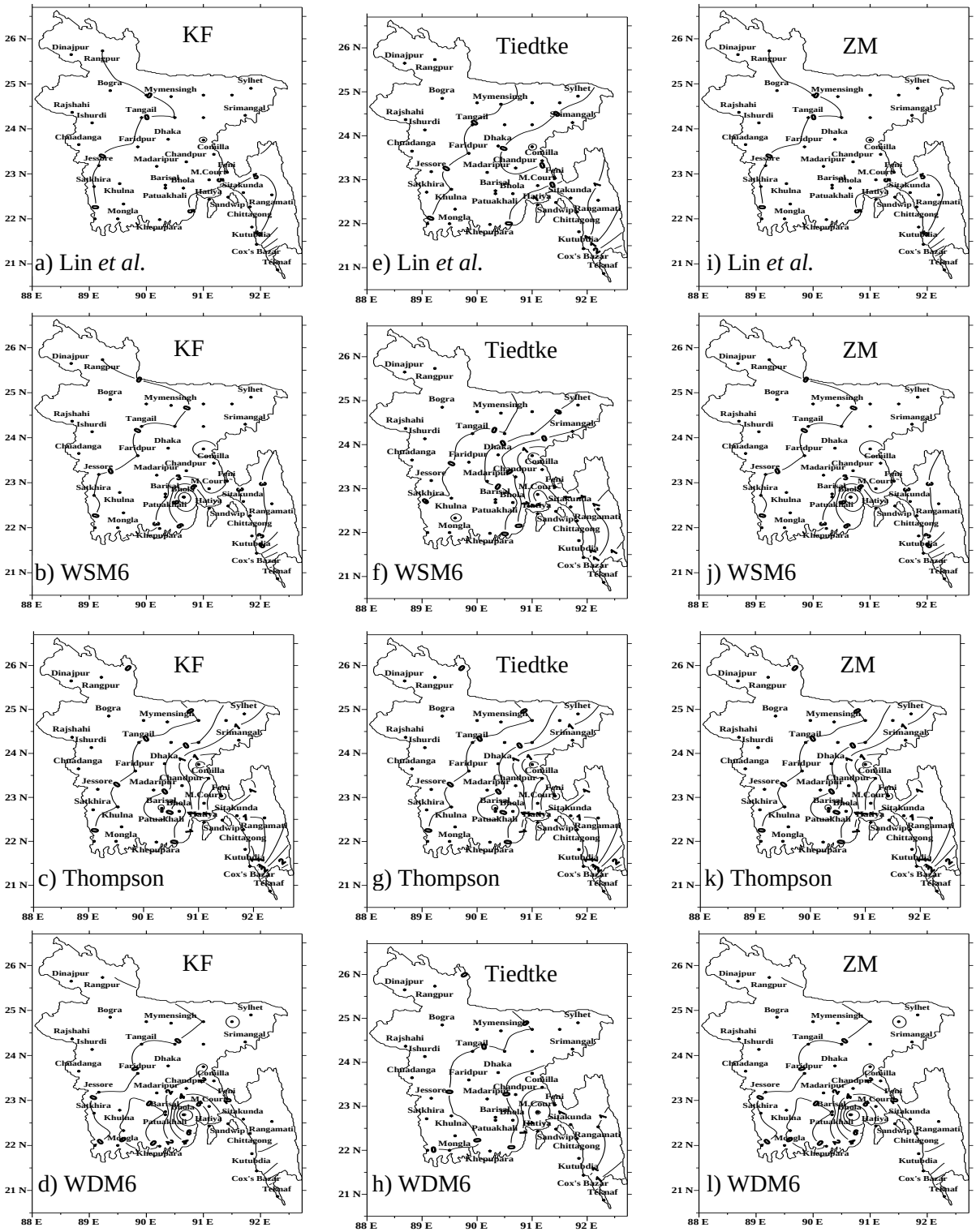

Figure 25: Distribution of model simulated (a–l) convective rain using Lin *et al.*, WSM6, Thompson and WDM6 schemes in combination with KF, Tiedtke and ZM schemes on 16 May with the initial condition at 0000 UTC of 16 May 2013.

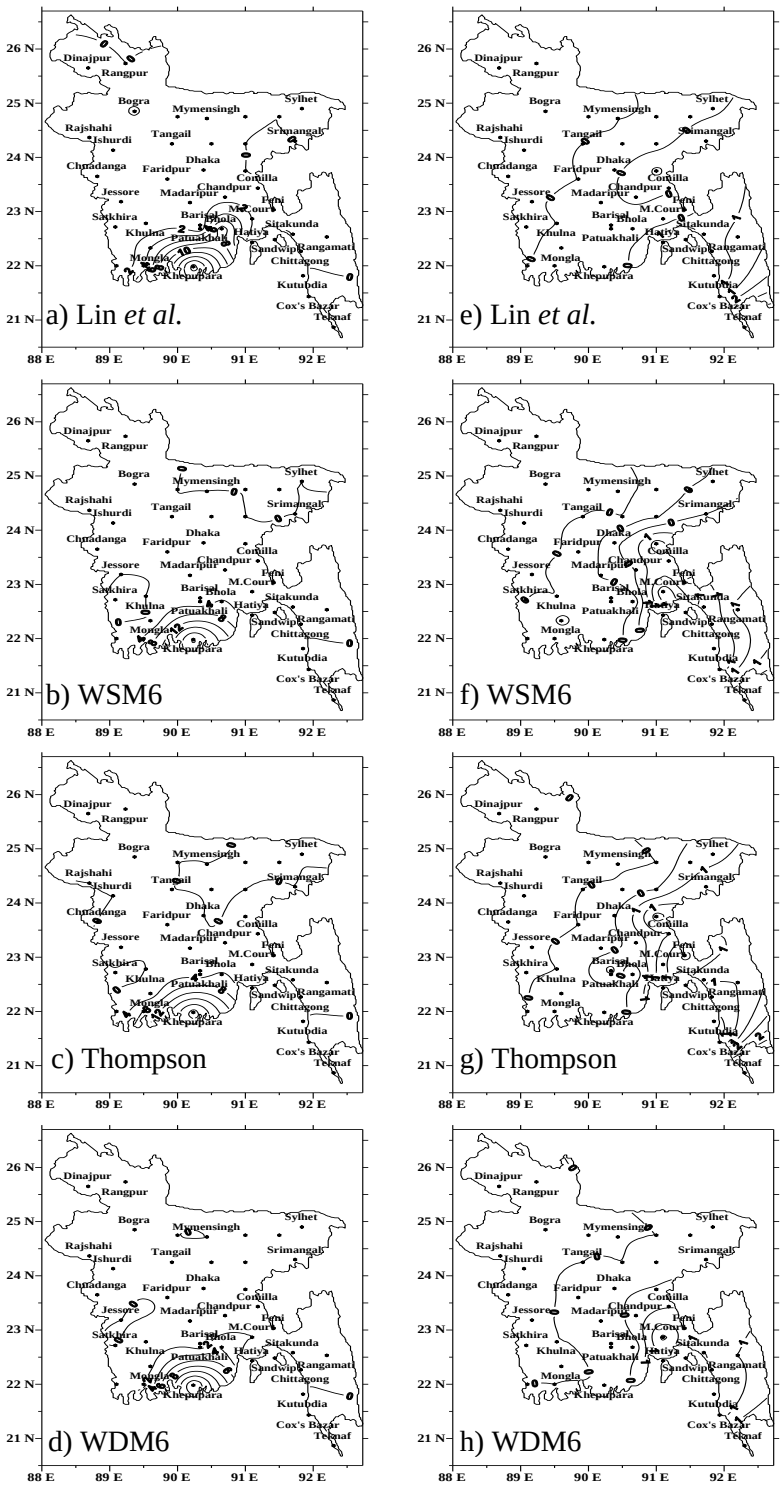

Figure 26: Distribution of model simulated convective rain using Lin *et al.*, WSM6, Thompson and WDM6 schemes in combination with MSKF scheme on 15 May (a–d) and 16 May (e–h) with the initial conditions at 0000 UTC of 15 and 16 May respectively.

rainfall in other regions of the country. Maximum amount of rainfall is found at Barisal, Chandpur, Dhaka, Feni, Hatiya, Khepupara, Khulna, Madaripur, M.Court, Mongla and Patuakhali regions where the rainfall amounts are 93, 56, 52, 46, 47, 382, 45, 147, 49, 121

and 78 mm for WSM6–Tiedtke (Figure 22f), 81, 64, 67, 51, 43, 316, 62, 112, 47, 134 and 75 mm for Thompson–Tiedtke (Figure 22g) and 116, 51, 51, 48, 58, 380, 40, 135, 71, 115 and 93 mm for WDM6–Tiedtke (Figure 22h) combinations respectively.

The ZM scheme coupling with Lin *et al.*, WSM6, Thompson and WDM6 schemes has simulated heavy rainfall at Barisal, Chandpur, Dhaka, Feni, Hatiya, Khepupara, Khulna, Madaripur, Mongla and Patuakhali regions where the rainfall amounts are 124, 84, 77, 45, 50, 350, 67, 133, 161 and 106 mm for Lin–ZM (Figure 22i), 104, 46, 68, 55, 35, 309, 44, 115, 127 and 96 mm for WSM6–ZM (Figure 22j), 81, 64, 67, 51, 43, 316, 62, 112, 134 and 75 mm for Thompson–ZM (Figure 22k) and 98, 42, 59, 34, 46, 344, 39, 121, 127 and 90 mm for WDM6–ZM (Figure 22l) combinations respectively.

The MSKF scheme coupling with Lin *et al.*, WSM6, Thompson and WDM6 schemes has simulated heavy rainfall at Barisal, Chandpur, Dhaka, Feni, Hatiya, Khepupara, Khulna, Madaripur, M.Court, Mongla and Patuakhali regions where the rainfall amounts are 122, 82, 55, 50, 42, 445, 58, 154, 30, 176 and 110 mm for Lin–MSKF (Figure 23e), 93, 56, 52, 46, 47, 382, 45, 147, 49, 121 and 78 mm for WSM6–MSKF (Figure 23f), 74, 60, 69, 50, 49, 323, 65, 109, 53, 141 and 82 mm for Thompson–MSKF (Figure 23g) and 116, 51, 51, 48, 58, 380, 40, 135, 71, 115 and 93 mm for WDM6–MSKF (Figure 23h) combinations respectively.

The model simulated maximum rainfall is almost matched with the observed rainfall on 16 May 2013 for all CPs in combinations all MPs in the southern region but the model simulated heavy rainfall position is found to shift from Barisal–Patuakhali regions to Khepupara region. On both the days the heavy rainfall position is found to shift towards west for all MPs in combination with all CPs of model run.

4.2.3 Model Simulated Convective Rain on 15 May 2013

The model simulated convective rain using four different MP schemes coupling with four different CP schemes on 15 May 2013 is presented in Figures 24(a–l) and Figures 26(a–d) respectively for the initial conditions at 0000 UTC of 15 May. The Lin–KF combination has simulated (Figure 24a) light convective rain in the southern region and no convective rain in other regions. The WSM6–KF has simulated (Figure 24b) moderate convective rain in the SW region and no convective rain in other regions of the country. The KF scheme coupling with Thompson and WDM6 schemes have simulated moderate convective rain (Figures 24(c–d)) in Bhola and Khepupara regions and no convective rain in other regions of the country. The Tiedtke scheme coupling with Lin *et al.*, WSM6, Thompson and WDM6

schemes have simulated moderate convective rain at Khepupara region and no convective rain in other regions as shown in Figures 24(e–h).

The Lin–ZM combination has simulated (Figure 24i) light convective rain in the southern region and no convective rain in other regions. The WSM6–ZM has simulated (Figure 24j) heavy convective rain in the SW region and no convective rain in other regions of the country. The ZM scheme coupling with Thompson and WDM6 schemes has simulated heavy convective rain (Figures 24(k–l)) in Bhola and SW region and no convective rain in other regions of the country. The MSKF scheme coupling with Lin *et al.*, WSM6, Thompson and WDM6 schemes has simulated (Figures 26(a–d)) moderate convective rain in Khepupara region and almost no convective rain in other regions of Bangladesh.

All MPs in combination with different CPs have simulated moderate convective rain in the southern region of the country and have not simulated any convective rain in all other regions on 15 May 2013.

4.2.4 Model Simulated Convective Rain on 16 May 2013

The model simulated convective rain using four different MP schemes coupling with four different CPs on 16 May 2013 is presented in Figures 25(a–l) and Figures 26(e–h) respectively for the initial conditions at 0000 UTC of 16 May. The KF scheme coupling with Lin *et al.*, WSM6, Thompson and WDM6 schemes has simulated little amount of convective rain in the south–southeastern regions as shown in Figures 25(a–d) and almost no convective rain in other regions of Bangladesh. The Tiedtke (Figures 25(e–h)), ZM (Figures 25(i–l)) and MSKF (Figures 26(e–h)) schemes coupling with Lin *et al.*, WSM6, Thompson and WDM6 schemes have simulated little amount of convective rain in regions where the rainfall amounts.

All MPs in combination with different CPs have simulated moderate convective rain in the eastern to southeastern region of the country and all other regions have not simulated any convective rain on 16 May 2013.

4.2.5 Model Simulated Non–convective Rain on 15 May 2013

The model simulated NC rain using four different MP schemes coupling with four different CPs on 15 May 2013 is presented in Figure 27(a–l) and Figure 29(a–d) respectively for the initial condition at 0000 UTC of 15 May. The Lin–KF combination has simulated significant amount of NC rain (Figure 27a) at Mongla and Patuakhali regions where the rainfall amounts

are 261 and 50 mm respectively. The WSM6–KF has simulated moderate NC rain (Figure 27b) at Bhola region and no NC rain in other regions of Bangladesh. The KF scheme coupling with Thompson and WDM6 schemes have simulated moderate NC rain (Figure 27(c–d)) in the SW region of the country and almost no NC rain in other regions.

The Tiedtke scheme in combination with Lin *et al.*, WSM6, Thompson and WDM6 schemes have simulated significant amount of NC rain at Barisal, Mongla and Patuakhali regions where the rainfall amounts are 78, 275 and 84 mm for Lin–Tiedtke (Figure 27e), 78, 310 and 89 mm for WSM6–Tiedtke (Figure 27f), 72, 185 and 67 mm for Thompson–Tiedtke (Figure 27g) and 46, 44, 274 and 48 mm WDM6–Tiedtke (Figure 27h) combinations respectively.

The WSM6–ZM has simulated moderate NC rain (Figure 27i) at Bhola region and no NC rain in other regions of Bangladesh. The Lin–ZM combination has simulated significant amount of NC rain (Figure 27j) at Chandpur, Mongla and Patuakhali regions where the rainfall amounts are 41, 266 and 57 mm respectively and slight NC rain in other regions of the country. The ZM scheme coupling with Thompson and WDM6 schemes have simulated moderate NC rain (Figure 27(k–l)) in the S–SW regions of the country and almost no NC rain in other regions of Bangladesh.

The Lin–MSKF has simulated moderate NC rain (Figure 29a) in the SW region of the country and almost no NC rain in other regions of Bangladesh. The MSKF scheme in combination with WSM6, Thompson and WDM6 schemes have simulated significant amount of NC rain (Figure 29(b–d)) in the SW region and almost no NC rain in other regions of the country. Maximum amount of NC rain has been simulated at Barisal, Mongla and Patuakhali regions where the rainfall amounts are 75, 277 and 81 mm for WSM6–MSKF (Figure 29b), 73, 188 and 64 mm for Thompson–MSKF (Figure 29c) and 80, 319 and 82 mm for WDM6–MSKF (Figure 29d) combinations respectively.

All MPs in combination with different CPs have simulated heavy NC rain in the S–SW regions of the country and all other regions have simulated almost no NC rain on 15 May 2013.

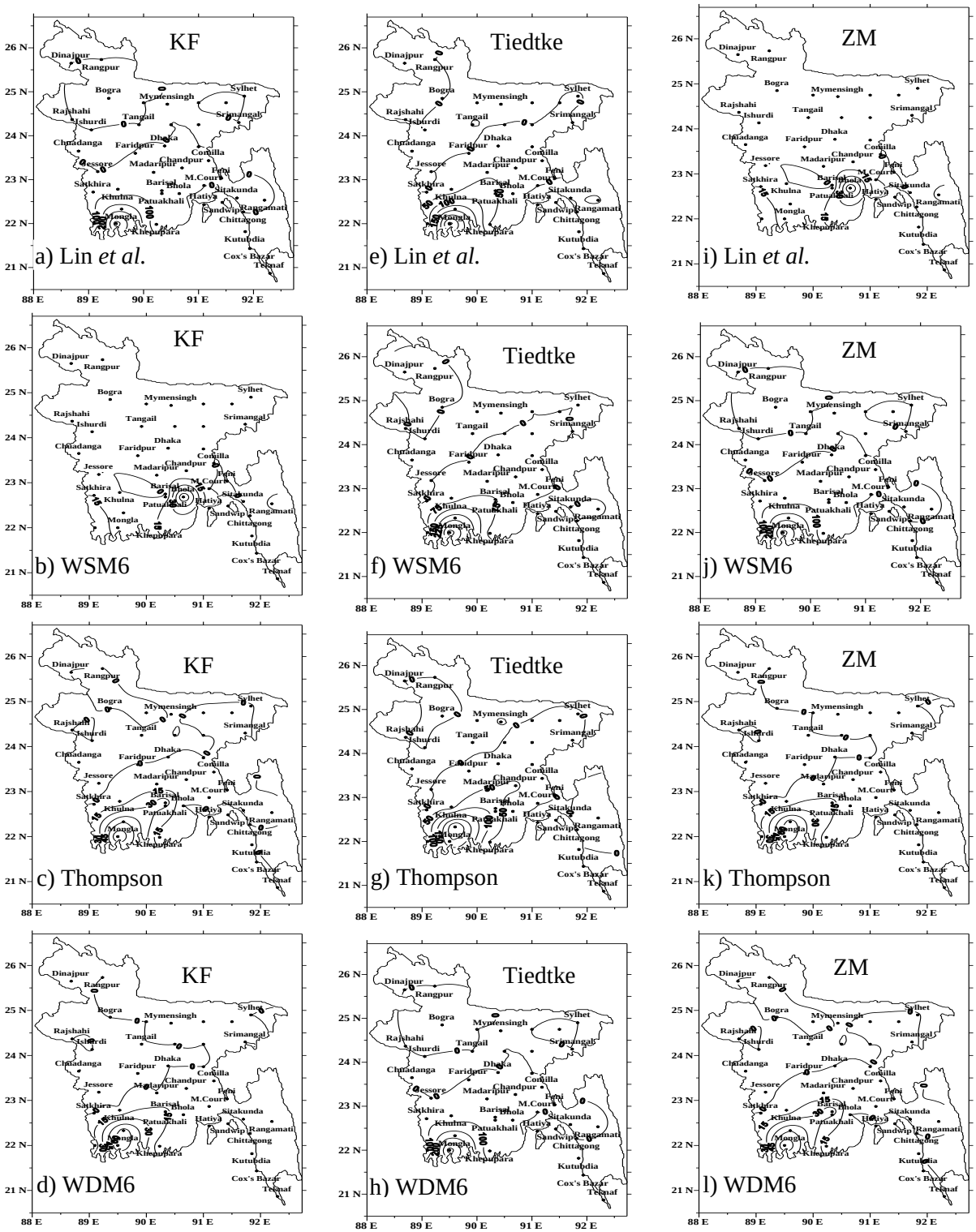

Figure 27: Distribution of model simulated (a–l) non–convective rain using Lin *et al.*, WSM6, Thompson and WDM6 schemes in combination with KF, Tiedtke and ZM schemes on 15 May with the initial conditions at 0000 UTC of 15 May 2013.

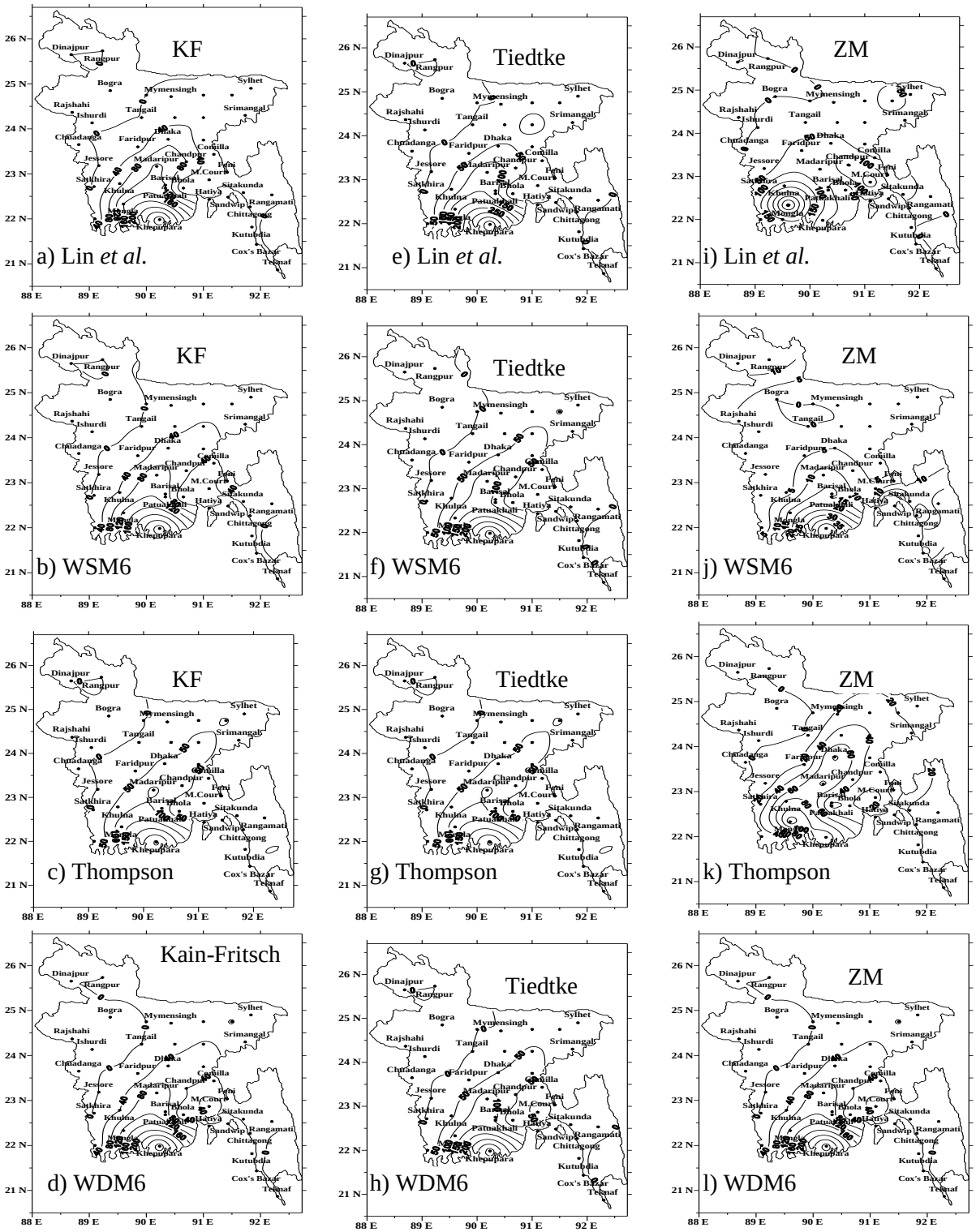

Figure 28: Distribution of model simulated (a–l) non–convective rain using Lin *et al.*, WSM6, Thompson and WDM6 schemes in combination with KF, Tiedtke and ZM schemes on 16 May with the initial conditions at 0000 UTC of 16 May 2013.

4.2.6 Model Simulated Non–convective Rain on 16 May 2013

The model simulated NC rain using four different MP schemes coupling with four different CP schemes on 16 May 2013 is presented in Figure 28(a–l) and Figure 29(e–h) respectively

for the initial conditions at 0000 UTC of 16 May. The KF scheme coupling with Lin *et al.*, WSM6, Thompson and WDM6 schemes have simulated significant amount of NC rain (Figure 28(a–d)) in the central to south–SW regions of the country and slight NC rain in other regions. Maximum amount of NC rain is found at Barisal, Chandpur, Dhaka, Khepupara, Khulna, Madaripur, Mongla and Patuakhali regions where the rainfall amounts are 121, 81, 76, 350, 66, 130, 161 and 103 mm for Lin–KF (Figure 28a), 103, 45, 66, 306, 43, 114, 127 and 95 mm for WSM6–KF (Figure 28b), 80, 63, 66, 316, 62, 111, 134 and 74 mm for Thompson–KF (Figure 28c) and 97, 40, 58, 344, 38, 120, 127 and 90 mm for WDM6–KF (Figure 28d) combinations respectively.

The Tiedtke scheme coupling with Lin *et al.*, WSM6, Thompson and WDM6 schemes has simulated significant amount of NC rain (Figure 28(e–h)) in the central to south–SW regions of Bangladesh and slight NC rain in other regions. Maximum amounts of NC rain are found at Barisal, Chandpur, Dhaka, Feni, Khepupara, Khulna, Madaripur, M.Court, Mongla and Patuakhali regions where the rainfall amounts are 122, 82, 54, 50, 445, 58, 154, 30, 176 and 109 mm for Lin–Tiedtke (Figure 28e), 92, 56, 52, 45, 382, 45, 147, 48, 121 and 78 mm for WSM6–Tiedtke (Figure 28f), 75, 60, 69, 50, 307, 71, 102, 49, 141 and 82 mm for Thompson–Tiedtke (Figure 28g) and 116, 51, 51, 47, 380, 40, 135, 69, 115 and 93 mm for WDM6–Tiedtke (Figure 28h) combinations respectively.

The ZM scheme coupling with Lin *et al.*, WSM6, Thompson and WDM6 schemes has simulated significant amount of NC rain (Figures 28(i–l)) in the central to south–SW regions of the country and slight NC rain in other regions. Maximum amounts of NC rain are found at Barisal, Chandpur, Dhaka, Khepupara, Khulna, Madaripur, Mongla and Patuakhali regions where the rainfall amounts are 51, 157, 68, 57, 179, 46, 426 and 69 mm for Lin–ZM (Figure 28i), 9, 19, 51, 122, 126, 70, 94 and 14 mm for WSM6–ZM (Figure 28j), 20, 48, 84, 115, 83, 85, 133 and 14 mm for Thompson–ZM (Figure 28k) and 85, 18, 33, 113, 136, 58, 109 and 166 mm for WDM6–ZM (Figure 28l) combinations respectively.

The MSKF scheme coupling with Lin *et al.*, WSM6, Thompson and WDM6 schemes has simulated significant amount of NC rain (Figures 29(e–h)) in the central to south–SW regions of the country and slight NC rain in other regions. Maximum amounts of NC rain are found at Barisal, Chandpur, Dhaka, Khepupara, Khulna, Madaripur, Mongla and Patuakhali regions where the rainfall amounts are 98, 90, 115, 64, 230, 142, 195 and 131 mm for Lin–MSKF (Figure 29e), 167, 128, 131, 83, 198, 144, 470 and 151 mm for WSM6–MSKF (Figure 29f), 128, 73, 86, 21, 193, 121, 269 and 125 mm for Thompson–MSKF (Figure 29g) and 55, 160,

63, 61, 180, 51, 431 and 70 mm for WDM6–MSKF (Figure 29h) combinations respectively. The significant amount of NC rain is simulated in the S–SW region by almost all CPs coupling with all MPs on 16 May 2013.

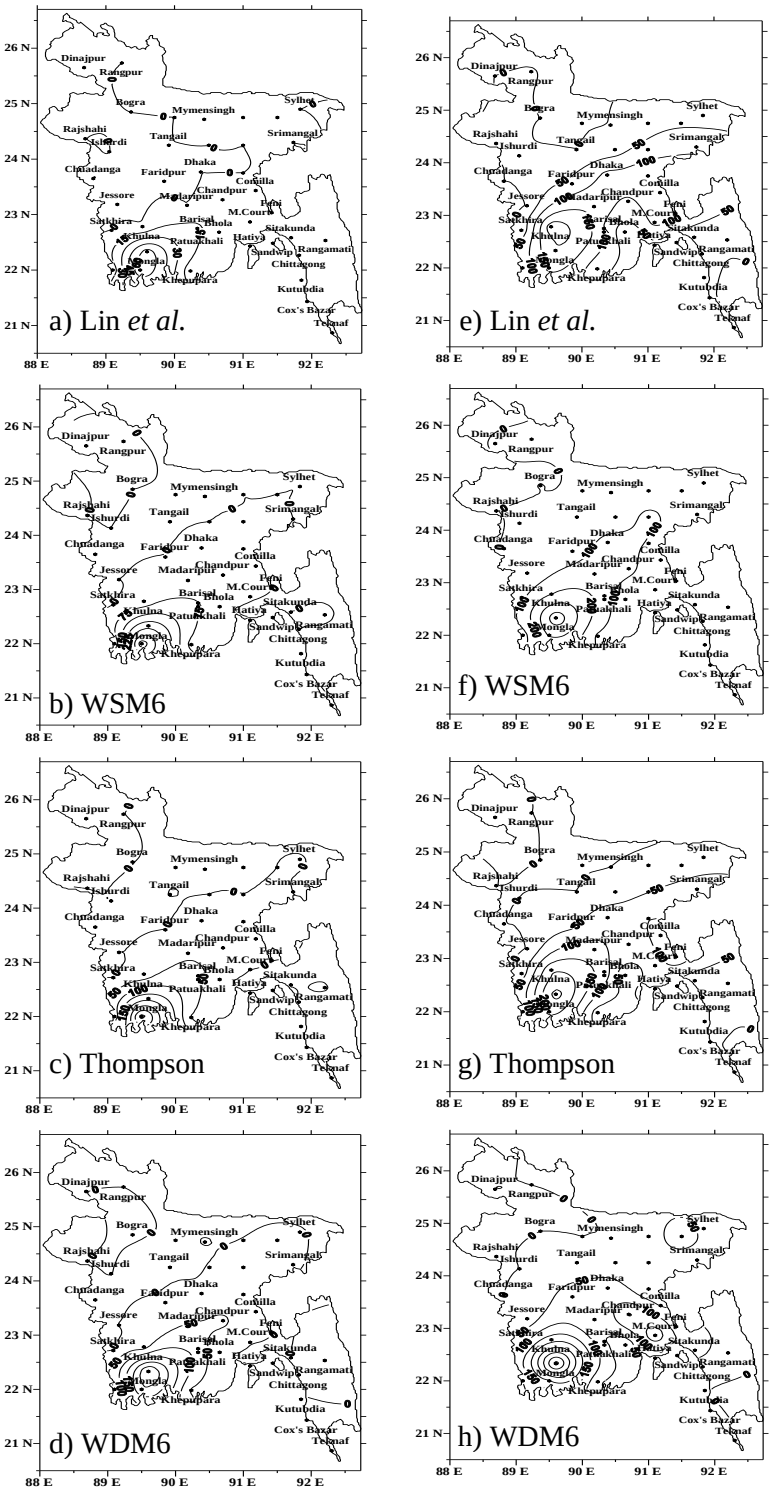

Figure 29: Distribution of model simulated non–convective rain using Lin *et al*., WSM6, Thompson and WDM6 schemes in combination with MSKF on (a–d) 15 and (e–h) 16 May with the initial conditions at 0000 UTC of 15 and 16 May respectively.

4.2.7 Area average rainfall during 15–16 May 2013

All Bangladesh observed and model simulated station average rainfall and station average observed and model simulated heavy rainfall in the S–SE region of the country using different MPs in combination with different CPs during 15–16 May 2013 are presented in Figures 30(a–d) respectively. The Tiedtke scheme coupling with all MPs have simulated (Figure 30a) almost similar amount of average rainfall with observed from 35 meteorological stations of all over Bangladesh on 15 May 2013. Lin–KF, WSM6–ZM and WSM6–MSKF combinations have also simulated similar amount of average rainfall to that of observed all over Bangladesh on this day.

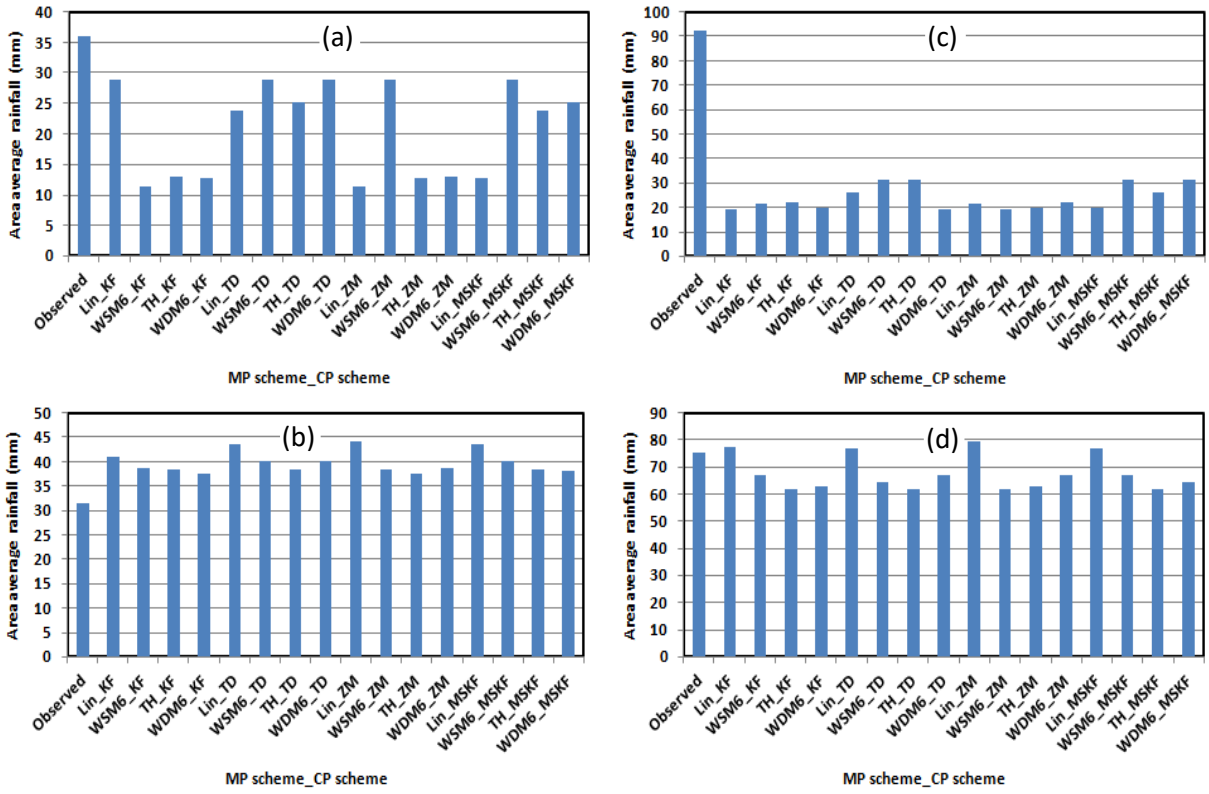

Figure 30: Station average (a–b) all Bangladesh observed and model simulated rainfall and (c–d) heavy rainfall in the S–SE region of the country using different MPs in combination with different CPs during 15–16 May 2013 respectively.

The WSM6, Thompson and WDM6 schemes in combination with all CPs have simulated (Figure 30b) higher average rainfall to that of observed from all Bangladesh 35 meteorological stations rainfall on 16 May 2013. The Lin *et al.* schemes coupling with Tiedtke, ZM and MSKF schemes have simulated much higher station average rainfall than that of observed from all Bangladesh on 16 May.

The KF, Tiedtke, ZM and MSKF schemes coupling with all MPs have simulated (Figure 30c) very little rain in comparison with the observed in the heavy rainfall area on 15 May 2013. On 16 May Lin *et al.* scheme coupling with all CP schemes have simulated (Figure 30d) almost similar amount of station average rain in the heavy rainfall region and all other combinations have simulated slightly lower rainfall than that of observed.

Tiedtke scheme in combination with four different MPs has simulated near about all Bangladesh observed rain and all MPs coupling with all CPs have simulated very much less rainfall in the heavy rainfall area on 15 May. On 16 May, all MPs coupling with all CPs have simulated higher rain in all over Bangladesh but slightly lower rain in heavy rainfall region except Lin *et al.* scheme coupling with all CPs to that of observed.

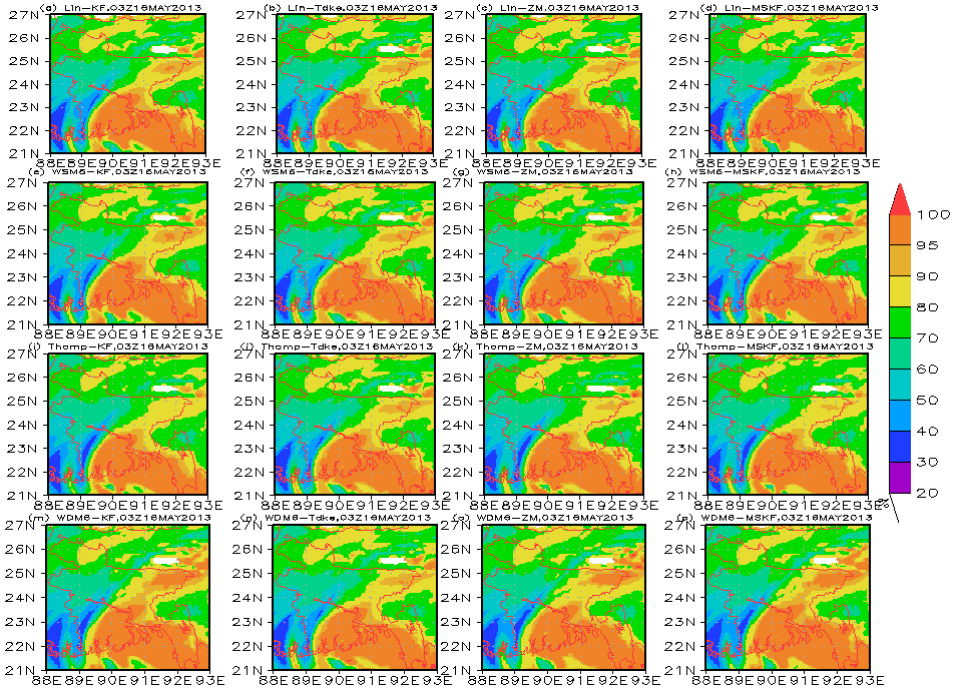

Figure 31: Model simulated RH at 850 hPa level using (a–d) Lin *et al.*, (e–h) WSM6, (i–l) Thompson and (m–p) WDM6 schemes in combination with KF, Tiedtke, ZM and MSKF schemes respectively at 0300 UTC of 16 May with the initial conditions at 0000 UTC of 16 May 2013.

4.2.8 Relative Humidity during 15–16 May 2013

The model simulated RH at 850 hPa level has been analyzed at 2100 and 0300 UTC for the heavy rainfall events of 15 (Figure not shown) and 16 (Figure 31(a–p)) May for the initial conditions at 0000 UTC of 15 and 16 May 2013 using four different MP schemes coupling with four different CP schemes respectively. All MPs coupling with all CPs have simulated high RH (95–100%) in the south–southeastern region of Bangladesh and also oceanic region

and low RH (50–70%) in the western region with little anomalies at 2100 UTC of 15 May with the initial conditions of 0000 UTC of 15 May. All MPs coupling with all CPs have simulated high RH (95–100%) in the south–southeastern and also northeastern region of Bangladesh and also oceanic region and low RH (50–70%) in the western region with little anomalies at 0300 UTC of 16 May with the initial conditions of 0000 UTC of 16 May. The heavy rainfall observed on 15 and 16 May on the western side of heavy rainfall area. All CPs coupling with all MPs have simulated high RH in the S-SE regions of the country on 15 and 16 May and NE region of on 16 May 2013. The maximum amount of rainfall is simulated in a region where RH is significantly high. This suggests that the amount of rainfalls in an area is directly proportional to the RH of that area.

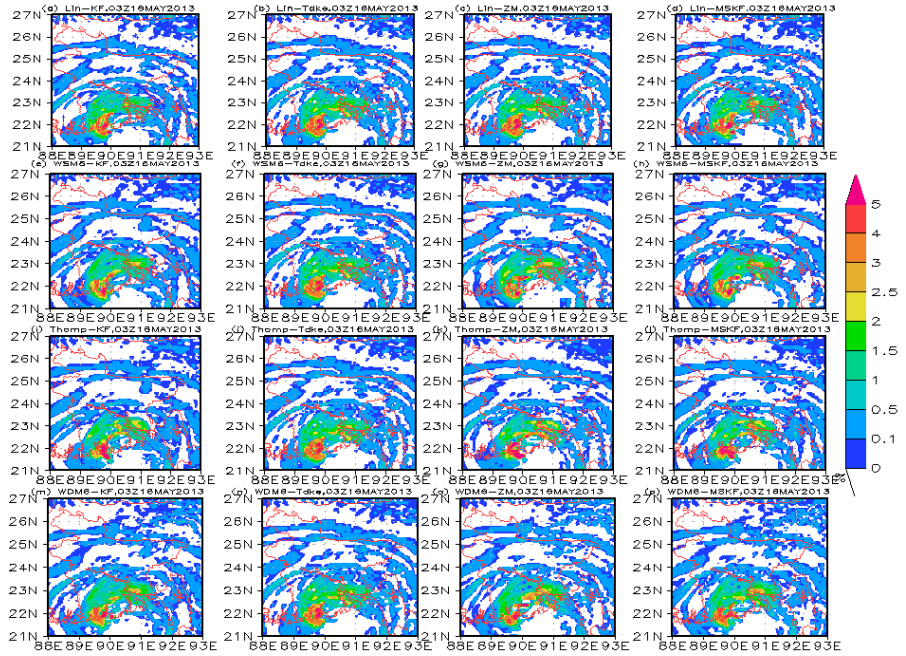

Figure 32: Model simulated vertical velocity at 300 hPa level using (a–d) Lin *et al.*, (e–h) WSM6, (i–l) Thompson and (m–p) WDM6 schemes in combination with KF, Tiedtke, ZM and MSKF schemes respectively at 0300 UTC of 16 May with the initial conditions at 0000 UTC of 16 May 2013.

4.2.9 Vertical Velocity during 15–16 May 2013

The model simulated vertical velocity at 300 hPa level has been analyzed at 2100 and 0300 UTC of 15 (Figure not shown) and 16 (Figure 32(a–p)) May respectively for the initial conditions at 0000 UTC of 15 and 16 May 2013 using four different MP schemes coupling with four different CP schemes. The KF and MSKF schemes coupling with all MP schemes have simulated maximum vertical velocity 4–5 ms^{-1} in the S–SW region of the country at

2100 UTC of 15 May with the initial condition at 0000 UTC of 15 May. The Tiedtke and ZM schemes coupling with all MP schemes have simulated vertical velocity below 1 ms^{-1} in almost all over the country.

All MPs coupling with all CPs have simulated maximum vertical velocity 4–5 ms^{-1} in the S–SW region of Bangladesh at 0300 UTC of 16 May with the initial conditions at 0000 UTC of 16 May. The simulated vertical velocity on 15 May is not significant for Tiedtke and ZM schemes but the rainfall is found significant for all MPs and CPs in the S–SW region. On 16 May, vertical velocity is related significantly with the maximum amount of rainfall in the S–SW regions. Higher vertical velocity means more convection and more rainfall to occur.

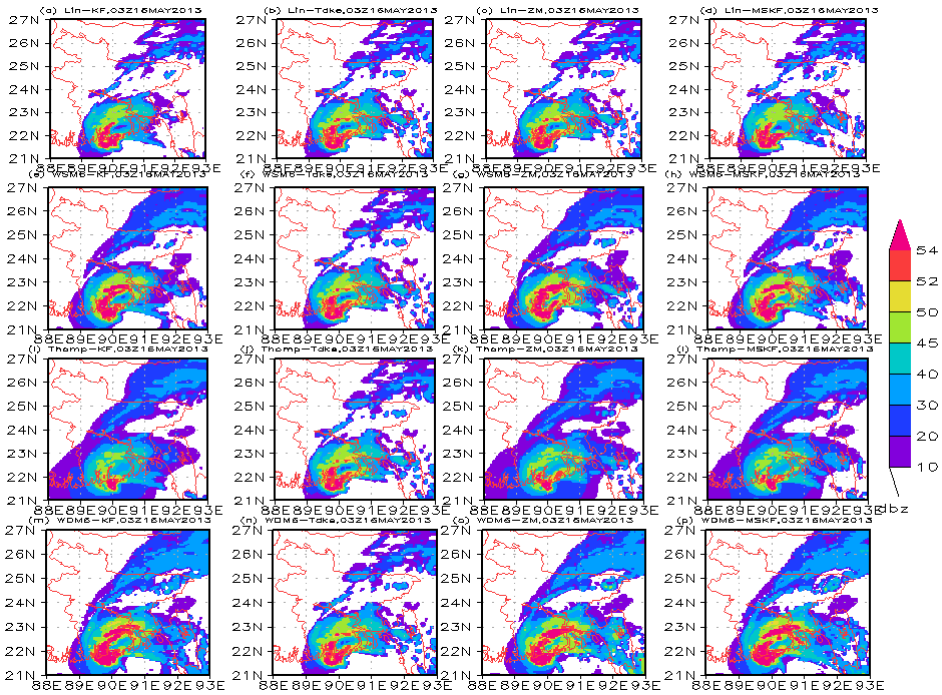

Figure 33: Model simulated reflectivity at 850 hPa level using (a–d) Lin *et al*., (e–h) WSM6, (i–l) Thompson and (m–p) WDM6 schemes in combination with KF, Tiedtke, ZM and MSKF schemes respectively at 0300 UTC of 16 May with the initial conditions at 0000 UTC of 16 May 2013.

4.2.10 Reflectivity during 15–16 May 2013

The model simulated reflectivity at 850 hPa level has been analyzed at 2100 and 0300 UTC of 15 (Figure not shown) and 16 (Figures 33(a–p)) May respectively for the initial conditions at 0000 UTC of 15 and 16 May 2013 using four different MPs coupling with four different CPs. The KF and MSKF schemes in combination with different MPs have simulated maximum reflectivity around 54 dBZ in the SW region of Bangladesh and a band of

reflectivity has found from southwest to northeasterly direction at 2100 UTC of 15 May except little anomalies with the initial condition at 0000 UTC of 15 May. The Tiedtke and ZM schemes coupling with all MPs have simulated maximum reflectivity of 20–30 dBZ in the southern region of the country.

The KF, Tiedtke, ZM and MSKF schemes in combination with four different MPs have been simulated maximum reflectivity of 54 dBZ in the SW region of Bangladesh (Figure 33(a–p)) at 0300 UTC of 16 May with the initial condition at 0000 UTC of 16 May. The structure of the cloud is determined on the basis of reflectivity of the system. The area, where the reflectivity >54 dBZ of the system is found maximum, the maximum amount of rain is also identified on that area. Maximum amount of reflectivity is observed at 850 hPa level on 15 and 16 May for all MPs coupling with all CPs in region where the maximum amount of rainfall is simulated.

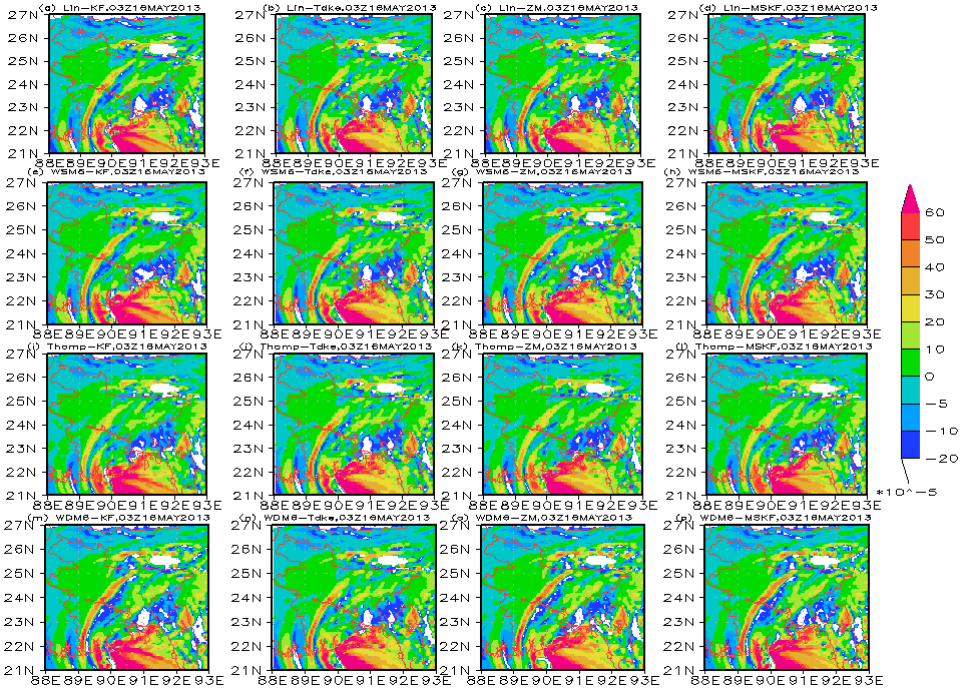

Figure 34: Model simulated vorticity at 850 hPa level using (a–d) Lin *et al*., (e–h) WSM6, (i–l) Thompson and (m–p) WDM6 schemes in combination with KF, Tiedtke, ZM and MSKF schemes respectively at 0300 UTC of 16 May with the initial conditions at 0000 UTC of 16 May 2013.

4.2.11 Vorticity during 15–16 May 2013

The model simulated vorticity at 850 hPa level has been analyzed at 2100 UTC and 0300 UTC of 15 (Figure not shown) and 16 (Figures 34(a–p)) May respectively for the initial conditions at 0000 UTC of 15 and 16 May 2013 using four different MPs coupling with four

different CPs. The KF and MSKF schemes in combination with four different MPs have simulated maximum vorticity of 60×10^{-5}/s in the SW region of the country and in other regions the value is –10 to 10×10^{-5}/s at 2100 UTC of 15 May with the initial condition at 0000 UTC of 15 May. The Tiedtke and ZM schemes in combination with all MPs have not simulated sufficient vorticity all over the country on 15 May.

The KF, Tiedtke, ZM and MSKF schemes coupling with four different MPs have simulated maximum vorticity of 60×10^{-5}/s in the southern region of the country and also oceanic region (Figures 34(a–p)) at 0300 UTC of 16 May with the initial condition at 0000 UTC of 16 May. The maximum vorticity simulated in a region where the rainfall, vertical velocity, reflectivity and RH are found maximum. The maximum vorticity 60×10^{-5}/s simulated at 2100 and 0300 UTC of 15 and 16 May for all MPs coupling with all CPs in a region where the rainfall, vertical velocity, reflectivity and RH are also found maximum.

4.2.12 Different verification methods of rainfall during 15–16 May 2013

For the prediction of correct forecast, TS, ETS, BS and SD have been estimated for the heavy rainfall events of 15–16 May. The model simulated heavy rain predicted region, predicted area (km^2), observed heavy rainfall region and intersected regions and intersected area (km^2) have been identified for different combination of MPs and CPs on 15 and 16 May 2013 and are presented in Tables 4 & 5 for the initial conditions of 0000 UTC of 15 and 16 May respectively. The observed heavy rain region lies between 89.0–91.4ºE and 21.9–23.1ºN and the observed area is 33198.203 km^2 for 15 May for 16 May the heavy rain observed region lies between 89.7–91.6ºE and 21.9–24.3ºN and the observed area is 52330.07 km^2.

The highest and lowest values of TS are found 0.640 and 0.229 for WSM6–MSKF and WSM6–KF combinations respectively. The highest and lowest values of ETS are found from WSM6–MSKF and WSM6–KF combinations and are 0.611 and 0.209 respectively. The highest value of BS is found from Thompson–ZM and Thompson–MSKF combinations and is 0.988 and lowest value of BS found from WSM6–KF is 0.229. The highest and lowest values of SD are found from Lin–KF and WSM6–KF combinations are 94.65 and 19.14 respectively.

TS are applicable to validate the accuracy of forecasts without the contribution from the correct rejections events. The accuracy of forecasts is higher as TS approaches to the maximum value of unity. The obtained TS and ETS scores suggest that the WSM6–MSKF and WSM6–KF combinations give the better and worse forecast among all studied

combinations respectively. The bias score is less than 1 for all MPs in combination with all CPs and suggests that all MPs–CPs combinations under–predicts rain occurrence on 15 May. The bias score is 0.988 for both Thompson–ZM and Thompson–MSKF combinations indicate the better performance.

Table 4: TS, ETS, BS and SD for the heavy rainfall region on 15 May for different combinations of MPs and CPs with the initial conditions at 0000 UTC of 15 May

CPs	MPs	Threat Score TS = H/(O+F–H)	Equitable Threat Score ETS = (H–R)/(O+F–H–R)	Bias Score BS = F/O	Standard Deviation
KF	Lin *et al*.	0.469	0.440	0.469	94.65
	WSM6	0.229	0.209	0.229	19.14
	Thompson	0.285	0.260	0.316	28.73
	WDM6	0.521	0.492	0.521	19.45
Tiedtke	Lin *et al*.	0.503	0.473	0.555	92.35
	WSM6	0.278	0.246	0.438	88.11
	Thompson	0.340	0.315	0.340	62.96
	WDM6	0.389	0.362	0.389	65.32
ZM	Lin *et al*.	0.503	0.473	0.555	89.61
	WSM6	0.588	0.558	0.649	20.24
	Thompson	0.605	0.567	0.988	28.73
	WDM6	0.495	0.453	0.887	19.45
MSKF	Lin *et al*.	0.588	0.561	0.611	93.55
	WSM6	0.640	0.611	0.708	88.11
	Thompson	0.605	0.567	0.988	62.96
	WDM6	0.577	0.544	0.708	65.32

O = Observed heavy rain area; F = Model predicted heavy rain area; H = Intersected area between observed (O) and model predicted (F) heavy rain area; R = O*(F/N), where N = Entire verification domain.

The maximum values of TS and ETS are found 0.64 and 0.611 respectively for WSM6–MSKF combination. The maximum value of BS is found 0.988 from both Thompson–ZM and Thompson–MSKF combinations and lowest value of SD is found 19.14 from WSM6–KF.

The highest and lowest values of TS are found 0.742 and 0.321 for Thompson–KF and WSM6–KF combinations respectively. The highest and lowest values of ETS are found from Thompson–KF and WSM6–KF combinations and are 0.693 and 0.265 respectively. The highest value of BS is found from WSM6–Tiedtke is 1.206 and lowest value from WSM6–KF, WSM6–ZM and WDM6–ZM combinations is 0.229. The highest and lowest values of SD are found from Lin–Tiedtke and Thompson–KF combinations and are 78.12 and 55.59 respectively. The maximum values of TS and ETS are found 0.742 and 0.693 respectively for

Thompson–KF combination. The maximum value of BS is found 1.206 from WSM6–Tiedtke and lowest value of SD is found 55.59 from Thompson–KF combination.

Table 5: TS, ETS, BS and SD for the heavy rainfall region on 16 May for different combinations of MPs and CPs with the initial conditions at 0000 UTC of 16 May

CPs	MPs	Threat Score TS = H/(O+F–H)	Equitable Threat Score ETS = (H–R)/(O+F–H–R)	Bias Score BS = F/O	Standard Deviation
KF	Lin *et al*.	0.376	0.315	0.593	64.19
	WSM6	0.321	0.265	0.495	55.91
	Thompson	0.742	0.693	1.139	55.59
	WDM6	0.350	0.293	0.528	60.58
Tiedtke	Lin *et al*.	0.370	0.312	0.563	78.12
	WSM6	0.618	0.549	1.206	65.56
	Thompson	0.687	0.632	1.104	57.79
	WDM6	0.672	0.613	1.096	65.86
ZM	Lin *et al*.	0.424	0.367	0.593	64.19
	WSM6	0.360	0.307	0.495	55.91
	Thompson	0.688	0.629	1.196	59.52
	WDM6	0.360	0.307	0.495	60.58
MSKF	Lin *et al*.	0.403	0.347	0.561	75.22
	WSM6	0.712	0.658	1.151	65.56
	Thompson	0.687	0.629	1.196	58.57
	WDM6	0.672	0.613	1.096	65.86

Chapter V
Conclusions

In the present study, the Advanced Research WRF (ARW) v3.8.1 model has been used to simulate the heavy rainfall events in the southeastern regions of Bangladesh during 4, 6 and 7 May 2013 and southern region during 15-16 May 2013. In this research Lin *et al*., WSM6, Thompson and WDM6 microphysics schemes and Kain-Fritsch, Tiedtke, Zhang-McFarlane and Multi-scale Kain-Fritsch cumulus parameterization schemes are used to simulate the heavy rainfall events. The conclusions have been drawn on convective rain, non-convective rain, area average rainfall, relative humidity, vertical velocity, reflectivity and vorticity have been simulated and threat score, equitable threat score, bias score and standard deviation.

The model simulated maximum rainfall position is almost matched with the observed rainfall for KF, ZM and MSKF schemes in combination with all MPs on 4, 6 and 7 May 2013 but the observed heavy rainfall position is found to shift from its original position. The significant amount of convective rain is simulated in the heavy rainfall regions with little exceptions by KF, Tiedtke and ZM schemes on 4 May, Tiedtke, ZM and MSKF schemes on 6 May and KF, ZM and MSKF schemes on 7 May coupling with all MPs. The significant amount of NC rain is simulated in the central to eastern and NE regions by KF and MSKF schemes on 4 May, KF, ZM and MSKF schemes on 6 May and MSKF scheme on 7 May 2013 coupling with all MPs. Tiedtke scheme has simulated lower rainfall in combination with all chosen MPs over whole Bangladesh and also heavy rainfall area on 4, 6 and 7 May. KF scheme coupling with all MPs has simulated similar average rainfall all over Bangladesh on 4 May and WDM6 coupling with KF, ZM and MSKF schemes has simulated almost similar amount of rain in the heavy rainfall region on 7 May.

The model simulated heavy rainfall region is shifted from Khepupara to Mongla on 15 May in case of all MPs and CPs and on 16 May, observed maximum rain at Barisal and Patuakhali is found with the simulated rainfall but higher rain area is found at Khepupara. Simulated convective rain position matched with the observed maximum rain on 15 May but the amount is not significant for all MPs and CPs and on 16 May, insufficient Convective Rain has been simulated. Maximum amount of rain is found mainly non-convective for all MPs and CPs. On 16 May, Lin *et al.* scheme coupling with all CPs has simulated almost similar results in the heavy rain area and all MPs give higher results all over Bangladesh. Tiedtke scheme in combination with four different MPs has simulated almost similar amount of average rainfalls of all over Bangladesh observed rain (i.e. average rain of 33 stations of BMD) and all MPs coupling with all CPs have simulated very much less rainfall in the heavy rainfall area on 15 May. On 16 May, all MPs coupling with all CPs have simulated higher rain in all over

Bangladesh but slightly lower rain in heavy rainfall region except Lin *et al.* scheme coupling with all CPs to that of observed.

KF and MSKF schemes in combination with four different MP schemes have simulated maximum reflectivity of 54 dBZ in a region where the maximum amount of rainfall has been simulated at 4, 6 and 7 May 2013 and 15-16 May 2013. The vorticity is found maximum (60×10^{-5}/s) for different microphysics schemes in combination with KF, ZM and MSKF schemes in a region where the simulated rain is maximum for both the events on 4, 6 and 7 May 2013 and during 15-16 May 2013. The vertical velocity is found maximum for different microphysics schemes in combination with KF and MSKF schemes in a region where the model has simulated maximum rain for both the events on 4, 6 and 7 May 2013 and during 15-16 May 2013. All CPs coupling with all MPs have simulated high RH in the eastern and NE regions of the country on 4 May and almost all over Bangladesh on 6 and 7 May 2013 and in the south-southeastern region of the country during 15-16 May 2013. This high relative humidity has been responsible to cause heavy rainfall in different regions.

The maximum values of TS, ETS and BS and minimum values of SD are found 0.662, 0.615, 0.90 and 15.43 for WDM6–ZM combination on 4 May 2013, 0.801, 0.742, 1.16 and 33.19 for WSM6–ZM combination on 6 May and 0.522, 0.478, 2.48 and 26.13 for WDM6–MSKF combination on 7 May 2013, 0.588, 0.588, 0.649 and 20.24 for WSM6–ZM combination on 15 May and 0.712, 0.658, 1.15 and 65.56 for WSM6–MSKF combination on 16 May 2013.

WSM6 and WDM6 schemes coupling with ZM and MSKF schemes give the better performance on the basis of Threat Score, Equivalent Threat Score and Bias Score on 4, 6 and May 2013 and during 15-16 May 2013.

References

Ahmed, R., 1989: Probabilistic estimates of rainfall extremes in Bangladesh during the pre–monsoon season. Indian Geogr. J., 64, 39–53.

Alam, M. M., 2014: Impact of cloud microphysics and cumulus parameterization on simulation of heavy rainfall event during 7–9 October 2007 over Bangladesh, J. Earth Syst. Sci. 123, 2, 259–279.

Alexander, L. V., X. Zhang, T. C. Peterson, J. Caesar, B. Gleason, A. M. G. Klein Tank, M. Haylock, D. Collins, B. Trewin, F. Rahimzadeh, A. Tagipour, R. K. Kumar, J. Ravedekar, G. Griffiths, L. Vincent, D. B. Stephenson, J. Burn, E. Aguilar, M. Brunet, M. Taylor, M. New, P. Zhai, M. Rusticucci, and J. L. Vazquez–Aguirre, 2006: Global observed changes in daily climate extremes of temperature and precipitation. J Geophy Res 111 (DO5109), Doi: 10.1029/ 2005JD006290.

Anderson, D., and Coauthors, 2007: Seasonal forecasting system 3. ECMWF Tech. Memo. 503, pp. 58.

Arakawa, A., and W. H. Schubert, 1974: Interaction of a cumulus cloud ensemble with the large–scale environment, Part I. J. Atmos. Sci., 31, 674–701.

Awan, N. K., H. Truhetz, and A. Gobiet, 2011: Parameterization induced error characteristics of MM5 and WRF operated in a climate mode over the Alpine region: An ensemble–based analysis. J. Climate, 24, 3107–3123.

Baldwin, M. E., and J. S. Kain, 2006: Sensitivity of several performance measures to displacement error, bias, and event frequency, Wea. Forecasting, 21, 636–648, doi:10.1175/WAF933.1.

Bechtold, P., E. Bazile, F. Guichard, P. Mascart, and E. Richard, 2001: A mass–flux convection scheme for regional and global models. Quart. J. Roy. Meteor. Soc., 127, 869–886.

Bhanu, K. O. S. R. U., P. Suneetha, R. S. Rao, and S. M. Kumar, 2012: Simulation of Heavy Rainfall Events during Retreat Phase of Summer Monsoon Season over Parts of Andhra Pradesh, International Journal of Geosciences, 3, 737–748.

Bhowmik, S. K. R., and V. R. Durai, 2008: Multi–model ensemble forecasting of rainfall over Indian monsoon region, Atmósfera 21, 3, 225–239.

Bukovsky, M. S., and D. J. Karoly, 2009: Precipitation simulations using WRF as a nested regional climate model. J. Appl. Meteor. Climatol, 48, 2152–2159.

Cartwright, T. J., and T. N. Krishnamurti, 2007: Warm season mesoscale super ensemble precipitation forecasts in the southeastern United States, Wea. Forecasting, 22, 873–886, doi:10.1175/WAF1023.1.

Chen, G. T. J., C. C. Wang, and D. T. W. Lin, 2005: Characteristics of low–level jets over northern Taiwan in Mei–Yu season and their relationship to heavy rain events, Monthly weather review 133, 1, 20–43.

Chen, G. T. J., and C. C. Yu, 1988: Study of low–level jet and extremely heavy rainfall over northern Taiwan in the Mei–Yu season, Monthly weather review 116, 4, 884–891.

Chen, J. Y., and Y. Sun, 2002: Hydrolysis of lignocellulosic materials for ethanol production, a review, Bi ore source technology 83, 1, 1–11.

Chen, Y. L., and J. Li, 1995: Large–scale conditions favorable for the development of heavy rainfall during TAMEX IOP 3, Monthly weather review 123, 10, 2978–3002.

Chiew, F. H. S., 2006: Estimation of rainfall elasticity of stream flow in Australia. Hydrol. Sci. J. 51, 4, 613–625.

Chowdhury, M. R., 2003: The El Nino–Southern Oscillation (ENSO) and seasonal flooding – Bangladesh, Theoretical and Applied Climatology, 76, 105–124.

Clark, A. J., W. A. Gallus Jr., and T. C. Chen, 2007: Comparison of the Diurnal Precipitation Cycle in Convection–Resolving and Non–Convection–Resolving Mesoscale Models, Mon. Wea. Rev., 135, 3456–3473.

Clark, A. J., W. A. Gallus Jr., M. Xue, and F. Kong, 2009: A Comparison of Precipitation Forecast Skill between Small Convection–Allowing and Large Convection–Parameterizing Ensembles, Weather and Forecasting, 24, 1121–1140.

Das, S., M. M. Rahman, and J. Singh, 2012: Simulation of Seasonal Monsoon rainfall over the SAARC Region by Dynamical Downscaling using WRF Model, SMRC Report No. 42, 1–38.

Das, S., R. Ashrit, G. R. Iyengar, S. M. Mohandas, D. Gupta, J. P. George, E. N. Rajagopal, and S. K. Dutta, 2008: Skills of different mesoscale models over Indian region during monsoon season: Forecast errors, J. Earth Syst. Sci., 117, 5, 603–620.

Deardorff, J. W., 1972: Parameterization of the planetary boundary layer for use in general circulation models, Mon. Wea. Rev., 100, 93–106.

Ding, Y., 1992: Summer monsoon rainfalls in China. J. Meteor. Soc. Japan, 70, 373–396.

Donner, L. J., 1993: A cumulus parameterization including mass fluxes, vertical momentum dynamics, and mesoscale effects. J. Atmos. Sci., 50, 889–906.

Dudhia, J., 1989: Numerical study of convection observed during the winter monsoon experiment using mesoscale two–dimensional models, J. Atmos. Sci., 46, 3077–3107.

Ebert, E. E., 2001: Ability of a poor man's ensemble to predict the probability and distribution of precipitation, Mon. Wea. Rev., 129, 2461–2480, doi: 10.1175/1520–0493(2001)129.

Ek, M. A. A., K. E. Mitchell, Y. Lin, E. Rogers, P. Grundmann, V. Koren, G. Gayno, and J. D. Tarpley, 2003: Implementation of Noah land surface model advances in the National Centers for Environmental Prediction operational mesoscale Eta model, Journal of Geophysical Research, 108, D22, 8851, doi:10.1029/2002 JD003296

Ferretti, R., T. Paolucci, W. Zheng and G. Visconti, 2000: Analyses of the Precipitation Pattern on the Alpine Region Using Different Cumulus Convection Parameterizations, Journal of Applied Meteorology, 39, 2, 182–200.

Ferrier, B. S., W. –K. Tao, and J. Simpson, 1995: A double moment multiple phase four–class bulk ice scheme, Part II: Simulations of convective storms in different large–scale environments and comparisons with other bulk parameterizations. J. Atmos Sci., 52, 1001–1033.

Fritsch, J. M. and C. F. Chappell, 1980: Numerical Prediction of Convective Driven Mesoscale Pressure Systems, Part I: Convective Parameterization, J. Atoms. Sci., 37, 1722– 1733.

Fritsch, J. M., and R. E. Carbone, 2004: Improving quantitative precipitation forecasts in the warm season: A USWRP research and development strategy. Bull. Amer. Meteor. Soc., 85, 955–965, doi:10.1175/BAMS–85–7–955.

Fujinami, H., D. Hatsuzuka, T. Yasunari, T. Hayashi, T. Terao, F. Murata, M. Kiguchi, Y. Yamane, J. Matsumoto, M. N. Islam, A. Habib, 2011: Characteristic intraseasonal oscillation of rainfall and its effect on interannual variability over Bangladesh during boreal summer, Int. J. Climatol., 31, 1192–1204. Doi: 10.1002/joc. 2146.

Gadgil, Sulochana, M. Rajeevan, and R. Nanjundiah, 2005: Monsoon prediction–Why yet another failure? Current science, 88, 9, 1389–1400.

Groisman, P. Y., T. R. Karl, D. R. Easterling, R. W. Knight, P. F. Jameson, K. J. Hennessy, R. Suppiah, C.M. Page, J. Wibig, K. Fortuniak, V. N. Razuvaev, A. Douglas, E. Forland, and P. M. Zhai, 1999: Changes in the probability of heavy precipitation: important indicators of climatic change, Clim. Change., 42:243–283.

Hong, S. Y., Y. Noh, and J. Dudhia, 2006: A new vertical diffusion package with an explicit treatment of entrainment processes. Mon. Wea. Rev., 134, 2318–2341.

Hong, S. Y., and J. O. J. Lim, 2006: The WRF Single Moment 6–Class Microphysics Scheme (WSM6), J Korean Meteorol. Soc., 42, 2, 129–151.

Hong, S. Y., J. Dudhia and S. H. Chen, 2004: A Revised Approach to Ice Microphysical Processes for the Bulk Parameterization of Clouds and Precipitation, Mon. Wea. Rev., 132, 103–120.

Hong, S. Y., J. Dudhia, and S. H. Chen, 2004: A Revised Approach to Ice Microphysical Processes for the Bulk Parameterization of Clouds and Precipitation, Mon. Wea. Rev., 132, 103–120.

Houze, R. A. Jr., S. G. Geotis, F. D. Marks Jr., and A. K. West, 1981: Winter monsoon convection in the vicinity of north Borneo. Part I: Structure and time variation of the clouds and precipitation, Mon. Wea. Rev., 109, 1595–1614.

Iwashima, T., R. Yamamoto, and Y. Sakurai, 2002: Long–term trends of extremely heavy precipitation intensity in Japan in recent 100 years, Recent Res Devel Meteorol 1, 1–9.

Kain J. S., and J. M. Fritsch, 1990: A one–dimensional entraining/detraining plume model and its application in convective parameterization. J. Atmos. Sci., 47, 2684–2702.

Kain, J. S., and J. M. Fritsch, 1993: Convective parameterization for mesoscale models: the Kain–Fritsch scheme. The representation of cumulus convection in numerical models, Meteo. Monogr, No. 46 Amer. Meteor. Soc., 165 – 170.

Karl, T. R., and R. W. Knight, 1998: Secular trends of precipitation amount, frequency and intensity of the United States. Bull Am Meteorol Soc 79, 223–241.

Karmakar, S., and A. Khatun, 1995: Variability and probabilistic estimates of rainfall extremes in Bangladesh during the southwest monsoon season. Mausam 46, 1, 47–56.

Khairoutdinov, M., and Y. Kogan, 2000: A new cloud physics parameterization in a large–eddy simulation model of marine stratocumulus, Monthly weather review 128, 1, 229–243.

Khaladkar, R. M., S. G. Narkhedkar, and P. N. Mahajan, 2007: Performance of NCMRWF Models in Predicting High Rainfall Spells During SW Monsoon Season –A Study for Some Cases in July 2004, ISSN 0252–1075 IITM Research Report No. RR–116,1–21.

Kim, H. W., and D. K. Lee, 2006: An observational study of mesoscale convective systems with heavy rainfall over the Korean Peninsula. Wea. Forecasting, 21, 125–148.

Kodama, Y. M., A. Ohta, M. Katsumata, S. Mori, S. Satoh, and H. Ueda, 2005: Seasonal transition of predominant precipitation type and lightning activity over tropical monsoon areas derived from TRMM observations. Geophys. Res. Lett., 32, L14710, doi: 10.1029/2005GL022986.

Kotroni, V., and K. Lagouvardos, 2001: Precipitation forecast skill of different convective parameterization and microphysical schemes: application for the cold, Geophysical research letters 28, 10, 1977–1980.

Kreitzberg, C. W., and D. J. Perkey, 1976: Release of potential instability: Part I. A sequential plume model within a hydrostatic primitive equation model. J. Atmos. Sci., 33, 456–475.

Kumar, R. A., J. Dudhia, and S. K. R. Bhowmik, 2010: Evaluation of Physics options of the Weather Research and Forecasting (WRF) Model to simulate high impact heavy rainfall events over Indian Monsoon region, Geofizika 27, 101–125.

Kuo, Y. –H., and G. T. –J. Chen, 1990: The Taiwan Area Mesoscale Experiment (TAMEX): An overview. Bull. Amer. Meteor. Soc., 71, 488–503.

Lambert, J. H., 1772: Tobler, Waldo, ed. Notes and Comments on the Composition of Terrestrial and Celestial Maps (Translated and Introduced by W. R. Tobler, 1972). ESRI Press. ISBN 978–1–58948–281–4.

Leung, L. R., Y. –H. Kuo, and J. Tribbia, 2006: Research needs and directions of regional climate modeling using WRF and CCSM. Bull. Amer. Meteor. Soc., 87, 1747–1751.

Li, J., and Y. L. Chen, 1998: Barrier jets during TAMEX, Mon. Wea. Rev., 126, 959–971.

Lin, Y. L., R. D. Farley, and H. D. Orville, 1983: Bulk parameterization of the snow field in a cloud model, J. Climate Appl. Meteor., 22, 1065–1092.

Mason, I. B., 2003: Binary events. Forecast Verification—A Practitioner's Guide in Atmospheric Science, I. T. Jolliffe and D. B. Stephenson, Eds., Wiley and Sons, 37–76.

McCumber, M., W. –K. Tao, and J. Simpson, R. Penc, and S. –T. Soong, 1991: Comparison of ice–phase microphysical parameterization schemes using numerical simulations of tropical convection. J. Appl. Meteorol., 30, 985–1004.

Mesinger, F., Z. I. Janjić, S. Nicković, D. Gavrilov, and D. G. Deaven, 1988: The step–mountain coordinate: Model description and performance for cases of Alpine lee cyclogenesis and for a case of an Appalachian redevelopment, Mon. Wea. Rev., 116, 1493–1518.

Mlawer, E. J., S. J. Taubman, P. D. Brown, M. J. Lacono and S. A. Clough, 1997: Radiative transfer for inhomogeneous atmosphere: RRTM, a validated correlated–k model for the longwave, J. Geophys. Res., 102(D14), 16663–16682.

Murata, F., T. Terao, T. Hayashi, H. Asada, J. Matsumoto, 2008: Relationship between atmospheric conditions at Dhaka, Bangladesh, and rainfall at Cherrapunjee, India. Nat Hazards 44:399–410. Doi: 10.1007/s11069–007–9125–2.

Nesbitt, S. W. and E. J. Zipser, 2002: The Diurnal Cycle of Rainfall and Convective Intensity according to Three Years of TRMM Measurements, Journal of Climate, 16, 1456–1475.

Ohsawa, T., T. Hayashi, Y. Mitsuta, and J. Matsumoto, 2000: Intraseasonal variation of monsoon activities associated with the rainfall over Bangladesh during the 1995 summer monsoon season. J Geophys Res Atmos 105, 29445–29459.

Olson, D. A., N. W. Junker, and B. Korty, 1995: Evaluation of 33 years of quantitative precipitation forecasting at the NMC. Wea. Forecasting, 10, 498–511, doi:10.1175/1520–0434(1995)010,0498.

Pasaric, Z., and J. Juras, 2011: Comments on ''Applying a general analytic method for assessing bias sensitivity to bias–adjusted threat and equitable threat scores'', Wea. Forecasting, 26, 122–125, doi:10.1175/2010WAF2222453.1.

Pleim, J., 2007: A combined local and non–local closure model for the atmospheric boundary layer. Part II: Application and evaluation in a mesoscale meteorological model, J.Applied Meteor. Climatology, 46, 1396–1409.

Ramage, C. S., 1971: Monsoon Meteorology, Academic Press, New York, p.6.

Ranadhur, R. P. S., K. Pal, and P. C. Joshi, 2009: Impacts of Satellite–Observed Winds and Total Precipitable Water on WRF Short–Range Forecasts over the Indian Region during the 2006 Summer Monsoon, Weather and Forecasting, 24, 1706–1731.

Rodrigo, F. S., 2002: Changes in climate variability and seasonal rainfall extremes: a case study from San Fernando (Spain), 1821–2000, TheorApplClimatol 72, 3, 193–207.

Romatschke U., and R. A. Houze Jr., 2001: Characteristics of Precipitating Convective Systems in the Premonsoon Season of South Asia, Journal of Hydrometeorology, 12, 157–180.

Routray, A., U. C. Mohanty, D. Niyogi, S. R. H. Rizvi, and K. K. Osuri, 2010: Simulation of heavy rainfall events over Indian monsoon region using WRF–3DVAR data assimilation system, MeteorolAtmosPhys, 106, 107–125.

Schaefer, J. T., 1990: The critical success index as an indicator of warning skill. Wea. Forecasting, 5, 570–575, doi:10.1175/1520–0434(1990)005,0570.

Schumacher, R. S., and R. H. Johnson, 2005: Organization and environmental properties of extreme–rainproducingmesoscale convective systems. Mon. Wea. Rev., 133, 961–976.

Shin, H. H., and S. Y. Hong, 2011: Intercomparison of Planetary Boundary–Layer Parametrizations in the WRF Model for a Single Day from CASES–99, Boundary–Layer Meteorol, 139, 261–281.

Skamarock, W. C., J. B. Klemp, J. Dudhia, D. O. Gill, D. M. Barker, W. Wang, and J. G. Powers, 2008: A description of the Advanced Research WRF version 3. NCAR Tech. Note 4751STR, 113.

Su, B. D., T. Jiang, W. B. Jin, 2006: Recent trends in observed temperature and precipitation extremes in the Yangtze River basin, China. TheorApplClimatol 83, 139–151.

Tao, W. K., and Coauthors, 2003: Microphysics, radiation and surface processes in the Goddard Cumulus Ensemble (GEC) model. Meteor. Atmos. Phys., 82, 97–137.

Tao, W. K., J. Simpson, S. Lang, M. McCumber, R. Adler and R. Penc, 1990: An algorithm to estimate the heating budget from vertical hydrometeor profiles. J. Appl. Meteor., 29, 1232–1244.

Thompson, A. M., R. B. Chatfield, H. G. J. Hguan, Smit, 2007: Mechanisms for the intraseasonal variability of ozone during the India winter monsoon, J. Geophys. Res., 112, D10303.

Tripoli, G. J., and W. R. Cotton, 1980: A numerical investigation of several factors contributing to the observed variable intensity of deep convection over south Florida, Journal of Applied Meteorology 19, 9, 1037–1063.

Vitrat, F., and Molteni, F., 2009: Dynamical Extended–Range Prediction of Early Monsoon Rainfall over India, Monthly Weather Review, 137, 1480–1492.

Wang, W., and N. L. Seaman, 1997: A comparison study of convective parameterization schemes in a mesoscale model, Monthly Weather Review 125, 2, 252–278.

Wilks, D. S., 1995: Statistical Methods in the Atmospheric Sciences: An Introduction. Academic Press, pp. 467

WMO/UNDP/BGD/79/013, 1986: Bangladesh Meteorological Department Climatological data and charts (1961–80), Tech. Note No.9.

Wu, X., W. D. Hall, W. W. Grabowski, M. W. Moncrieff, W. D. Collins, and J. T. Kiehl, 1999: Long–term behavior of cloud systems in TOGA COARE and their interactions with radiative and surface processes. Part II: Effects of ice microphysics on cloud–radiation interaction. J. Atmos. Sci., 56, 3177–3195.

Xukai, Z., and R. Fumin, 2015: Changes in regional heavy rainfall events in China during 1961–2012, Advances in Atmospheric Sciences 32, 5, 704.

Zhang, D. –L., and J. M. Fritsch, 1986: Numerical simulation of the mesoscale structure and evolution of the 1977 Johnstown flood. Part I: Model description and verification. J. Atmos. Sci., 43, 1913–1943.

Zhang, Q., K. H. Lau, Y. H. Kuo, and S. J. Chen, 2003: A Numerical study of a mesoscale convective system over the Taiwan Strait. Mon. Wea. Rev., 131, 1150–1170.